Thermal Considerations in Bulk Acoustic Wave Devices towards Optimised Acoustofluidics

Corato, Enrico

2025

Thermal Considerations in Bulk Acoustic Wave Devices towards Optimised Acoustofluidics

Enrico Corato

LUND
UNIVERSITY

Doctoral Dissertation

by due permission of the Faculty of Engineering, Lund University, Sweden.

To be defended in E:1406, Ole Römers väg 3, Lund.

April 11th, 2025 at 9:00

Faculty opponent
Professor Martyn Hill

Organization **LUND UNIVERSITY** Department of Biomedical Engineering Lunds Tekniska Högskola Box 118 221 00, Lund, Sweden	**Document name** DOCTORAL DISSERTATION **Date of issue** March 13, 2025
Author Enrico Corato	**Sponsoring organization** Swedish Foundation for Strategic Research (Grant Agreement FFL18-0122) and European Research Council (ERC) under the European Union's Horizon 2020 Research and Innovation Programme (Grant Agreements 852590)

Title: Thermal Considerations in Bulk Acoustic Wave Devices towards Optimised Acoustofluidics

Abstract

The main goal of my studies was obtaining bulk acoustofluidic devices able to achieve high energy density inside a water-filled cavity. This led us to explore the interplay of sound and thermal effects more in details. Hence, this thesis covers both thermoacoustic effects in Bulk Acoustic Wave devices and a revisited approach for designing them, focusing on achieving good performance. Thermoacoustic effects arise every time an acoustic field interacts with a temperature gradient. Its working mechanism relies on the change in physical properties that heat induces in every substance. By changing the temperature of a fluid, its interaction with sound will also change, hence creating acoustic forces that depend on the temperature distribution. We studied this phenomenon in various configurations, by inducing differential heating either by conduction at the channel boundaries or light absorption within the fluid itself. We employed tracing particles to characterize the resulting thermoacoustic streaming in three-dimensions for each configuration. Comparing our measurements with simulations performed with a finite-element method software, we could probe the limits of our understanding of thermoacoustics.I also studied how to generate strong acoustic fields inside a water-filled cavity, mainly using so-called mechanical interfaces. With this term, I refer to any material that we interposed between the actuator and resonator, namely in between the piezoelectric element(s) and the microfluidic chip. In this thesis, I present two approaches: using a bulky double-parabolic structure made in aluminium to input strong vibration and using a thin sheet of copper to shield the microfluidic chip from unwanted heat from the actuator. With this latter setup, we could achieve temperature-controlled acoustic focusing in a microchannel with a relatively simple design, opening up to robust and reliable acoustophoresis at various flow rates and input electrical power. As another approach, we employed a double-parabolic reflector through which we could couple a small microfluidic chip with two large piezoelectric elements. With this design, we could achieve very strong acoustic energy density in the water cavity, as we reported the highest measured energy density in literature as of today. However, our investigation showed that this design is not optimized for focusing a clean mode of sound waves. This means that there is still much more research to be done, which would potentially lead to even higher acoustic energy inside the microchannel.

This thesis contributes to the development of acoustofluidics by investigating the interplay of sound and heat and presenting few novel approaches to couple actuators and resonators. Employing mechanical interfaces allows for good sound transmission into the microfluidic channel, whilst preventing unwanted heat form reaching the analytes.

Key words: Ultrasonics, Microfluidics, Acoustofluidics, Acoustic forces, Thermoacoustics, Nonlinear acoustics, Transducers, Mechanical interface

Classification system and/or index terms (if any)

Supplementary bibliographical information	ISNR: LUTEDX/TEEM-1141-SE Report No. 2/25	**Language:** English
ISSN and key title		**ISBN:** 978-91-8104-443-0 (print) 978-91-8104-444-7 (electronic)
Recipient's notes	**Number of pages:** 185	**Price**
	Security classification	

Signature _____ Date 2025-03-13

To Roberto Masiero
who taught me how fun it is trying to understand

It's all about vibez...
and warmth !

Public defence
April 11th 2025, 9:00 in E:1406, E-huset, Ole Römers väg 3, 223 62 Lund, Sweden

Supervisor
Associate Professor Per Augustsson
Department of Biomedical Engineering, Lund University, Sweden
Co-supervisors
Assistant Professor Wei Qiu and Dr. Michael Gerlt
Department of Biomedical Engineering, Lund University, Sweden

Faculty opponent
Professor Martyn Hill
Faculty of Engineering and the Environment, University of Southampton, United Kingdom

Examination board
Assistant Professor Himani Garg
Department of Energy Sciences, Lund University, Sweden
Professor Lars Hoff
Department of Microsystems, University of South-Eastern Norway, Norway
Professor Karin Maria Tenje
Department of Materials Science and Engineering, Uppsala University, Sweden
Deputy member: Associate Professor Nina Reistad
Department of Physics, Lund University, Sweden

Chairman
Associate Professor Christian Antfolk
Department of Biomedical Engineering, Lund University, Sweden

Cover illustration
A galaxy of vibrating possibilities. Central image shows 10-µm fluorescent particles focusing in the presence of thermoacoustic streaming. The surrounding structures are four different time instants showing the simulated velocities inside a parabolic structure.

ISBN: 978-91-8104-443-0 (printed version)
ISBN: 978-91-8104-444-7 (electronic version)
Report No. 2/25
ISRN: LUTEDX/TEEM-1141-SE
Printed by Tryckeriet i E-huset, Lund, Sweden

Popular Science Summary

I feel that the title of this thesis sounds little cryptic and scary. If you recognise yourself in the previous sentence, this page is for you! Here I will explain what acoustofluidics is and why temperature effects are important to consider when building acoustofluidic devices, which happens to be the topic of my PhD work.

The whole concept behind acoustofluidics is that we can use sound to move small objects floating in a fluid. How so? And mostly, why should we do so? Let's first address this latter question. The reason for using sound to move small objects is that it has been proven to be precise and gentle. This is because it is a non-contact process, which is really important when handling delicate samples, such as cells and other biological structures. Then, let's see how we can impose movement with sound. Sound itself is a vibration that propagates in a material. We are used to hear sound and we thus do not acknowledge the mechanical nature of it, our ears do it for us. However, you can try to place a hand on a loudspeaker and you will perceive vibration as the membrane and cone of the speaker move up and down. Ok, but how does this translate to movement of objects? Well, sound is a wave and it travels in a medium. When it encounters an obstacle along its path, sound bounces on it and it gets scattered around. This exerts a gentle "push" on the object, making it move a little bit. And the stronger the sound amplitude, the faster the movement. This is the basic mechanism of acoustophoresis, which literally mean "separation by sound". And this is the niche in which this thesis sits.

Now let's imagine that instead of an object, we have a portion of fluid with slightly different density compared to its surroundings, for example a drop of salty water in fresh water. From the sound point of view, this drop will look exactly as an object on its path, namely an obstacle that has different acoustic properties compared to the medium through which it arrived. Hence, this salty drop will also scatter sound and, consequently, it will be moved. This is the essence of fluid relocation, which is analogous to particle acoustophoresis.

Here's where temperature gets into the mix. We all know that if we change the temperature of a substance, its physical properties will change. For example, when heating a gas, its density will decrease. This is the principle that makes a hot air balloon fly. In our work, we change the temperature locally inside a water-filled channel by constant heating/cooling. Once sound is introduced, it will encounter water with slightly different density depending on the temperature distribution, hence pushing it away from that location. However, as soon as the water moves, it changes temperature, as this is dependent on the position inside the channel. We can thus create and sustain fast recirculation of liquid by combining sound and heat: the so-called *thermoacoustic streaming*.

Cool. But why are we doing this? As all science, this phenomenon is neutral, meaning that it does not carry any specific purpose nor meaning within itself. We investigated it so to broaden our understanding of acoustofluidics and to optimize the design of devices. In fact, we also studied how metal can act as an interface between the material that emits sound and the water-filled channel. Metals have rather high heat conductivity and they can be employed to modulate the temperature inside the channel. For example, we showed how a thin sheet of copper can act as a shield and prevent heat from reaching the water cavity. Moreover, we also tried to use a metal structure to "funnel" sound from two large sources into a much smaller channel, enabling very fast movements of particles within a water-filled channel.

Overall, this thesis is an exploratory work for how heat affects the acoustic effects in very small channels filled with water. We proved that heat must be considered and that it can be controlled by employing metallic structures in the design. We also showed how these structures can help us achieve very

high-performing devices, as we measured the highest energy density ever reported in literature (as of today).

Welcome to the future of bulk-wave acoustofluidics !!

Riassunto Divulgativo

Il titolo di questa tesi mi sembra un po' criptico e spaventoso. Se ti riconosci nella frase precedente, questa pagina è per te! Di seguito spiegherò cos'è l'acustofluidica e del perché sia importante considerare gli effetti della temperatura quando si costruiscono dispositivi acustofluidici, che fatalità è proprio il tema del mio dottorato.

Il concetto alla base dell'acustofluidica è usare il suono per muovere piccoli oggetti che fluttuano in un fluido. Come? E soprattutto, perché mai dovremmo farlo? Affrontiamo prima quest'ultima domanda. Si utilizza il suono per muovere piccoli oggetti poiché è stato dimostrato essere molto preciso e delicato, essendo un processo privo di contatto: ciò è molto importante quando si maneggiano campioni delicati, come cellule e altre strutture biologiche. Vediamo quindi come possiamo muovere oggetti con il suono. Il suono in sé è una vibrazione che si propaga in un materiale. Siamo abituati a sentire il suono e quindi non ne riconosciamo la natura meccanica, abbiamo le orecchie che lo fanno per noi. Tuttavia, provando a mettere una mano su un altoparlante, percepirai le vibrazioni della membrana e del cono che si muovono su e giù. Ok, ma come si traduce questo nel movimento degli oggetti? Beh, il suono è un'onda e viaggia in un mezzo. Quando incontra un ostacolo lungo il suo percorso, il suono rimbalza su di esso e si disperde. Questo esercita una leggera "spinta" sull'oggetto, facendolo muovere un po'. E più forte è l'ampiezza del suono, più veloce è il movimento. Questo è il meccanismo di base dell'acustoforesi, che letteralmente significa "separazione tramite suono".

Ed è questa la nicchia in cui questa tesi si inserisce.

Ora immaginiamo di avere, al posto di un oggetto, una porzione di fluido con densità leggermente diversa rispetto all'ambiente circostante, ad esempio una goccia di acqua salata in acqua dolce. Dal punto di vista del suono, questa goccia apparirà esattamente come un oggetto sul suo percorso, cioè un ostacolo che ha proprietà acustiche diverse rispetto al mezzo attraverso cui già viaggiava. Pertanto, anche questa goccia salata disperderà il suono e, di conseguenza, verrà spostata. Questa è l'essenza del ricollocamento di fluidi, che è analogo all'acustoforesi delle particelle.

Ed è qui che entra in gioco la temperatura. Sappiamo tutti che se cambiamo la temperatura di una sostanza, le sue proprietà fisiche varieranno. Ad esempio, quando si riscalda un gas, la sua densità diminuisce. Questo è il principio che fa volare una mongolfiera. Nel nostro lavoro, cambiamo la temperatura localmente all'interno di un canale riempito d'acqua mediante costante riscaldamento/raffreddamento. Una volta introdotto il suono, questo incontrerà acqua con densità leggermente diversa a seconda della sua temperatura, spingendola via da quella posizione. Tuttavia, non appena l'acqua si muove, cambia temperatura, poiché questa dipende dalla posizione all'interno del canale. Possiamo quindi creare e sostenere una rapida ricircolazione del liquido combinando suono e calore: la cosiddetta *circolazione termoacoustica* .

Bene. Ma perché lo stiamo facendo? Come tutta la scienza, questo fenomeno è neutrale, nel senso che non ha alcuno scopo o significato specifico in sé. Lo abbiamo studiato per ampliare la nostra comprensione dell'acustofluidica e per ottimizzare il design dei dispositivi. Infatti, abbiamo anche studiato come i metalli possano agire in qualità di interfaccia tra il materiale che emette il suono e il canale riempito d'acqua. I metalli hanno una conducibilità termica piuttosto elevata e possono essere utilizzati per modulare la temperatura all'interno del canale. Ad esempio, abbiamo dimostrato che un sottile foglio di rame può agire come uno scudo termico e impedire al calore di raggiungere la cavità con l'acqua. Inoltre, abbiamo anche utilizzato una struttura metallica per "convogliare" il suono da due grandi sorgenti in un canale molto più piccolo, muovendo delle particelle molto velocemente all'interno di un canale.

In sostanza, questa tesi è un lavoro esplorativo su come il calore influisca sugli effetti acustici in canali molto piccoli riempiti d'acqua. Abbiamo dimostrato che il calore deve essere considerato e che può essere controllato includendo strutture metalliche nel design. Abbiamo anche dimostrato come queste strutture possano aiutarci a ottenere dispositivi ad alte prestazioni, poiché abbiamo misurato la più alta densità di energia mai riportata in letteratura (finora).

Benvenuti nel futuro dell'acustofluidica a onde di volume !!

Abstract

Acoustic fields can generate forces and streaming phenomena in fluids, which can then be used to manipulate suspended particles, such as cells or bacteria. The main goal of my studies was obtaining bulk acoustofluidic devices able to achieve high energy density inside a water-filled cavity, a necessary step to apply acoustofluidics to real-world diagnostics. This led us to explore the interplay of sound and thermal effects in more detail. Hence, this thesis covers both thermoacoustic effects in bulk acoustic wave devices and a revisited approach for designing them, focusing on achieving good performance.

Thermoacoustic effects arise every time an acoustic field interacts with a temperature gradient. Its working mechanism relies on the change in physical properties that heat induces in every substance. By changing the temperature of a fluid, its interaction with sound will also change, hence creating acoustic forces that depend on the temperature distribution. We studied this phenomenon in various configurations, by inducing differential heating either by conduction through the channel boundaries or light absorption within the fluid itself. We traced particles suspended in the fluid to characterize the resulting thermoacoustic streaming in three-dimensions for each configuration. Comparing our measurements with simulations performed with a finite-element method software, we could probe the limits of our understanding of thermoacoustics.

We also studied how to generate strong acoustic fields inside a water-filled cavity, mainly using so-called mechanical interfaces. With this term, we refer to any material interposed between the actuator and resonator, i.e. between the piezoelectric element(s) and the microfluidic chip. In this thesis, I present two alternative approaches. The first approach employs a double-parabolic structure

made in aluminium to input strong vibration from two large piezoelectric elements into a small microfluidic chip. With this design, we could achieve a very high acoustic energy density in the water cavity, as we reported the highest measured energy density in literature as of today. However, our investigation showed that this design is not optimized for generating a clean mode of sound waves. This means that there is still much more research to be done, which would potentially lead to even higher acoustic energy inside the microchannel. The second approach was based on interposing a thin sheet of copper between the piezoelectric element and the chip to divert unwanted heat from the actuator. With this latter setup, we could achieve temperature-controlled acoustic focusing in a microchannel with a relatively simple design, opening for robust and reliable acoustophoresis at various flow rates and input electrical power.

This thesis contributes to the development of acoustofluidics by investigating the interplay of sound and heat and by presenting two novel approaches to couple actuators to resonators. Employing mechanical interfaces allows for good sound transmission into the microfluidic channel, whilst preventing unwanted heat from reaching the biological sample.

List of Papers

I. Fast Microscale Acoustic Streaming Driven by a Temperature-Gradient-Induced Nondissipative Acoustic Body Force

Wei Qiu, Jonas Helboe Joergensen, **Enrico Corato**, Henrik Bruus, and Per Augustsson

in *Physical Review Letters*, vol.127(6):064501, Published 3rd August 2021

Author's contribution: part of planning and performing the experiments, partial data commentary and preparation of the manuscript, revising the manuscript.

II. High-energy-density acoustofluidic device using a double parabolic ultrasonic transducer

Enrico Corato, Ola Jakobsson, Wei Qiu, Takeshi Morita, Per Augustsson

in *Physical Review Applied*, vol.23(2):024031, Published 12th February 2025

Author's contribution: conceptualizing, planning, and performing the experiments, data commentary and preparation of the manuscript, revising the manuscript.

III. Thermoacoustic streaming in a linear temperature gradient

Enrico Corato, David Van Assche, Ola Jakobsson, Wei Qiu, Per Augustsson
Submitted to *Physical Review E*

Author's contribution: conceptualizing, planning, and performing the experiments, data commentary and preparation of the manuscript.

IV. Preliminary investigation report: Simple temperature-controlled device for robust bulk acoustic wave acoustofluidics

Enrico Corato, Ola Jakobsson, Michael Gerlt, Wei Qiu, Per Augustsson
Preliminary investigation report

Author's contribution: planning and performing the experiments, data commentary and preparation of the manuscript.

V. Temporal evolution of thermoacoustic streaming around spatially confined temperature gradient

Franziska Martens, **Enrico Corato**, David Van Assche, Ola Jakobsson, Wei Qiu, Per Augustsson
Manuscript

Author's contribution: part of planning and performing the experiments, data commentary and preparation of the manuscript.

Acknowledgments

This thesis would have not come into existence without the help and support of many people, who must be acknowledged. This page might be the most difficult part to write, but I must give it a try.

First and foremost, I want to thank Per. You were the very first professor I met when I arrived in Lund and, almost from the beginning, you have entrusted me with a great deal of responsibility and freedom. Through you, I've indeed learned a lot about acoustofluidics, but also about academia, leadership styles, and, mostly, how to tie my shoes. I'm really grateful for all of that. Thanks to Wei. I appreciate your continuous support and the spontaneous conversations we had about any results, problems, and (im)possible projects. Thanks to Ola. You are a true wizard, and your greatest magic is the overwhelming positivity that you project all around you. I owe you a lot, and I owe your great attitude towards life even more. Thanks to Michael. You showed me how it's possible to juggle multiple projects together and maintain a trace of sanity in the process. Thanks to Franzi and Megan, my sisters-in-science. I appreciate all the companionship we built both within and around university. Thanks to Qing, for all the *fightinggg* in the office. Thanks to Richard, for showing me that the lab is not that scary at night. Thanks to Oskar, for demonstrating that CADding can always be better. Thanks to David. Although brief, I appreciate our encounter and our discussions about work and being, wish you the best for your future endeavours. And of course, thanks to deGreat Mahdi. You showed me how it is possible to abduct oneself, and still keep singing within. I

wholeheartedly appreciate our brotherhood.

Even more people outside my group have helped me during my time at BME. Thanks to Axel, my fabrication-sensei. I'm grateful for all the time you dedicated to teaching me, and all the wonderful podcast suggestions. Thanks to Ammi, Désirée, and Ulrika, for always being kind and helpful while I was trying to navigate the maze of the university's bureaucracy. Thanks to Johan and Thomas, for showing me how enthusiasm for research never fades. Thanks to Leif, for the always mesmerizing conversations about life&food, which in the end are the same thing. Thanks to Lorenzo G., for demonstrating how an Italian can survive the North. And talking about Italians, huge thanks to Lorenzo B. Thank you for mankeeping me, both in Lund and from the beautiful Tuscan hills.

Thanks to all the acoustic people in BMC, aka "the other side", Cecilia, Andreas, Thierry, Amal, Alex, and Axel, for all the interesting and welcoming acoustic meetings. Here I sadly cannot mention everyone that roamed around with me during my *longbrief* time at the department, otherwise I would never hand in this thesis. Hope I can make up for it when I give you this book. So, a big thanks to the whole BME family, it has been a great pleasure to live E-huset with all of you.

My thanks also to the people outside Lund University that have contributed to this thesis. Thanks to Mathias, for always being happy to discuss about all the exciting fabrication projects. Good luck with the 500 rinnovata. Thanks to Henrik and Jonas, for trying to make theory intelligible to a simple experimentalist like myself. Thanks to Morita-sensei, for the inspiring lab-tour and fruitful collaboration. Thanks to Nakamura-sensei, for welcoming me in your lab and trying to bridge power ultrasonics and acoustofluidics with me. And huge thanks to querida Azuma-san, your kindness will live with me forever.

If you are reading this and feel I've not mentioned you so far, you might have helped with this thesis. Or maybe not. But you have for sure helped me becoming the human I am. A somehow strange ape, but as real as I can get. In presence or in absence, I am truly happy that you have been taking part to the madness of my tribe. I owe you my growth and the fantastic discoveries about human life. Thank you from the bottom of my heart, that now I know I do possess.

Last but definitely not least, my deepest thanks to my blood family, especially my parents and brothers. You are my definition of unconditional love, and I truly appreciate the support and warmth you have always given me.

Thank you, Tack, Gracias, Merci, Danke, Xièxie, Grazie

Enrico
Lund, March 13th, 2025.

Contents

Acronyms and Abbreviations

BAW Bulk Acoustic Wave

BCECF 2',7'-Bis(2-CarboxyEthyl)-5(6)-CarboxyFluorescein

DNA DeoxyriboNucleic Acid

DEP DiElectroPhoresis

DLD Deterministic Lateral Displacement

LASER Light Amplification by Stimulated Emission of Radiation

LDV Laser Doppler Vibrometry

LED Light-Emitting Diode

LoC Laboratory-on-a-Chip

NASA National Aeronautics and Space Administration

PCR Polymerase Chain Reaction

PID Proportional-Integral-Derivative

PS Polystyrene

PZT lead(P)-zirconate(Z)-titanate(Ti)

SAW Surface Acoustic Wave

SDG Sustainable Development Goals

UN United Nations

USA United States of America

Part I

Overview of the research field

Chapter 1
Introduction

In the past N years, I've been playing with water and sound, as my brothers often like to point out. This thesis aims to explain to the wilful reader what I did, and how I made it happen. The subject I have explored is acoustofluidics and, more specifically, I have been mainly investigating the thermal effects in bulk acoustic wave devices. With this introduction, I would like to give the reader a simple understanding of the somehow baffling terms introduced in the previous sentence, along with a general explanation of the research gap we have attempted to fill during my journey. In the following chapters, there will be more detailed explanations and discussions of the herein presented concepts, together with their related bibliographical references.

1.1 Why sound and fluids at the micro-scale?

The name acoustofluidics explains already everything one has to know about it: *acousto-* relates to sound, *-fluidics* refers to fluids of course. Practically, this method employs mechanical vibration (i.e. sound) to create forces in a fluid-filled chamber, which are then used for the intended purpose. Acoustofluidics has been exploited as part of the broad range of microfluidic techniques that have been developed starting in the 1960s. Common for such techniques is that they take advantage of the different set of forces dominating at the micro-scale (i.e. in the range of several thousandths of a millimetre), where viscous forces, related to friction in the fluid, are much larger than inertial forces, which are related to mass and velocity. Hence, in such small devices, the flow is deterministic, as the fluid motion dominated by viscous forces does not incur turbulence, which is

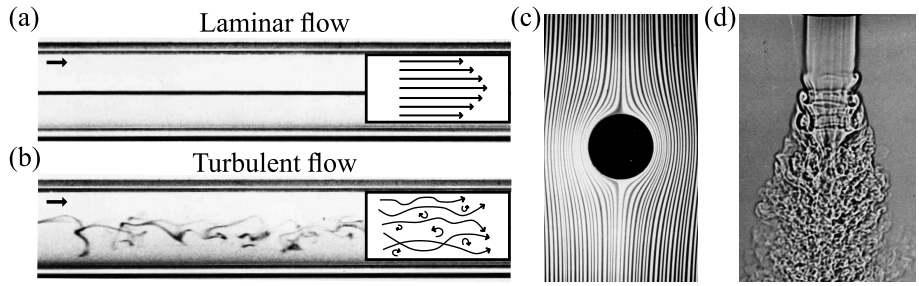

Figure 1.1: A filament of coloured water flowing in the (a) laminar and (b) turbulent regime. The arrows in the inserts represent a schematic of the fluid streamlines in each condition. (c) Visualisation of laminar flow creeping around an obstacle. (d) Transition from laminar to turbulent flow in a gas jet. Images adapted from [1], ©(1982) by the author.

the chaotic eddies and vortices that we all see when looking at fluid motion in our day-to-day life. The two different flow regimes are depicted in Figure 1.1.

An important feature differentiating acoustofluidic approaches from other microfluidic techniques is that the exerted forces only depend on the physical properties of the suspended object with respect to the surrounding medium. In simpler terms, this means that anything that is more or less compact than the fluid around it will be subjected to acoustic forces. Thus, no labelling or physical barrier is needed to achieve separation of the desired analyte. For these reasons, from the early 2000s, acoustofluidics has been applied in the life sciences as it allows gentle, non-contact, and label-free manipulation of objects in suspension flowing in microfluidics devices. With all these benefits, it has the potential to revolutionize diagnostics, with people in the field envisioning automated, precise, and low-cost analysis of biological fluids, especially when handling small sample volumes.

In the past two decades, seminal works applying acoustofluidics have been published, mainly exploring the concept of liquid biopsy, which is the analysis of non-solid biological samples. Encouraging results have shown how acoustofluidics can help to find cancer cells circulating in the blood, opening for better understanding of metastasis and disease or treatment monitoring with minimally invasive techniques.

Nevertheless, acoustofluidics has so far failed to fulfil its promises and to

become more than a mere research tool used only in university laboratories. As an example, high enough throughput has yet not been achieved to fulfil the requirements for many clinical applications, as it performs still one order of magnitude below what is desired for most real-world diagnostic applications. Moreover, reproducibility has been a recurring issue in the field, meaning that two identical devices perform differently due to the highly sensitive coupling between their components. This boils down to very practical considerations on how the different parts are glued together and how the whole assembly is packaged. Another long-standing issue has been temperature control, as regulating heat generation and dissipation remains a crucial step when dealing with biological samples. When actuating acoustofluidic devices, heat is an inherited by-product of its resonating behaviour and it affects not only the fluid, but also the magnitude and mode of vibration of the actuator itself.

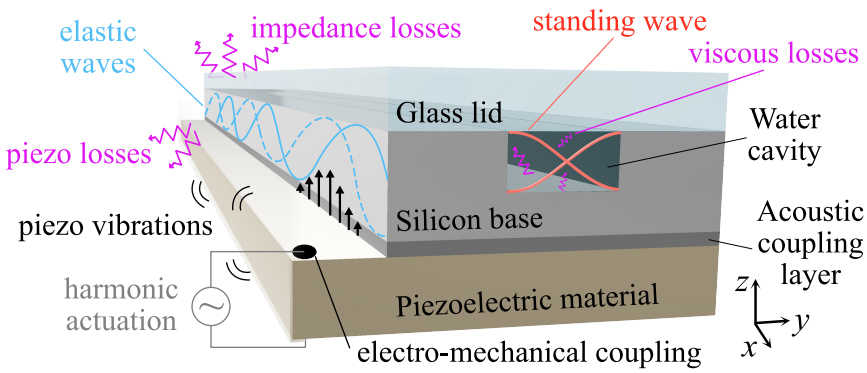

Figure 1.2: Sketch of the prototypical Bulk Acoustic Wave device (not to scale). The piezoelectric element vibrates when subjected to an alternate electrical current, vibrating mainly at the actuation frequency. A coupling layer assures good acoustic coupling between the piezoelectric element and the glass-silicon chip, which the elastic waves propagate into. The harmonic actuation aims to induce resonant modes of vibration which result in a pressure standing wave inside the water cavity. The behaviour of the device is heavily affected by different types of energy loss.

This thesis deals with bulk acoustic wave devices, which means that in our systems the whole bulk of the device vibrates to obtain a resonance inside the

fluid cavity. Hence, we used stiff materials able to store a lot of energy without too much dissipation. As an example, glass is quite stiff (i.e. it has a high elastic modulus) and thus, once a vibration is applied to it, it will vibrate for quite some time. Conversely, rubber is soft (i.e. low elastic modulus) and an applied vibration will dissipate rather fast. Prototypical bulk acoustic wave devices (Fig. 1.2) comprise a micro-channel fabricated in either silicon or glass, bonded to a lid, which is usually glass to allow for optical visualisation, with some holes to allow for fluid inlets and outlets, and an actuator to excite vibrations, usually a hard-type piezoelectric material. Explaining piezoelectricity is well beyond the scope of this thesis, but, in a nutshell, it is the ability of some materials to generate electrical currents when subjected to mechanical deformation (direct piezoelectric effect) and vice versa (inverse piezoelectric effect). In our research, we exploit this latter effect and thus, when we apply an alternate current to a piezoelectric material, it responds with mechanical vibrations at the same frequency.

In summary, the prototypical bulk acoustofluidic device has the piezoelectric element directly in contact with the glass/silicon that includes the channel, usually with an acoustic coupling agent in between (a glue or similar) to ensure good mechanical contact. An advantage of this configuration is that it allows for efficient energy transfer from the actuator (piezo) to the resonator (channel). However, a clear drawback is that heat can easily spread from the actuator, where it is inevitably generated, to the fluid cavity. Temperature changes affect the physical properties of the fluid and thus the stability of the acoustofluidic device. Moreover, having biomedical applications as an overarching goal, temperature must be tightly regulated, as biological samples are notoriously sensitive to heat.

1.2 Motivation of the thesis

The aim of my research is to tackle the current limitations of acoustofluidics, mainly focusing on the low throughput and adverse temperature effects. With the initial goal of building the best performing acoustofluidic device ever, we soon realised that the lack of understanding of how heat affects our devices was the main hindrance to obtaining reliable and bio-compatible diagnostic tools based on this technology.

This thesis has two main objectives: investigate thermoacoustic effects in

microchannels by studying the fluid flow arising from the interaction of sound and heat in different configurations (**Paper I**, **III**, and **V**); devise novel actuation strategies for bulk-acoustic wave devices, capable of achieving high acoustic energy density without inducing unwanted heating in the microchannel (**Paper II** and **IV**).

1.3 Overview of the thesis' work

On the one hand, we investigated the effects of temperature fields inside the fluidic chamber by generating heat both via light absorption and conduction. Thanks to our collaborators at the Technical University of Denmark, we validated a comprehensive theory that explains in detail the interplay between thermal and acoustic fields and attempted to show the implications that temperature gradients have on acoustofluidic devices.

We used heat conduction to generate and sustain temperature differences

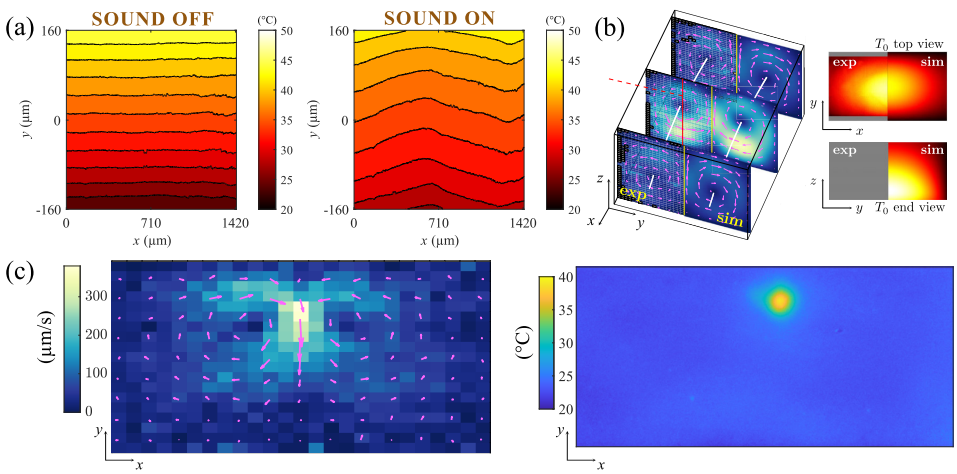

Figure 1.3: Thermoacoustics in microfluidic channels. (a) Linear temperature gradient by heat conduction, deformed when sound is ON (**Paper III**). (b) Thermoacoustic streaming via spherical temperature gradient by LED heating (**Paper I**). (c) Localised thermoacoustic streaming via spot temperature gradient by laser heating (**Paper V**).

between the two side walls of a microfluidic channel and we studied the re-

sulting forces and streaming patterns, Figure 1.3(a). This study has bearing on how the heat spreads from the vibrating actuator to the fluid channel in acoustofluidic devices, as the piezoelectric element is usually directly in contact with the microfluidic chip.

Further, by employing light absorption, we were able to generate localised heating in a microfluidic channel, with thermal gradients in three dimensions, Figure 1.3(b) and 1.3(c). Besides a few potential applications that we can already foresee, these investigations concern the unwanted thermal effects that might arise by simply monitoring the channel with a fluorescent microscope, whose light might heat the sample to be observed. Hence, these experiments indeed shone some more light on the young micro-scale thermoacoustic research field, which studies how sound and heat interact with each other.

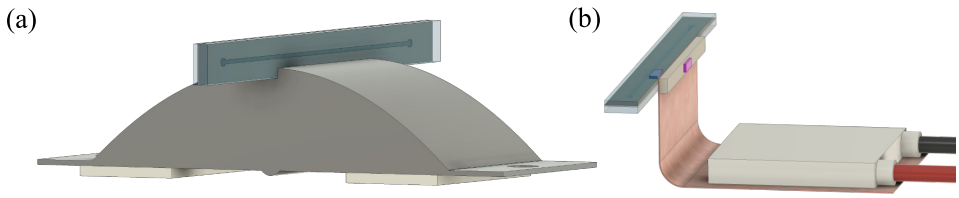

Figure 1.4: Three-dimensional drawings of the mechanical interfaces introduced in this thesis. (a) LDPLUS: a double parabolic reflector in aluminium couples two large piezos (on the bottom) with a microfluidic chip on top (**Paper II**). (b) Heat Pipe: a thin copper sheet is interposed between the piezo and the chip, and a peltier element controls the temperature on the chip (**Paper IV**).

On the other hand, we also investigated a few novel ways in which the piezoelectric elements can be coupled to the microfluidic chamber. First, we tried to use a structure for harvesting vibrations from two large actuators and focusing the sound onto the much smaller microfluidic chip, Figure 1.4(a). Our reasoning was fairly simple: by keeping the energy constant and reducing the area over which this is applied, we would obtain a much larger vibration amplitude. For this purpose, we adapted a design already existing in literature, whose working mechanism was explained as being similar to how we use parabolas to focus electromagnetic waves. With our prototype, we indeed achieved very high acoustic energy density inside the fluid cavity and thus reached quite high throughput (5 ml/min). However,

our study also shook the foundation of our reasoning when choosing this design, clearly showing that it was not an optimal solution to obtain highly focused acoustic energy cleanly delivered onto the microfluidic chip. Treasuring this experience, we then investigated a simpler setup that differs from the prototypical acoustofluidic device only by having a thin sheet of copper sandwiched between the piezoelectric elements and the chip, Figure 1.4(b). By doing this, we wanted to shield the fluid from the heat generated by the vibrating actuator, dissipating it through the copper film. Our study showed that acoustic manipulation is very sensitive to temperature changes and we proposed a relatively simple design to maintain constant performance of an acoustofluidic chip, regardless of the intended application.

Our work will help the researchers in our field understand and address the effects that heat has on acoustofluidic devices. Moreover, I hope that our work will inspire others to further investigate the feasibility of adding mechanical interfaces between actuators and resonators, for which we have shown their potential in reaching both high acoustic energy and robust temperature control.

1.4 Societal impact

Our work aligns with the Sustainable Development Goals (SDG) promoted by the UN. More precisely, our investigations pertain to SDG #3, *Good Health and Well-Being*, as we strive to build automated, precise, and cheap diagnostic tools. However, I see huge potential for acoustofluidics also in SDG #6, *Clean Water and Sanitation*. This issue could be tackled thanks to microfluidic devices distributed along the water grid that monitor and send real-time information about the water quality. Again, I reckon that acoustofluidics can play a significant role due to the relative simplicity of the devices: they comprise no moving parts and are less susceptible to clogging than other microfluidic techniques, potentially making them less prone to failure and demanding less maintenance. Moreover, I can also foresee applications of more mature acoustofluidics related to SDG #12, *Responsible Consumption and Production*, namely for the latter target. For example, with the aid of microfluidic and acoustic forces, the production of chemicals can become more efficient, with higher reuse of reagents and less wasteful recycling.

1.5 Ethical implications

This thesis addresses fundamental issues that are at the ground level of our understanding of acoustofluidic devices. Hence, from a utilitarian perspective, it could be argued that my whole work has no immediate application and is, if not completely useless, not a priority for society as a whole. However, I strongly reject these claims. This argument holds only in a world with finite resources, both human and material. While it can be argued that material resources are indeed finite, human resources are not. And I believe that research and technological advancement are the pinnacle of humanity, the very characteristics that differentiate us from the rest of the animal kingdom. By pursuing a PhD, I feel I have made my small contribution to the massive body of knowledge upon which our society stands and progresses. And history taught us that no one knows what can sprout from basic research in the future!

However, I do find that Biomedical Engineering as a field has some critical aspects. First and foremost, significant energies and resources are spent to understand and treat diseases that affect primarily only a fraction of the world's population, the richest fraction. This is an injustice that runs deep in the history of human societies and has escalated with modern medicine. A second, and perhaps related, issue is that funding for research often goes to selected topics that are "hyped" in the community, leaving other fields underfunded. As a result, scientist have the incentive to pursue similar topics. This has indeed the benefit of fostering fast progress in the subject and leading to new insights and breakthroughs. Still, these findings then open new research avenues, acting as a self-fulfilling prophecy that draws even more funding to the specific topic. I do not have any solution for this issue, and I am unsure if there is any better way to distribute funding in the research community (which are always never enough!). Nevertheless, I strongly believe that this is an issue scientists must evaluate when choosing what to dedicate their lives to investigating.

1.6 Structure of the thesis

This thesis aims to contextualize the research work that my collaborators and I have published. Besides this introduction, there is a brief overview of the field, from the general *Microfluidics* to the niche of *Acoustofluidics*, where I will explain

the theory necessary to understand the publications and the limitations that my work has tried to tackle. Before the paper summary, I stress the possibility of employing mechanical interfaces between actuators and resonators as an untapped means of obtaining more reliable and stable devices. The thesis ends with the conclusions I deem more significant and few possible outlooks that build on the knowledge and experience we gathered during my PhD studies. The included chapters of the thesis are:

1. **Introduction**, giving a broad perspective on the research subject in an accessible manner, together with the motivation of the thesis and its societal impact.

2. **Microfluidics**, briefly explaining fluid dynamics at the small scale and the concept of Lab-on-a-Chip. A section on thermal control in microfluidics system is also included.

3. **Acoustofluidics**, introducing the theory which my experimental work relies on. Here I focus mainly on the forces exerted in the resonating cavity and their interplay with thermal gradients. The chapter ends with the limitations that affect current acoustofluidic devices.

4. **Interface between actuator and resonator**, stressing the unexploited possibilities of adding materials between the piezoelectric element(s) and the microfluidic chip.

5. **Summary of the included papers**, giving a succinct summary of the findings of each paper, along with their motivation.

6. **Conclusions and outlook**, providing an epilogue to this thesis and puzzling together all the projects I have worked on during my journey. The chapter ends with few outlooks and suggestions regarding future research based on this thesis' findings.

Chapter 2
Microfluidics

Here I introduce the concept of *microfluidics*. For the work presented in this thesis on acoustofluidics, the small scale has helped not only for the precise control of the fluid flow, presented in this chapter, but also for the acoustic forces we employ in our devices. Since the acoustic forces scale with frequency, which in turn scales with the inverse of the wavelength, micro-scale resonators allow us to exert strong acoustic forces. While acoustics is presented in the following chapter, Ch.3, this chapter on microfluidics starts with a brief history of the field, followed by some basic equations necessary to understand fluid dynamics at the sub-millimetre scale. Then, the idea of *Lab-on-a-Chip* is introduced, together with the most commonly employed separation techniques. The chapter ends with a section on thermal considerations in microfluidic systems, where techniques for temperature monitoring and control at this small scale are introduced.

2.1 Historical background

Microfluidics is an interdisciplinary field that focuses on developing and applying technologies for handling fluids at the micro-scale. In simple terms, this means that the chamber containing the fluid has at least one dimension below 1 mm. Working at such small dimensions has several benefits, including precise flow control, small sample volume, and strong automation potential. The reduction of the dimensions from centimetres (10^{-2} m), e.g. a classic test-tube, to hundreds of micrometres (10^{-4} m), e.g. a classic microfluidic channel, allows for ~ 6 orders of magnitude reduction in sample volumes to

be processed, as it scales with the dimensions to the cube. Microfluidics has been applied to several fields such as chemistry and biology, while the focus of this thesis is biomedical engineering. The birth of microfluidics is conventionally set with the publication of a groundbreaking paper published in 1979 by researchers at Stanford University [2]. In this work, Terry and colleagues managed to perform gas chromatography onto a coiled capillary etched in a 5 cm silicon wafer, which comprises not only the fluidic chamber but also the necessary detectors. They integrated a 1.5 m long capillary onto that small platform, enabling them to process a volume as small as 1 nl with comparable results as the standard, and bulky, devices at the time. It was indeed the first micro-Total Analysis System ante litteram [3]. Since silicon etching became the go-to method to produce devices for microfluidics, these were called *microfluidic chips*, like their electronic counterparts that have analogous fabrication procedures. A significant leap forward in the field was brought about by the Human Genome Project, a concerted effort funded by the USA government aiming at sequencing and mapping the whole human genome. Due to the massive task at hand, conventional methods would have required too much time and enormous amount of labour and reagents. Hence, microfluidic solutions were developed for DNA separation [4] and polymerase chain reactions [5] for nl-volume samples, enabling the project to be successfully concluded in 2003.

After this brief historical excursus, I refer the interested readers to a review specifically focused on the progress of microfluidics from the 1980s to the 2010s [6], while here we proceed with contextualizing this thesis work. In conclusion, why do we use microfluidics in the biomedical field? The answer is not univocal, but in my view it is the small sample volume, linked to rapid processing, and the ease of automation that make microfluidics one of the best candidates for a future healthcare that is more efficient, affordable, and precise.

2.2 Fluid dynamics at the micro-scale

At the small scale, a different set of forces becomes dominant compared to the macro-scale that we are used to in everyday life. Considering a fluid flowing at smaller and smaller scale, inertial forces (related to mass and velocity) become less relevant compared to viscous forces, which arise from the friction the fluid experiences within itself and relative to the solid along which it flows. To

quantify the contribution of these two sets of forces, Reynolds proposed a dimensionless number (Re) taking into consideration the ratio between inertial and viscous forces [7]:

$$Re = \frac{\rho_0 v D}{\eta} \tag{2.1}$$

in which ρ_0 is the density of the fluid, η its dynamic viscosity, and v and D the characteristic velocity and dimension, respectively. Re accounts for inertial forces through $\rho_0 \cdot v$ and for viscous forces through η/D.

If $Re \gg 1$, the inertial forces dominate. Conversely, if $Re \ll 1$, the viscous forces are dominant in the system. With very high Reynolds numbers, the flow is defined as *turbulent*, meaning that the flow has a chaotic behaviour whose motion comprises several vortices (called eddies) added to the general flow direction. These eddies exist at different scales, disrupting the flow and eventually dissipating the fluid energy as heat below the micro-scale. The strength of microfluidics relies on reducing the characteristic dimension D of the systems, thus greatly reducing the contribution of inertial forces. With $Re \ll 1$, the flow is defined as *laminar*, meaning that it behaves as if various lamellae of fluid flow one on top of another, held together by the intermolecular forces whose effect we commonly refer to as viscosity. As a result, the fluid can smoothly flow in an orderly and deterministic manner. This greatly enhances our ability to precisely process, separate, and analyse fluids and the objects suspended within them, as long as the microfluidic system is specifically tailored for the intended function.

2.2.1 Flow in a microfluidic channel

Here I describe the typical flow inside a microchannel such the ones that I have used in my experimental works. Considering a Newtonian fluid flowing in the laminar regime and solving the Navier-Stokes equation in the case of a steady-state flow driven by a constant pressure difference Δp along a channel of length L, we obtain [7]:

$$[\partial_y^2 + \partial_z^2] v_x(y,z) = -\frac{\Delta p}{\eta L} \qquad \text{for} (y,z) \in \Omega \tag{2.2a}$$

$$v_x(y,z) = 0 \qquad \text{for} (y,z) \in \partial\Omega \tag{2.2b}$$

in which Ω refers to the fluid domain and $\partial\Omega$ to its boundaries.

By applying these equations to a channel defined by two infinite parallel plates at a distance H, i.e. an approximation of a rectangular microfluidic channel with high aspect ratio, we obtain:

$$\partial_z^2 v_x(z) = -\frac{\Delta p}{\eta L} \tag{2.3a}$$

$$v_x(0) = v_x(H) = 0 \tag{2.3b}$$

whose solution is a parabola:

$$v_x(z) = \frac{\Delta p}{2\eta L}(H - z)z \tag{2.4}$$

This solution is a good approximation of a shallow enclosure through which a fluid flows. A microfluidic channel can also be modelled as shallow and wide, but for channels of aspect ratio close to one, the side walls affect the velocity due to their no-slip condition, thus affecting the derivation of an analytical expression for the velocity.

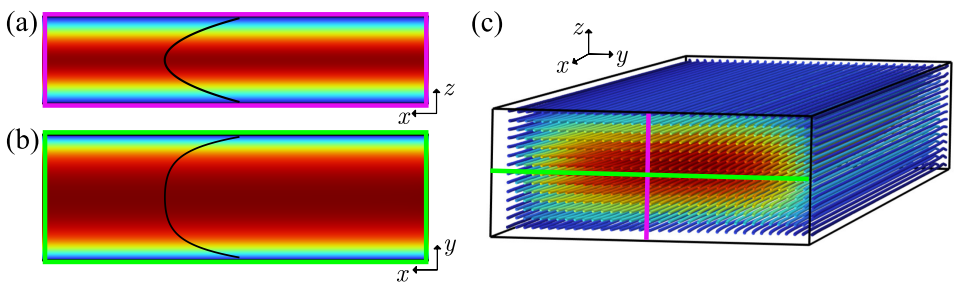

Figure 2.1: Simulation of three-dimensional flow inside a microchannel 375-µm wide and 150-µm high, performed in COMSOL Multiphysics [8]. (a) Flow velocity as seen from the side, displaying a parabolic profile. (b) Flow velocity as seen from the top, displaying a capped parabolic profile. (c) Full three-dimensional view of the fluid velocity.

Figure 2.1 (a) and (b) show the velocity profiles for water flowing in a channel with the dimensions I used in most of the experiments during my PhD work,

namely a rectangular channel 375-µm wide (W) and 150-µm high (H). Figure 2.1(a) shows a parabolic profile that resembles what could be calculated using Eq. 2.4. However, as aforementioned, that equation assumes two infinite parallel plates confining the fluid. In this case, the solution must also account for the presence of the side walls, especially as the aspect ratio W/H of such a channel is only 2.5, hence very different from the infinite-plate assumption. Along the width of the channel, the velocity profile resemble a capped parabola, Figure 2.1(b). Since the flow is affected much more by the top- and bottom-wall, the maximum velocity amplitude is mainly influenced by the stresses along the channel height, as in the aforementioned parallel plate case. However, the velocity must also to fulfil the no-slip boundary condition at the side-walls, thus resulting in such profile. The reader interested in deepening this topic is referred to [7].

2.2.2 Stokes' drag

Having the flow velocity field, I now introduce the forces that the moving fluid exerts onto a suspended object. Consider a stationary spherical particle of radius a, surrounded by a fluid of dynamic viscosity η, moving with uniform velocity v_∞ in the laminar regime ($Re < 0.1$). By neglecting gravity and applying the linearized Navier-Stokes equation and the continuity equation, along with the no-slip boundary condition at the surface of the sphere, we obtain an expression for the radial and tangential velocity distribution and for the pressure in the immediate vicinity of the sphere [7, 9].

By integrating the normal stresses on the surface of the sphere, we get:

$$F_{\text{drag}}^{(n)} = 2\pi\eta a v_\infty \tag{2.5}$$

which is the so-called *form drag*. It relates to the shape of the suspended object and it is caused by the flow separation when the fluid flows along the object, creating a low-pressure area behind it. By integrating the tangential stresses on the surface of the sphere, we get:

$$F_{\text{drag}}^{(t)} = 4\pi\eta a v_\infty \tag{2.6}$$

which is the so-called *friction drag*. It relates to the viscous friction between the fluid and the surface of the suspended object, and it is heavily influenced by

factors such as the surface roughness of the object. By summing the contribution from Eq. 2.5 and 2.6, we obtain the full drag force acting on a spherical particle:

$$F_{\text{drag}} = F_{\text{drag}}^{(n)} + F_{\text{drag}}^{(t)} = 6\pi\eta a v_{\infty} \tag{2.7}$$

also known as *Stokes' drag*. Finally, Eq. 2.7 can be generalised for a particle moving with velocity $\boldsymbol{v}_{\text{p}}$ in a fluid with velocity $\boldsymbol{v}$ (as with no particle present):

$$\boldsymbol{F}_{\text{drag}} = 6\pi\eta a(\boldsymbol{v} - \boldsymbol{v}_{\text{p}}) \tag{2.8}$$

The Stokes' drag will be useful to understand the balance between the forces acting on a particle in an acoustic field. However, this simple formulation of the fluid drag is limited to very low Reynolds numbers, as it is already 10% too low for $Re = 1$. For higher Reynolds numbers, the non-linear terms of the Navier-Stokes equation cannot be neglected, resulting in an adjusted formulation of Eq. 2.7 including factors proportional to Re [9].

2.3 Lab-on-a-Chip

My work aligns with the theme of Laboratory-on-a-Chip (LoC), a concept in bioengineering that aims to perform many of the operations currently conducted in clinical laboratories on small microfluidic chips. This implies the smooth integration of fluid control, separation, and detection onto a small device capable of automated analysis. In fact, LoC is a concept that translates the micro-Total Analysis Systems in the bio-field. Nevertheless, it is fair to state that nowadays LoC is not a reality. What has emerged is a "chip-in-a-lab", meaning that microfluidics has entered the clinical laboratories for specific purposes and tasks rather than LoC as a whole-encompassing analytical solution [6].

Ideal LoC instruments comprise an apparatus that includes the electronic and mechanical drivers, optical components for the intended tests, and single-use cartridges through which the sample flows. The cartridge with the analytes is loaded into the driving unit, which automatically performs the programmed analysis. The result is then shown either by the driving unit itself or through a computer.

Microfluidics, applied within the LoC concept, offers a viable way to tackle the inequality of the healthcare systems in different countries. Most medical equipment requires constant electricity supply, a reliable supply chain of reagents and equipment, and refrigerated chemicals, among other even stricter requirements. LoC devices, thanks to their compactness, integration, and automated analysis, have the potential to allow access to good healthcare also in resources-limited settings [10].

2.4 Separation at the micro-scale

An important aspect of LoC is the ability to separate the sample in what is intended to be analysed from what is not. Such a statement does sound obvious and straight-forward, but its implementation is far from trivial. Biological samples processed in microfluidics have very diverse compositions, but, for the purpose of this thesis, they can all be thought of as a carrier liquid with suspended objects within it. Depending on the adapted strategy, one can separate single populations of suspended particles or diverse populations that share specific characteristics, such as expressing the same surface markers or having similar physical properties. A lot of research effort has been focused on this latter approach to achieve separation through differences in the inherent physical characteristics of the objects, such as size or density. This results in label-free separation, meaning that the sample does not need any pre-processing steps and it can be processed without employing specific reagents, thus reducing operational complexity and costs.

In this section, I will briefly describe a few common passive and active separation techniques in LoC devices, along with their strengths and weaknesses. Acoustophoresis has a more detailed and lengthier subsection, as it is the technique that my PhD work was based on. The theoretical background for acoustophoresis is described in Chapter 3.

2.4.1 Passive separation

Passive techniques rely on the structure of the microfluidic chamber to achieve separation. The flow itself exerts forces on the suspended objects, enabling

separation with no external fields applied thanks to the deterministic behaviour of the hydrodynamic forces in the microfluidic system [11].

Inertial focusing

This technique relies on relatively high Re, up to values of a few hundred, which differentiates it from other microfluidic approaches. It needs such high flows to induce significant inertial forces in the fluid, and it then utilizes the shape, size, and deformability of the suspended objects to achieve separation [12]. Operating at such a high flowrate, inertial focusing is one of the few microfluidic techniques that offers high throughput by default. Nevertheless, most biological samples need considerable dilution to be processed with this technique. The main forces involved in inertial focusing are due to the lift caused by either wall effects or shear gradients. They both rely on asymmetric pressure distribution across the suspended objects flowing with the fluid, which results in net displacement in the direction perpendicular to the flow. Another effect is often exploited in curved channels, namely Dean flow [13, 14] . Centrifugal forces in curved fluid flows create streaming that drags suspended objects along recirculating vortices in the channel cross-section. By tuning the channel dimensions and the velocity of the flow, precise separation can be achieved based on the objects' properties. However, inertial focusing tends to be application-specific, meaning that the channel dimensions must be precisely tailored for each new application, as deriving the precise working mechanisms from first principles is still rather complex [15].

Deterministic lateral displacement

Deterministic lateral displacement (DLD) relies on obstacles along the fluid path to affect the particle's trajectories based on their size [16]. DLD offers extremely good size-resolution and, for this reason, it has been employed for the separation of nanoparticles such as bacteria, viruses, and even DNA [17]. However, the fluid flow inside DLD devices is rather complex, as it depends not only on the posts' shape but also on their spatial distribution and the flowrate. Analytical solutions still fail to describe the exact behaviour of DLD devices, making it necessary to employ numerical simulations and subsequent experimental validation for each design [18].

Filtration

This technique is based on the volume and deformability of the suspended objects. The simplest approach is to use physical barriers such as membranes [19]. Its biggest advantages are that they are simple, flexible, and fast. However, they present major drawbacks, such as being prone to clogging [20] and inducing significant mechanical stresses on the analytes. These stresses, in case of biological samples, can cause cell lysis and cell activation, impairing the diagnostic purpose [21].

2.4.2 Active separation

Active techniques rely on external forces applied to the fluid or the suspended objects while flowing through the microfluidic system [22, 23]. In general, they require more complex setups compared to passive techniques. However, the fluidic chambers themselves can usually have simpler designs, while the driving of external fields significantly complicates the system. The suspended objects are affected by the external force field which affects their flow trajectory. Different populations can then be independently collected by carefully positioning the outlets.

Magnetophoresis

Magnetophoresis allows for selective separation of magnetic objects suspended in a fluid that can be magnetic or not [24, 25]. The suspended objects can be naturally susceptible to the magnetic field [26] or labelled with affinity-based magnetic beads [27]. The particles susceptible to the magnetic field are deflected from their streamlines, while non-target objects are not. The sample of interest can then be collected from the outlets. While this technique allows for high purity of the target objects, it requires fairly strong magnetic forces, related to either the strength of the magnetic field or to the concentration of the magnetic beads to be attached to the target. Several challenges remain for this technology, among which are the bio-compatibility of the employed fluids and the prolonged exposure of living specimen to strong magnetic fields [25].

Dielectrophoresis

Dielectrophoresis (DEP) is a separation technique that relies on the dielectric properties of the suspended objects through the accumulation of electric charges at the object-fluid interface when applying a non-uniform electric field [28]. The forces applied to the suspended objects are influenced by several parameters, such as direct or alternating currents, their frequency, and the geometry of the electrodes. DEP has many advantages, such as being label-free and bio-compatible [29], but it usually requires a rather complex design for the microfluidic chip and has limited throughput [30].

Acoustophoresis

The first instance of *acoustophoresis* can be traced back to 1992, when the term was defined by Heyman in a patent (assigned to NASA) [31]. Due to acoustic scattering and non-linearities, the sound waves apply forces on the suspended objects while propagating in the fluid. Acoustophoresis relies on piezoelectric materials to induce acoustic vibration inside the fluid cavity and its separation capabilities are based on the physical properties of the suspended particles, such as their size, density, and compressibility. There are two main categories of acoustophoretic devices: bulk acoustic wave (BAW) and surface acoustic waves (SAW).

SAW devices employ acoustic waves that propagate along the surface of the piezoelectric material, excited by using interdigital transducers, which then propagate inside the fluid [32]. They can be differentiated into travelling SAW (TSAW) and standing SAW (SSAW). Thanks to their actuation method, SAW devices can apply sound waves at really high frequencies in confined regions and thus manipulate really small suspended objects [33]. However, these devices usually comprise of soft materials to build the fluid channel, thus undergoing significant heating due to acoustic waves leaking from the fluid into the material [34].

BAW devices rely on the vibration of the whole bulk of the chip and are therefore made of stiff materials [35]. Thanks to the hard walls, standing sound waves inside the fluid cavity form relatively easily at actuation frequencies close to its ideal one-dimensional resonances. It is also possible to employ more lossy materials, such as polymers, but then the whole-system resonance needs to be accounted for [36]. The underlying physics that allows for particle manipulation

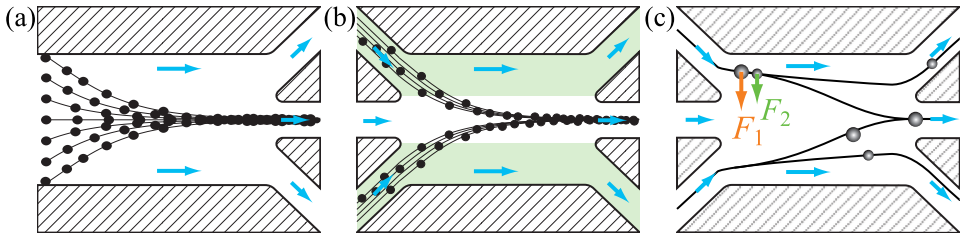

Figure 2.2: Illustration of a few applications of acoustophoresis: (a) enrichment; (b) buffer exchange; (c) separation of subpopulations. Figures adapted from [37], courtesy of Per Augustsson.

in acoustofluidic systems is introduced in the following chapter, Ch.3.

Acoustophoresis can be employed for different purposes in microfluidic devices. For example, it can be used to enrich target objects, Fig. 2.2(a) [38], re-suspend objects in a different medium, Fig. 2.2(b) [39], and separate objects in different populations based on their physical properties, Fig. 2.2(c) [40]. Hence, it has been extensively applied for cell washing [41], haematocrit determination [42], plasmapheresis [43], isolation of rare-cells [44], isolation of bacteria [45], and many more applications [46, 47, 48].

2.5 Thermal considerations in microfluidic systems

Here I describe the fundamental concept of heat, especially concerning microfluidic devices. The explanations are quite succinct, but the interested reader is referred to [9], where all the theory herein introduced is discussed and explained in detail.

2.5.1 Heat

Temperature T is one of those concepts that we intuitively and naturally understand in real life, yet its physical meaning is puzzling for most of us. The simplest explanation of temperature is that it relates to the average kinetic energy of the single constituents of a substance. Every molecule or atom in a material has some degrees of freedom to move, and thus kinetic energy. In solids, particles have mostly vibrational energy around a fixed position. In liquids, they have

also rotational and some translational energy, translation which is somewhat confined by the inter-particle interactions. In gases, the particles have the most freedom of movement, as they are far apart from each other.

Although the kinetic theory of temperature works well only for ideal monatomic gases, it offers an intuitive understanding of the concept of temperature [9]. Most material properties depend on temperature. Density, for example, relates to the mass (i.e. the amount of molecules) per unit of volume. Hence, the higher the temperature, the faster the particles are, and fewer particles will be present in the interrogation volume, resulting in decreased density.

Heat (Q) can be thought of as the transfer of thermal energy. Considering two insulated bodies at temperatures $T_1 > T_2$ and placing them in thermal contact, there will be a heat flux from body 1 to 2, a process termed *thermalisation*. The relation between heat and temperature can be expressed in terms of heat capacity C_p:

$$C_p = \frac{\mathrm{d}Q}{\mathrm{d}T} \tag{2.9}$$

where the amount of heat $\mathrm{d}Q$ introduced in a system relates to its temperature change $\mathrm{d}T$. This quantity can be expressed independently of the mass of the system m by considering the specific heat capacity c_p:

$$c_p = \frac{C_p}{m} \tag{2.10}$$

This is an intrinsic property of a substance and it defines the amount of heat needed to increase its temperature per unit mass. Various factors, such as constant pressure or volume, can influence how heat is distributed and thus how temperature changes. Therefore, c_p has been mapped in tables for various constraints, such as pressure.

Thermal energy can be transferred in different ways:

- **Conduction** is related to how molecules transfer heat to each other. It is presented in more detail below 2.5.1.

- **Advection** is related to the motion of the fluid bulk. It depends on the forces acting on the fluid and is the main heat transport mechanism at the macro-scale. For example, it describes how a radiator heats a room or how ocean currents distribute heat across the globe.
- **Radiation** is related to the absorption of electromagnetic waves and is the only heat transfer mechanism that does not require physical contact. For example, radiation is how the Sun warms the Earth.

In real-world scenarios, advection and conduction work in a complementary way: advection carries heat across large distances, while conduction distributes heat evenly inside the domain.

Heat conduction and the heat equation

From experimental observations, Fourier derived the law of thermal conductivity, linking the heat flowing normally through a surface A, i.e. the heat flux $q = Q/A$, to the temperature difference across a distance Δx via the heat conductivity of the material k_{th}:

$$q_x = \frac{Q_x}{A} = -k_{\text{th}} \frac{\Delta T}{\Delta x} \tag{2.11}$$

where the negative sign indicates that the heat flows opposite to the gradient of temperature, namely from hot to cold. Generalizing this equation for the limit $\Delta x \to 0$ and expanding it in three dimensions, one can write:

$$\boldsymbol{q} = -k_{\text{th}} \nabla T \tag{2.12}$$

in which $\boldsymbol{q}$ is a vector representing the heat flux in the three spatial dimensions. Eq. 2.12 holds in the case of an isotropic material, i.e. having the same heat conductivity in all dimensions. An example of isotropic material used in this thesis' work is water. When considering anisotropic materials, such as silicon, one can use the thermal conductivity tensor $\boldsymbol{k}_{\text{th}}$. This is a second-order symmetric tensor representing the ease of heat flow in each direction combination (i, j), namely $k_{\text{th}}^{ij} = k_{\text{th}}^{ji}$. Like the heat capacity, the thermal conductivity is a material property that has been mapped for various substances, with state-chart curves that express k_{th} as function of temperature and pressure.

To understand how temperature changes in time, one can derive the heat equation by equilibrating the heat leaving a system and its change in internal energy, and inserting Eq. 2.12 one can write:

$$\frac{\partial T}{\partial t} = \frac{k_{\text{th}}}{\rho c_p} \nabla^2 T = \alpha \nabla^2 T \tag{2.13}$$

in which the thermal diffusivity $\alpha = k_{\text{th}}/\rho c_p$ has been introduced.

2.5.2 Time scales for heat transport

To understand how heat gets distributed in a system, one can compute the different contributions to heat transport. The relative contribution of advection to conduction can be described by the Péclet number Pe:

$$Pe = \frac{Lv}{\alpha} = \frac{Lv\eta/\eta}{k_{\text{th}}/\rho_0 c_p} = \frac{\rho_0 Lv}{\eta} \cdot \frac{c_p \eta}{k_{\text{th}}} = Re \cdot Pr \tag{2.14}$$

in which L is the characteristic length of the system, v the fluid velocity, α the thermal diffusivity, and $Pr = c_p \eta / k_{\text{th}} = \nu/\alpha$ is the Prandtl number. Hence, Pe combines the flow regime (Re) with the ratio of momentum to thermal diffusivity of the fluid (Pr).

The Péclet number can be expressed also in terms of time-scales. Rearranging Eq. 2.14:

$$Pe = \frac{Lv}{\alpha} = \frac{v/L}{\alpha/L^2} = \frac{L^2/\alpha}{L/v} \tag{2.15}$$

The time for diffusion in one dimension can be calculated from Eq. 2.13 as:

$$t_{\text{1D}}^{\text{diff}} = \frac{L^2}{2\alpha} \tag{2.16}$$

and the time-scale for advection can be derived by the definition of velocity:

$$t^{\text{adv}} = \frac{L}{v} \tag{2.17}$$

In microfluidic systems, usually $Pe \ll 1$ and thus thermal diffusion is the main mechanism of heat transport.

2.5.3 Temperature control

Paper I, **III**, and **V** required precise regulation of the temperature inside the microfluidic channel. In general, controlling the temperature in microfluidic devices is crucial for several applications [49, 50, 51]. The strategies for thermal control can be broadly divided in two: external and integrated.

External control of temperature relies on setting the temperature outside of the fluidic chamber and it exploits thermal diffusion to then impose such temperature on the fluid. One strategy employs hot/cold fluids flowing parallel to the fluidic chamber, allowing temperature gradients to be generated in it [52]. A drawback of this approach is temperature stability, as changes in the temperature of the reservoirs will inevitably reflect onto the temperature of the fluidic channels. Another extensively used strategy for external control is to use thermoelectric elements (resistors or Peltier elements) placed in contact with the microfluidic device [53]. On the one hand, resistors rely on Joule effect to induce heating inside the fluidic chamber and they are thus limited to only adding the to the system. On the other hand, Peltier elements rely on the Peltier effect [54] to either add or subtract heat flowing electrical current through semiconductor pn-junctions in opposite directions, thus offering much more flexibility. By using small junctions on Peltier elements, researchers were able to control the temperature in very localised regions, enabling heating/cooling of fluids at the nano-litre scale [55]. However, controlling the temperature of such small volumes makes it necessary to integrate thermal control inside the microfluidic device itself.

Integrated thermal control has the considerable advantage of enabling control of temperature very close to the fluidic chamber, thus confining the cooled or heated area and being, on average, very fast due to the small distances involved. However, it usually requires more complex designs of the microfluidic system. One strategy relies on chemical or physical reactions occurring in channels parallel to the analytic chamber [56]. By either using endothermal (e.g. evaporation) or exothermal (e.g. dissolution of acid) reactions, the temperature in the analyte channel can be decreased or increased, respectively. By tuning the flowrates of reagents and the geometry of their channel, the temperature can be precisely controlled [57]. Another commonly employed integrated strategy relies on Joule heating of small resistors (usually wires made of platinum or gold). By embedding them in the microfluidic device

close to the fluidic chamber, the wires can heat the liquid in a precise and fast manner by controlling the electrical current that flows through them [58]. Moreover, wires can be patterned in arrays to achieve higher uniformity of the thermal field [59]. As aforementioned, a major drawback of relying on Joule effect is that it cannot subtract heat from the system. This issue can be tackled by integrating liquid cooling alongside Joule heating, implemented by flowing coolant liquid through dedicated channels carefully placed within the microfluidic chip [60].

Employing electromagnetic waves to heat the fluid in a microfluidic device differs from both external and integrated strategies for temperature control, as the heating device does not need to be in direct contact with the microfluidic device itself. For example, it is well known that microwaves can heat liquids and, by integrating miniaturized microwave heaters in microfluidic devices, precise and fast temperature increases can be achieved in confined locations along the fluid path [61]. Further, light absorption can also be employed to heat a fluid. Especially lasers, thanks to their very high spatial resolution, offer a means to precisely heat small volumes of fluid. This strategy has been successfully employed in a wide range of applications, such as polymerase chain reaction [62, 63] and bubbles control via thermocapillary effect [64].

In our group, we used light absorption to create temperature gradients across the whole channel width (via LED light absorption, **Paper I**) or in a localised spot in the microchannel (via laser light absorption, [65] and **Paper V**).

In **Paper III**, we used external Peltier controllers to impose near-linear temperature gradients across a microfluidic channel, while in **Paper V** we employed it to maintain the channel side-walls to a set temperature to enable temperature calibration. Our control system comprises two Peltier elements in thermal contact with the side of the microfluidic chip, with a resistance temperature detector glued on each side. A feedback loop and a thermo-electric cooler controller allow for maintaining the temperature at the set value.

2.5.4 Temperature measurements

Quantifying the temperature inside a microfluidic system is notoriously difficult, but extensive research has explored this issue. The employed methods can be broadly classified by how impactful they are on the fluidic system: invasive, semi-invasive, and non-invasive.

Invasive techniques require the fabrication of embedded temperature probes in the microfluidic device. They are defined as invasive since the probe must be in direct contact with the medium whose temperature is to be measured. The most widely used probes comprise a metal whose resistivity changes with temperature, such as nickel [66] and platinum [5]. Invasive techniques are not widely employed in microfluidic devices: besides being difficult to fabricate, they also affect the flow pattern if in direct contact with the fluid and the integrated electronics might obstruct optical access to the channel.

Semi-invasive techniques imply medium modifications allowing measurement of temperature from a distance, usually using kinetic fluorescent probes. These are fluorescent molecules that change light emission depending on the temperature, such as Rhodamine B [67]. One major drawback of this technique is that it requires a calibration curve to link the fluorescence intensity to the temperature, even though this limitation can be tackled by particles doped with two fluorophores, one temperature-sensitive and another temperature-insensitive [68]. Nevertheless, all the intensity-based measurement techniques, albeit practical, suffer from drawbacks such as uncertainties in the optical path, instability of the light source, photobleaching, and more [69]. Fluorescence lifetime imaging, relying on the intrinsic characteristics of the fluorescent molecules, overcomes these limitations and offers a precise and reliable method for quantifying temperature in microfluidic systems [70, 71]. However, the setups required for such measurements can be rather complex.

Non-invasive techniques, as the name suggests, allow for measuring the temperature at a distance without any pre-treatment to the medium. A common technique is infrared thermography [72], which quantifies the amount of low-energy electromagnetic waves (wavelengths higher than the visible spectrum) that every body emits. This thermal energy spectrum is then converted into visible images whose intensity is linked to the object's temperature. However, calibration of such measurements can be difficult [73], as it entails perfect knowledge of the emissivity and the reflections of the object

at hand [74]. Thus, this technique is often used together with thermocouples [75, 59]. Another non-invasive technique is backscatter interferometry [76], which links the change in the refractive index of the medium to its temperature. Despite recent advances in compensation [77], this technique depends heavily on the property of the sample at hand and the optical path itself, thus requiring calibration [78].

In our work, we used semi-invasive techniques to quantify the temperature in the microchannel. In **Paper I** and **III**, we employed Rhodamine B as a temperature-sensitive fluorophore. In **Paper V**, we used BCECF for the same purpose. The process of temperature calibration and measurement is described in detail in the supplementary material of **Paper I** [79]. In simple terms, we employed two Peltier elements driven by a PID controller to set the temperature on the side of the chip. By acquiring images at known set temperatures, we obtained pixel-wise calibration curves linking the temperature to the fluorescence intensity. Then, the inverse relation was used to estimate the temperature inside the channel once an unknown thermal field was present.

Chapter 3
Acoustofluidics

In this chapter, I introduce the theory necessary to tackle the acoustofluidic issues I have been dealing with during my PhD studies. The reader interested in deepening the theoretical understanding of acoustofluidics is referred to these books [80, 81] and PhD thesis [82, 83, 84].

3.1 Sound and acoustic impedance

Sound can be described as a pressure difference that travels in a medium: it implies no net mass transport, as matter "oscillates" around an equilibrium position, but there is net energy transfer. Sound propagation through matter happens either with vibrations parallel to the sound propagation direction (longitudinal waves) or with vibrations perpendicular to the propagation direction (transverse waves). While solids can support both modes of vibration, fluids do not have shear elasticity and thus they cannot transmit transverse waves.

The medium which sound travels through affects its propagation. This concept is expressed by the *acoustic impedance* (Z) of the material. Analogous to electrical impedance, it is defined as the ratio between the driving force (pressure p) and the flow (velocity v):

$$Z = \frac{p}{v} = \rho_0 c_0 = \sqrt{\frac{\rho_0}{\kappa_0}} \tag{3.1}$$

in which c_0 is the speed of sound and $\kappa_0 = 1/\rho_0 c_0^2$ is the compressibility of the medium.

When sound encounters an interface between two materials with different acoustic impedance $Z_1 \neq Z_2$, one portion of the wave gets reflected, and another is transmitted through the interface. Considering a sound wave propagating from medium 1 to medium 2 and suitable boundary conditions, the ratio of energy intensity that is reflected I_r compared to the incident energy intensity I_i can be expressed as:

$$R_\mathrm{I} = \frac{I_\mathrm{r}}{I_\mathrm{i}} = \frac{(Z_2 - Z_1)^2}{(Z_1 + Z_2)^2} \tag{3.2}$$

in which R_I is the intensity reflection coefficient. Through energy conservation, the intensity transmission coefficient T_I can be directly calculated as $T_\mathrm{I} = 1 - R_\mathrm{I}$.

In the acoustofluidic setups used in this thesis, we employed microfluidic chips made of hard materials, such as silicon (si) and glass (gl), with a channel filled with aqueous solutions. Since we are interested in retaining acoustic energy inside the water cavity, it is useful to compute the amount of energy that gets reflected at the interface between water (w) and the hard walls that act as boundaries of the channel. By considering the system at 25 °C and the material parameters as in [82], Eq. 3.1 can be inserted in Eq. 3.2 and R_I at the glass-water and silicon-water interfaces becomes:

$$R_\mathrm{I}^{(\mathrm{gl-w})} = \frac{(Z_\mathrm{gl} - Z_\mathrm{w})^2}{(Z_\mathrm{w} + Z_\mathrm{gl})^2} \approx 79\% \tag{3.3a}$$

$$R_\mathrm{I}^{(\mathrm{si-w})} = \frac{(Z_\mathrm{si} - Z_\mathrm{w})^2}{(Z_\mathrm{w} + Z_\mathrm{si})^2} \approx 86\% \tag{3.3b}$$

Eq. 3.3 shows that, thanks to the large mismatch of acoustic impedance between water and the hard walls of the channel, most of the acoustic energy is reflected back into the cavity.

3.2 Resonance

The incident and reflected pressure waves interact with each other, a phenomenon called interference. At certain frequencies f, the interference is mainly constructive, giving rise to resonant modes of vibration. Resonance occurs when the oscillation of the actuation matches the natural frequency of

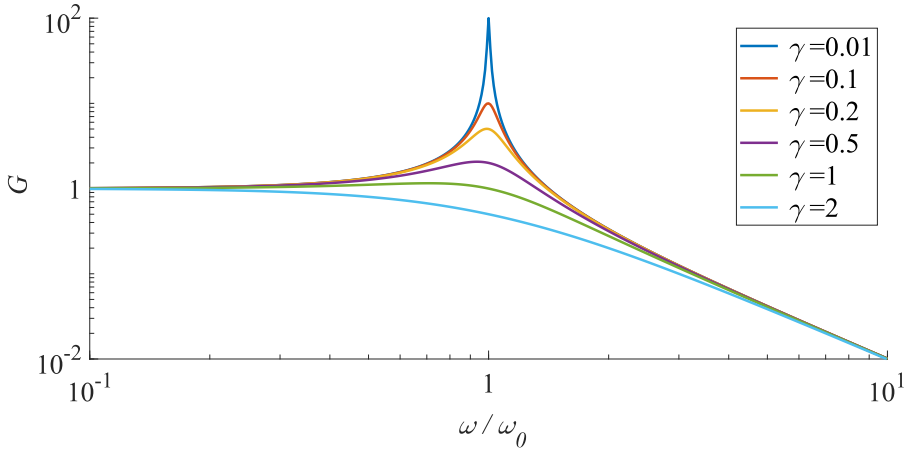

Figure 3.1: Gain G of a one-dimensional forced oscillator, as function of the actuation frequency ω divided by the natural frequency of the system ω_0. The smaller the damping γ, the higher the gain.

an object. At resonance, the acoustic energy density in the resonator is several orders of magnitude higher than off-resonance [85].

Considering a one-dimensional forced harmonic oscillator with small damping, the system gain G relates the oscillation amplitude of the system χ to the oscillation of the drive χ_0:

$$G = \frac{\chi}{\chi_0} \propto \frac{1}{\sqrt{(1-\tilde{\omega})^2 + \gamma^2 \tilde{\omega}^2}} \tag{3.4}$$

in which $\tilde{\omega} = \omega/\omega_0$, with $\omega = 2\pi f$ is the angular frequency and ω_0 the natural frequency of the system. γ is the damping of the system, which is related to its energy losses and mass. The natural frequency ω_0 depends on the physical properties of the system at hand, i.e. its geometry, mass, and materials. As shown in Fig. 3.1, the smaller the damping, the higher the gain. For a driven oscillator described by Eq. 3.4, one can derive the quality factor Q_m, which relates the stored and dissipated energy per cycle of oscillation at steady state. It can be defined as:

$$Q_\mathrm{m} = \frac{\text{Energy stored}}{\text{Energy dissipated}} = \frac{\omega_0}{2\gamma} \tag{3.5}$$

The quality factor Q_m is inversely proportional to the damping γ and this must

be minimized to obtain efficient systems, i.e. storing much more energy than they dissipate. This is the main reason why hard materials are employed in BAW devices. In real systems, Q_{m} can be derived from the electrical impedance spectrum of the piezoelectric actuator with reasonable uncertainty [86, 87], and thus linked to the acoustofluidic performance of the device [88, 89].

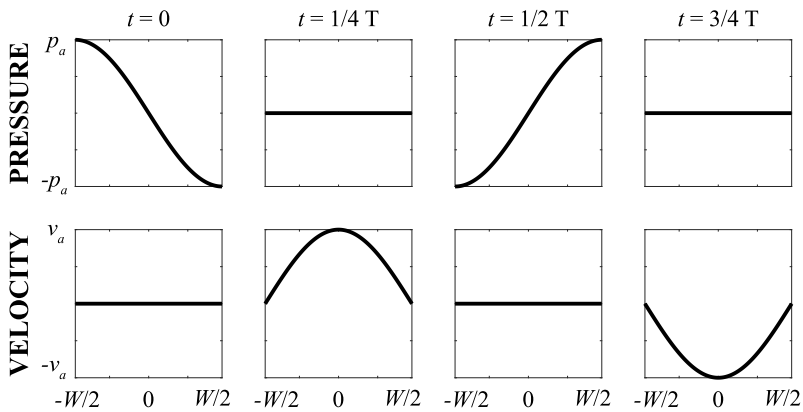

Figure 3.2: First-order pressure and velocity fields in a chamber with a single-node pressure standing wave across its width W. Each column corresponds to a different time instant along the period T of the acoustic wave. Pressure and velocity are out of phase both in space and in time.

In the experimental work presented in this thesis, we actuated the fundamental resonance across either the width or height of a water-filled channel. As an example, consider a one-dimensional standing sound wave across the width W of the channel, actuated at a frequency $f = c_0/\lambda = c_0/2W$, thus resulting in a single pressure-node in the centre of the channel. The expression in time t of the incident acoustic pressure p_1 and incident acoustic velocity v_1 along the width dimension y are given as:

$$p_1 = p_{\mathrm{a}} \cos\left[k_y\left(y + \frac{W}{2}\right)\right] \cos(\omega t) \tag{3.6a}$$

$$\boldsymbol{v}_1 = v_{\mathrm{a}} \sin\left[k_y\left(y + \frac{W}{2}\right)\right] \sin(\omega t)\mathbf{e}_y \tag{3.6b}$$

in which p_a is the pressure amplitude, v_a is the velocity amplitude, $k_y = 2\pi/\lambda$ is the angular wavenumber along the width of the channel, and $\mathbf{e}_y$ is the unit vector along y. The subscript $_1$ signifies *first-order* pressure and velocity, namely quantities that oscillate at the same time-scale as the actuation. This relates to the mathematical description of the resonating system through a perturbation scheme, valid with low acoustic amplitudes [85]. p_1 and v_1 are depicted in Fig. 3.2 along an actuation period $\mathrm{T} = 1/f$: as shown in Eq. 3.6, they are out of phase both in space and time.

The energy carried by the sound in the resonating chamber is a combination of potential and kinetic energy, oscillating in time between the two forms. For a one-dimensional system as in Eq. 3.6, the acoustic energy density E_{ac} can be simplified to:

$$E_{ac} = \frac{p_a^2}{4\rho_0 c_0^2} = \frac{1}{4}\kappa_0 p_a^2 = \frac{1}{4}\rho_0 v_a^2 \tag{3.7}$$

The acoustic energy density relates to all the second-order effects presented below. It is an useful quantity to measure in each system so to compare their performance.

3.3 Acoustic streaming

Acoustic streaming has been theoretically described first by Lord Rayleigh [90], who was inspired by the steady recirculation of gas in Kundt's tubes. By including friction at the boundaries, he described the streaming in the fluid bulk for an infinite parallel plate channel actuated with a sinusoidal first-order velocity parallel to the plates. His explanation was expanded by Schlichting, who derived the mathematical description of the streaming close to the boundaries of the resonator, in the so-called *viscous boundary layer*, where the fluid is subjected to strong non-uniform stresses due to the no-slip boundary condition [91]. The thickness of this boundary layer δ, for a fluid with kinematic viscosity $\nu = \eta/\rho_0$ and an acoustic field actuated at angular frequency $\omega = 2\pi f$, can be calculated as:

$$\delta = \sqrt{\frac{2\nu}{\omega}} = \sqrt{\frac{\eta}{\pi\rho_0 f}} \tag{3.8}$$

and it is ~ 0.4 µm for a 2 MHz ultrasound in water. Hence, acoustic streaming in the bulk of a resonator (Rayleigh streaming) can be explained by the slip velocity given by the streaming close to its boundaries (Schlichting streaming). Eventually, Lighthill generalized the description of acoustic streaming as the nonzero divergence of the time-averaged acoustic momentum-flux-density tensor [92]. In simple terms, it means that there is an imbalance in how the momentum carried by the sound wave is distributed in the fluid cavity during a full vibration cycle. This uneven distribution of the momentum causes the fluid recirculation that we call acoustic streaming. The theoretical explanation was further expanded including nonideal thermodynamic conditions [93] and curved elastic cavities vibrating at arbitrary velocity [94].

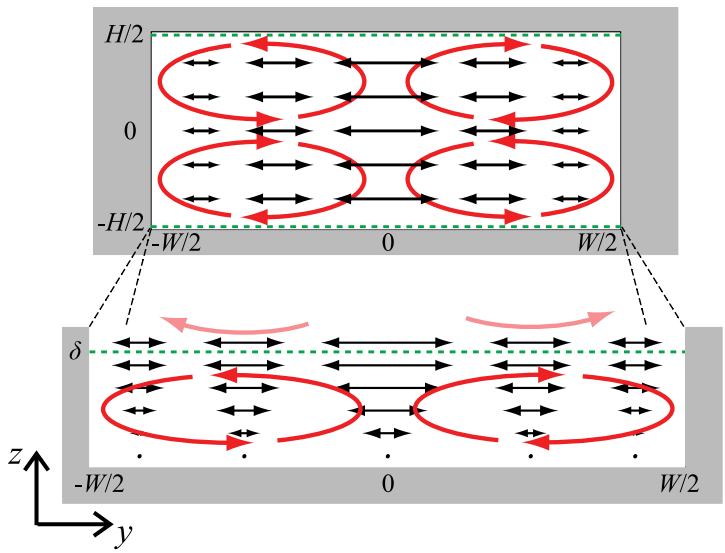

Figure 3.3: Rayleigh (red arrows, top) and Schlichting (red arrows, bottom) streaming in a fluid chamber with a single-node pressure standing wave across its width. The varying first-order velocity field (black arrows) rapidly decreases within the inner boundary layer δ, shown by the green dashed line. Figure adapted from [37], courtesy of Per Augustsson.

Figure 3.3 depicts boundary-driven acoustic streaming (Rayleigh streaming) in the cross-section of a microfluidic channel wide W and high H, with a

sound standing wave across its width. The streaming in the bulk is driven by the streaming at the boundaries parallel to the wave propagation direction (Schlichting streaming). This inner-boundary streaming originates from the uneven distribution of stresses in the thin boundary layer δ due to the no-slip boundary condition for the first-order velocity.

Given a sinusoidal actuation as in Eq. 3.6 along y and assuming $\lambda \gg H \gg \delta$, the components of the second-order streaming velocity in the bulk $\langle \boldsymbol{v}_2 \rangle$ can be described as [90]:

$$\langle v_{2y} \rangle = \frac{3}{16} \frac{v_a^2}{c_0} \sin\left[2k_y\left(y + \frac{W}{2}\right)\right]\left[1 - 3\frac{z^2}{(H/2)^2}\right] \tag{3.9a}$$

$$\langle v_{2z} \rangle = \frac{3}{16} \frac{v_a^2}{c_0} k_y h \cos\left[2k_y\left(y + \frac{W}{2}\right)\right]\left[\frac{z^3}{(H/2)^3} - \frac{z}{(H/2)}\right] \tag{3.9b}$$

At the channel mid-height ($z = 0$), the z-component of acoustic streaming $\langle v_{2z} \rangle$ vanishes, resulting in motion only across the channel width. However, Eq. 3.9 is expected not to fully represent the velocity we observe in our experimental work, as we have $\lambda \approx 5H$ for most of the channel geometries we used. The reader interested in more detailed descriptions of boundary-driven acoustic streaming is referred to these excellent PhD theses [82, 83, 84].

3.4 Acoustic radiation force

Particles suspended in an acoustic field scatter sound and this causes time-averaged forces, another second-order effect. The first study on these acoustic radiation forces dates back to 1934, when King formulated a theoretical description of the force acting on an incompressible particle in an inviscid fluid [95]. His work was expanded in 1955 by Yosioka and Kawasima, who included the compressibility of the suspended object [96]. In 1962, Gorkov generalised the mathematical formulation of the acoustic radiation force by using the time-averaged momentum flux through a closed surface around a particle [97]. Eventually, Settnes and Bruus expanded Gorkov's approach to include the viscosity of the fluid surrounding a particle [98]. Here I will present their formulation for the acoustic radiation force $\boldsymbol{F}_{\text{rad}}$ acting on a spherical particle of radius a, compressibility κ_p, and density ρ_p, suspended in a medium

of compressibility κ_0 and density ρ_0. The radius of the particle is assumed much smaller than the sound wavelength, i.e. $a \ll \lambda$.

$$\boldsymbol{F}_{\text{rad}} = -\pi a^3 \left[\frac{2\kappa_0}{3} \text{Re}[f_1 p_1 \nabla p_1] - \rho_0 \text{Re}[f_2 \boldsymbol{v}_1 \cdot \nabla \boldsymbol{v}_1] \right] \tag{3.10}$$

in which f_1 and f_2 are expressed as:

$$f_1(\tilde{\kappa}) = 1 - \tilde{\kappa}, \quad \text{with } \tilde{\kappa} = \frac{\kappa_p}{\kappa_0} \tag{3.11a}$$

$$f_2\left(\tilde{\kappa}, \tilde{\delta}\right) = \frac{2\left[1 - \Gamma\left(\tilde{\delta}\right)\right](\tilde{\rho} - 1)}{2\tilde{\rho} + 1 - 3\Gamma\left(\tilde{\delta}\right)}, \quad \text{with } \tilde{\rho} = \frac{\rho_p}{\rho_0} \tag{3.11b}$$

$$\Gamma\left(\tilde{\delta}\right) = -\frac{3}{2}\left[1 + \text{i}\left(1 + \tilde{\delta}\right)\right]\tilde{\delta}, \quad \text{with } \tilde{\delta} = \frac{\delta}{a} \tag{3.11c}$$

The acoustic radiation force $\boldsymbol{F}_{\text{rad}}$ (Eq. 3.10), proportional to the particle's volume, has two components. The first one represents the monopole scattering: it is dependent on the first-order pressure p_1 and it entails a compressible stationary particle (f_1). This term becomes null in the case of a particle with the same compressibility as the surrounding fluid (Eq. 3.11a). The second component relates to the dipole scattering of a translating incompressible particle that scatters sound due to the difference in density between the particle and the fluid (f_2). In fact, this term becomes null if $\rho_p = \rho_0$ (Eq. 3.11b). Γ is a correction factor due to the viscosity of the fluid (Eq. 3.11c), and it thus influences only f_2. Considering an inviscid fluid, the boundary layer thickness δ becomes zero (Eq. 3.8) and thus Eq. 3.10 and 3.11 have the same formulation as derived by Gorkov.

In the particular case of a resonant one-dimensional standing pressure wave along y, Eq.3.6, $\boldsymbol{F}_{\text{rad}}$ reduces to [98]:

$$\boldsymbol{F}_{\text{rad}} = 4\pi a^3 \Phi\left(\tilde{\kappa}, \tilde{\rho}, \tilde{\delta}\right) k_y E_{\text{ac}} \sin\left[2k_y\left(y + \frac{W}{2}\right)\right] \mathbf{e}_y \tag{3.12}$$

in which

$$\Phi\left(\tilde{\kappa}, \tilde{\rho}, \tilde{\delta}\right) = \frac{1}{3} f_1(\tilde{\kappa}) + \frac{1}{2} \text{Re}\left[f_2\left(\tilde{\rho}, \tilde{\delta}\right)\right] \tag{3.13}$$

is the so-called *acoustic contrast factor*, whose effect is depicted in Fig. 3.4.

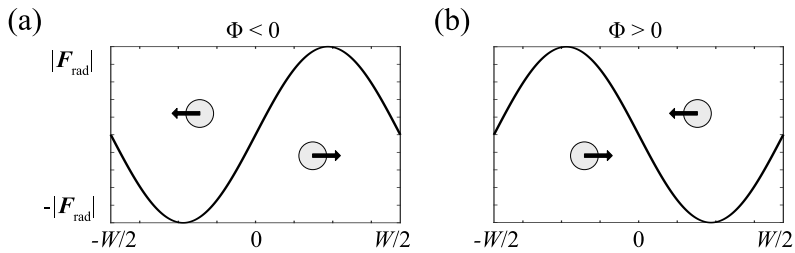

Figure 3.4: The effect of the contrast factor on the acoustic radiation force. (a) With negative contrast factor, the particles migrate towards the pressure anti-node of the channel. (b) On the contrary, particles with a positive contrast factor migrate towards the pressure node.

This can be either positive or negative, and its sign determines if the particle migrates towards the pressure node (positive contrast) or to the pressure anti-node (negative contrast).

In all the papers included in this thesis, we used particles with positive acoustic contrast factor ($\Phi \approx 0.17$) since we always employed polystyrene particles suspended in an aqueous solution [99]. In fact, polystyrene is denser and less compressible than water. Nevertheless, determining the exact physical properties of commercially available particles can be difficult [100]. Thus, for all the acoustofluidic devices herein presented, such particles gather always at the pressure node.

The full explanation of the forces acting on particles in acoustic fields in real systems is still in the making, but the equations herein presented are enough for the scope of this experimental thesis. The interested reader is referred to more recent theoretical [101, 102] and numerical approaches [103, 104, 105] for the most recent advances on the topic, including multi-body dynamics [106, 107] and thermoviscous effects [108].

3.5 Critical radius for acoustophoresis

By looking at Fig. 3.5, one can see that particles with small diameters get dragged along by the acoustic streaming. With increasing size, the particles eventually get (and stay) focused at the pressure node.

This can be explained by the competition of all the forces acting on a particle in a resonating microfluidic channel. The equation of motion for a spherical particle in a fluid-filled micro-resonator can be written as:

$$\frac{4}{3}\pi a^3 \rho_p \partial_t \boldsymbol{v}_\mathrm{p} = \boldsymbol{F}_\mathrm{rad} + \boldsymbol{F}_\mathrm{drag} + \boldsymbol{F}_\mathrm{buoy} \tag{3.14}$$

in which $\boldsymbol{v}_\mathrm{p}$ is the particle velocity, $\boldsymbol{F}_\mathrm{rad}$ is the acoustic radiation force (Eq. 3.12), $\boldsymbol{F}_\mathrm{drag}$ is the Stokes' force (Eq. 2.7), and $\boldsymbol{F}_\mathrm{buoy} = 4/3a^3(\rho_p - \rho_0)\boldsymbol{g}$ is the force due to buoyancy in the fluid, with $\boldsymbol{g}$ representing the gravitational acceleration, acting along the channel height.

By considering only the motion along the channel width, in our experimental work we can often neglect gravity thanks to the orientation of the setup. Further, the particle is assumed to not be affected by the side walls of the channel [99] and to not be influenced by the interactions with other particles [103]. By neglecting inertial terms [82], Eq. 3.14 can be directly solved for the particle velocity:

$$\boldsymbol{v}_\mathrm{p} = \frac{\boldsymbol{F}_\mathrm{rad}}{6\pi\eta a} + \langle \boldsymbol{v}_2 \rangle \tag{3.15}$$

In order to understand if the motion of the particle is dominated either by acoustic radiation force or by acoustic streaming-induced drag, one can compute the ratio between the two forces. By using Eq. 3.12 and 2.7 with the fluid velocity (Eq. 3.9) expressed in terms of the acoustic energy density E_ac (Eq. 3.7), at the channel mid-height ($z = 0$) one can write:

$$\frac{|\boldsymbol{F}_\mathrm{rad}|}{|\boldsymbol{F}_\mathrm{drag}|} = \frac{8}{9}\frac{\Phi a^2 \rho_0 \omega}{\eta} \tag{3.16}$$

When the ratio between the acoustic radiation force and the drag induced by the acoustic streaming equals unity, it means that the motion of the particle is equally influenced by the two forces [109]. By solving Eq. 3.16 for the particle

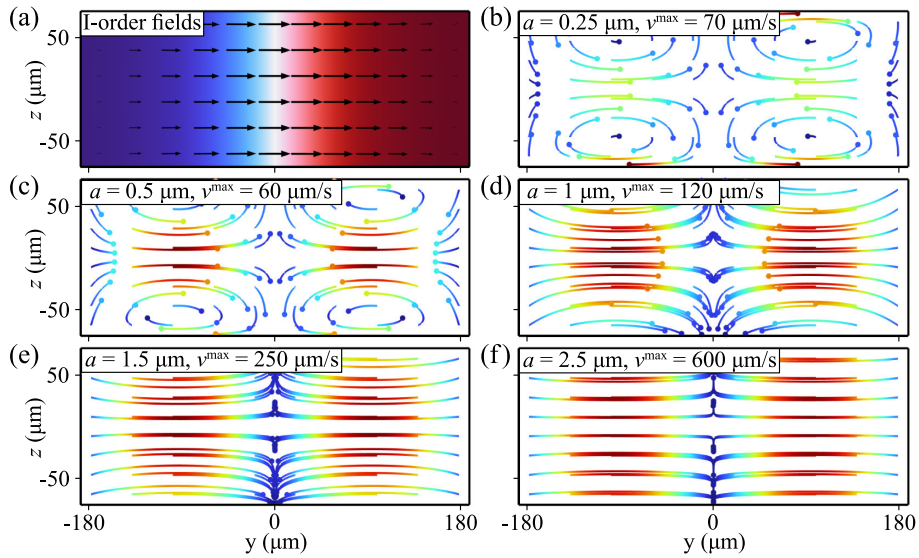

Figure 3.5: Two-dimensional simulation performed in COMSOL Multiphysics [8] for the cross-section of the microfluidic channel geometry used in this thesis' experimental work, i.e. $W = 375$ μm and $H = 150$ μm. (a) First- and (b-f) second-order effects in a water-filled microchannel with a sound standing wave across its width. (a) First-order velocity, depicted by the black arrows, and pressure, from low-blue to high-red. Here they are depicted together, but they are out of phase in time, i.e. $v_1(t = \mathrm{T}/4)$ and $p_1(t = \mathrm{T}/2)$. (b) and (c) depict boundary-driven acoustic streaming for particles of radius 0.25 μm and 0.5 μm, respectively. (d) represents the critical radius at which the particles are almost equally influenced by acoustic streaming and radiation force. (e) and (f) show particles that are well focused in the pressure node, of radius 1.5 μm and 2.5 μm, respectively, moving the faster the larger the particle.

radius:

$$a_c = \sqrt{\frac{9}{8}\frac{\eta}{\Phi\rho_0\omega}} \tag{3.17}$$

in which a_c is the so-called *critical particle radius*. If $a > a_c$, the motion is dominated by the acoustic radiation force. If $a < a_c$, the particle follows the acoustic streaming rolls. For the systems I have used the most during my PhD, namely a chamber filled with water and polystyrene particles in suspension

resonating at 2 MHz, $a_c \approx 1$ µm. Fig. 3.5 exemplifies the transition between the two regimes of motion with increasing particle size. Hence, acoustophoresis separates well particles with $a > a_c$, while smaller particles are more difficult to isolate. This has strong implication for bioparticles processing via acoustic fields [110, 111].

3.6 Acoustic body force

Inhomogeneities in the fluid domain create gradients of acoustic properties, reflected by changes in acoustic impedance of the fluid (∇Z) . In the presence of sound standing waves, the inhomogeneities induce a force acting along these gradients [112]. This is the so-called *acoustic body force* $\boldsymbol{f}_{\text{ac}}$:

$$\boldsymbol{f}_{\text{ac}} = -\frac{1}{4}|p_1|^2\nabla\kappa_0 - \frac{1}{4}|\boldsymbol{v}_1|^2\nabla\rho_0 \tag{3.18}$$

The first term in Eq. 3.18 relates to the first-order pressure and the gradient of compressibility, and it can be thought as the potential energy contribution. Conversely, the second term could be thought of as the kinetic energy contribution, and it is proportional to the first-order velocity and the gradient of density.

One way to introduce inhomogeneities in a microfluidic resonator is to use different solute concentrations of molecules. When flowing in the laminar regime, the fluid with the highest concentration of the solute is relocated at the pressure node once the sound is turned on [113]. The acoustic body force has been shown to be stronger than gravity even at low acoustic energy density and, for any symmetric initial configuration, to make the fluids reach the same organisation in the channel, with the denser medium at the pressure node [112]. This has paved the way to use acoustofluidics to reach size-insensitive cell separation [40]. The cells are moved to their so-called *isoacoustic* point, meaning the position in the gradient where their acoustic contrast factor is zero and they are thus "acoustically transparent". This method has been applied to separate subpopulations of cells in a label-free manner [114, 115] and to enrich circulating tumour cells [116].

Gradients of solutes in a micro-resonator have also been shown to affect acoustic streaming [117]. The acoustic body force originating from the gradient suppresses the streaming in the bulk, leaving only the inner-boundary layer streaming [118]. Streaming suppression has been employed to acoustically focus objects below the critical radius, opening up to sub-micrometre particles acoustophoresis, such as bacteria [45]. Nevertheless, the streaming suppression does not last long in a stationary system. First, diffusion is a mass-transport phenomenon that cannot be avoided, and it thus inevitably dissipates the gradient of solutes. Further, the inner-boundary layer streaming adds an advective term of mass transport, smoothing the gradient and thus reducing the magnitude of the acoustic body force. A weaker acoustic body force entails more acoustic streaming in the fluid bulk, which in turn diminishes the gradient even further. Eventually, the solute spreads homogenously in the whole channel and Rayleigh streaming dominates the fluid motion [119].

An alternative approach to generate inhomogeneities in a microfluidic channel is to employ differential heating. Temperature affects the physical properties of matter. Hence, by having a gradient of temperature inside a resonator, a gradient of acoustic properties can be induced. This phenomenon has been extensively studied for gases [120][121], as it is crucial for various applications, such as thermoacoustic engines [122] and Rijke tubes [123]. Recently, good qualitative agreement has been shown between experimental data [124] and theoretical explanations [125][126] for thermal gradients in gas resonators. The physical properties of water are of course affected by temperature [127][128], Fig. 3.6.

The formulation of the acoustic body force (Eq. 3.18) can be modified to account for inhomogeneities caused by thermal gradients:

$$\boldsymbol{f}_{\text{ac}} = -\frac{1}{4}\Big[|p_1|^2\Big(\frac{\partial \kappa_s}{\partial T}\Big)_{T_0} + |\boldsymbol{v}_1|^2\Big(\frac{\partial \rho}{\partial T}\Big)_{T_0}\Big]\nabla T_0 \tag{3.19}$$

which considers the dependency on temperature of both κ and ρ.

In **Paper I**, we showed how absorption of LED light induces fast fluid recirculation that deforms the Rayleigh streaming, even with gradients as small as 0.5 K/mm [79]. This phenomenon has been termed *thermoacoustic streaming*,

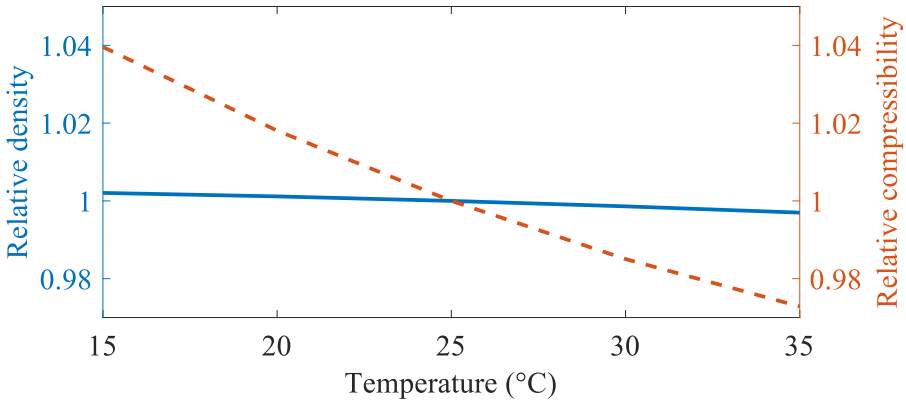

Figure 3.6: Temperature changes affect the physical properties of water. Its density, normalised with its value at 25 °C (solid line, left axis), changes much less than its compressibility, normalised with its value at 25 °C (dashed line, right axis). Data collected at BME department, Lund University.

which is driven by a nondissipative acoustic body force. Its theoretical explanation includes the compressibility terms that had been disregarded with gases, making it applicable to any fluid [129].

This work has been further expanded in our group. The natural follow-up was to confine the absorbed light in a much smaller spot by employing a laser to heat the sample [65]. In **Paper V**, we expanded our understanding of such phenomenon by characterizing the transient behaviour of thermoacoustic streaming, studying its onset and decay. We measured the temperature and the streaming in the channel when turning ON/OFF either the sound or the laser heating.

In **Paper III** we employed heat conduction at the side boundaries of the chip, generating a linear temperature gradient in the channel width. A sound standing wave was applied perpendicular to the thermal gradient, namely along the channel height.

Moreover, in the case of a channel whose walls are made of different materials (e.g., channel etched in silicon with glass lid), a transition from boundary-driven Rayleigh streaming to bulk-driven thermoacoustic streaming can be observed with increasing energy density [130]. This can be explained by the viscous

friction at the walls, where the first-order velocity of the fluid induces energy dissipation, and hence heat, which is differently conducted by the different materials. By increasing the acoustic energy density, the first-order velocity of the fluid also increases, thus increasing the energy dissipation into heat. Therefore, a thermal gradient arises in the channel, as the fluid in contact with the material having the lowest heat conductivity becomes hotter than the rest of the fluid. This phenomenon becomes increasingly important for devices capable of reaching very high acoustic energy.

3.7 Current limitations

Acoustofluidic devices have progressed a lot in recent years. This is both because the theoretical understanding of the phenomena involved has increased, and also because the experimental techniques have greatly improved [46, 48].

Nevertheless, substantial limitations still prevent the wide application of acoustofluidics in the real world. In my opinion, the biggest obstacle is the reliability and consistency of the devices, which is critical for commercial products. Two devices fabricated from identical chips and piezoelectric materials still perform differently. This is due to the complex 3D resonances arising in the assembly, which affect the optimal actuation frequency to achieve the best separation. The most crucial element is the acoustic coupling layer, which assures good mechanical contact between the actuator and the resonator. Further, the physics of the piezoelectric materials is complex [86] and this severely affects the reliability of the models. The electrical and mechanical behaviour of such materials are strongly coupled. Hence, mechanical loading and damping must be precisely accounted for to correctly model the physics of the device at hand. The concept of piezoelectricity and its implications are discussed in more detail in the following chapter 4.1.

Another substantial limitation is the low sample volume that current acoustofluidic devices can process in a time window useful for many biomedical applications. The benchmark of macro-scale techniques, capable of processing millilitres of sample in minutes, requires the throughput of BAW devices to increase at least an order of magnitude to be competitive. Recent publications in our group [131, 132] have shown that it is indeed possible to process samples with throughput high enough to be employed in clinical settings. However,

these studies must be further developed to assess the compatibility with biological samples [133], as well as their reliability in tackling the inevitable patient-to-patient variability in the composition of the analytes.

Last but not least, the temperature in devices employed to process biological samples must be tightly regulated. Since proteins and other organic compounds of interest are notoriously sensitive to heat [134], a few degrees too many could destroy relevant information, falsifying the test results. This will be discussed in more detail below 4.3.

Chapter 4
Mechanical interfaces

In this chapter, I introduce the concept of introducing a structure between the actuator, i.e. the piezoelectric element, and the resonator, i.e. the acoustofluidic chip. Considering it sits in between and needs to convey sound from one to the other, I refer to these structures as *mechanical interfaces*. During my PhD studies, we have explored these interfaces for two main, and separate, reasons: to increase the acoustic energy density and to thermally decouple the acoustofluidic channel from the piezoelectric actuator. After a brief introduction to piezoelectricity and how piezoelectric materials can act as heat sources, I present our studies on mechanical interfaces in the last two sections of this chapter, along with previous related examples in literature.

4.1 Actuators in BAW devices

The mechanical vibrations necessary for acoustofluidic applications are induced using piezoelectric materials. Piezoelectricity is the property of some materials to respond with an electrical field when subjected to mechanical stress (direct piezoelectric effect) and vice-versa (inverse piezoelectric effect). It was first discovered and explained by Pierre and Jacques Curie, who observed how some crystals, such as quartz, generate electric charge when mechanically stressed [135]. Piezoelectricity relies on the non-centrosymmetric structure of the crystals, resulting in a net electric dipole within the structure. When mechanical stress is applied to the structure, it results in a net electric displacement of the charges inside the material, hence inducing an electric field. Ferroelectric materials are usually employed to fabricate ceramics materials used in ultrasound

transducers [136]. The ceramic material is made of a matrix of randomly oriented ferroelectric crystallites, which are then re-oriented by applying a high electric field along a dimension of the structure, i.e. poling treatment. This induces strong orientation of the dipoles in the ceramic material, which then exhibits strong piezoelectric properties [136]. In the experimental work of this thesis, we have used lead zirconate titanate (PZT) as ultrasound actuators, namely a hard-type piezoelectric ceramic (Pz26) [137], poled along its thickness.

The constitutive equations for piezoelectric materials link the mechanical fields (stress and strain) to the electric fields (charge and electric field) [136]. The strain-charge constitutive equations of piezoelectric materials, expressed in tensor notation, are:

$$S_i = s_{ij}^E T_j + d_{im} E_m \tag{4.1a}$$

$$D_l = d_{lj} T_j + \epsilon_{ml}^T E_l \tag{4.1b}$$

in which $(i,j) = 1...6$, $(m,l) = 1...3$, S_i is the mechanical strain, T_j is the mechanical stress, E_m is the electric field, and D_l is the electric displacement field. s_{ij}^E is the elastic compliance under constant electric field, ϵ_{ml}^T is the dielectric permittivity under constant mechanical stress, and $d_{im} = d'_{lj}$ is the piezoelectric charge constant of the material.

The efficiency in converting electrical energy to mechanical energy for a piezoelectric material can be quantified via the electromechanical coupling factor k:

$$k^2 = \frac{d^2}{s^E \epsilon^T} \tag{4.2}$$

which describes the energy conversion in the different directions of the piezoelectric material. As an example, for the thickness-mode $k_{33}^2 = d_{33}^2 / s_{33}^E \epsilon_{33}^T$ and for a transverse-mode $k_{31}^2 = d_{31}^2 / s_{11}^E \epsilon_{33}^T$.

Losses in piezoelectric materials

Real piezoelectric materials are of course subjected to energy losses, which can be accounted for by introducing complex values for the material properties in

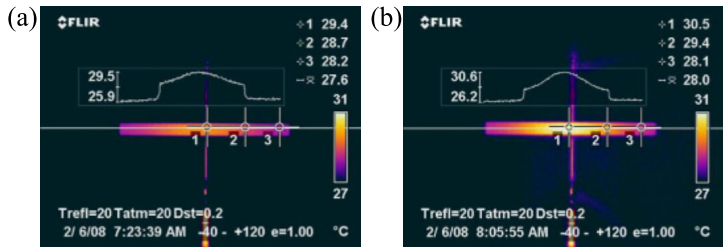

Figure 4.1: Infrared thermography of a PZT plate, driven under the same vibration velocity at (a) resonance and (b) antiresonance. Figure adapted from [139], ©(2009) by the Japanese Society of Applied Physics.

the constitutional equations (Eq. 4.1) [138]:

$$\hat{\epsilon}^T = \epsilon^T(1 - i\tan\zeta) \tag{4.3a}$$

$$\hat{s}^E = s^E(1 - i\tan\phi) \tag{4.3b}$$

$$\hat{d} = d(1 - i\tan\theta) \tag{4.3c}$$

in which $i = \sqrt{-1}$, ζ is the phase difference between electric displacement and applied electric field, ϕ is the phase difference between strain and applied stress, and θ is the phase difference between strain and applied electric field. The mechanical losses can be written also as a function of the mechanical quality factor Q_{m} (Eq. 3.5), i.e. $\tan\phi = 1/Q_{\mathrm{m}}$. All energy losses will eventually be dissipated into heat, meaning that a piezoelectric element will produce heat when actuated [139]. The heat generation is also dependent on the vibration mode of the piezoelectric material, especially when applying high electrical power, Fig.4.1. Moreover, all the losses in piezoelectric materials depend on the temperature, internal stresses, and the applied electrical power to the material at hand [140, 141, 142].

The reader interested in deepening this topic is referred to these publications [143, 141, 138, 144].

In conclusion, it is preferable to have piezoelectric materials with high Q_{m}-factor to drive BAW devices. However, the vibration mode of the actuator should be considered as well. For example, materials with a lower Q_{m}-factor but a higher ratio k_{33}/k_{31} could have vibration modes closer to an ideal thickness

mode, thus oscillating in a way more helpful to excite a standing wave in the micro-resonator. Further, the material properties of piezoelectric materials provided by the manufacturer are usually measured under very low applied power. For intermediate and high applied power, they can change quite dramatically, resulting in a Q_{m}-factor much lower than stated in the material specifications [145, 142]. These issues have been discussed in a recent study by my co-supervisor Wei Qiu [131]. Moreover, the shape and structure of the transducer itself can help obtain a vibration mode closer to the ideal thickness mode. For example, kerfing the piezoelectric material is an established technique that helps reduce its lateral mode of vibration [146]. A recent publication also explores how slanted transducers can effectively suppress such unwanted vibrations in the piezoelectric elements, resulting in more energy being converted into resonances useful to excite standing waves in the fluid cavity [147].

4.2 Need for high acoustic energy density devices

A high energy density in the acoustofluidic device can be an effective solution to tackle the low throughput that has generally characterized acoustofluidic devices so far. By increasing the acoustic energy density inside the microchannel, stronger radiation forces arise and thus acoustic focusing completes in a much shorter time. This implies that the flow rate can be increased, as it is this parameter that decides for how long the objects in suspension are subjected to the acoustic field when travelling over the actuation zone.

Several approaches can be used to achieve higher energy density inside a micro-resonator, among which tailoring the positioning of the channel in the bulk of the device [148] and optimizing the actuation scheme [149]. During my PhD, we wanted to use a hard material to be placed in between the actuator(s) and the resonator, whose dimensions and shape helped to induce strong vibration inside the resonator.

Previous studies have shown how to employ slanted transducers to couple piezoelectric plates much bigger than the microfluidic chip [150]. With a setup able to tune the angle of incidence of the transducer relative to the microfluidic chip, it was found that the acoustophoretic pattern inside the fluid cavity was heavily dependent on the incident angle [151]. However, the acoustic energy density in such devices was rather low, showing the need to optimise such

designs to deliver more energy into the fluid domain.

In **Paper II** [132], we investigated a double-parabolic ultrasonic reflector that coupled two large piezoelectric elements to a much smaller microfluidic chip. The main idea was to use the big parabola to focus longitudinal waves onto its focal point, and then use a small parabola, which had the same focal point, but opposite concavity, to redirect the sound waves as plane waves onto the microfluidic chip, Fig. 4.2. This concept had been explored previously with various versions of an axisymmetric device [152], which, for example, was used for tissue ablation [153], haemolysis [154], and nanoparticles cluster manipulation [155].

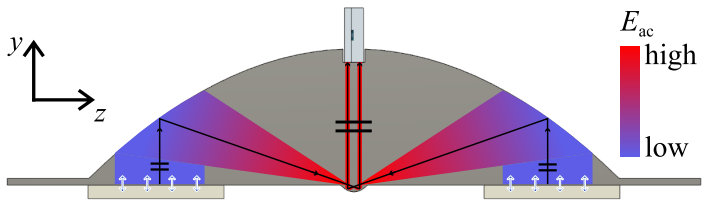

Figure 4.2: Drawing of the concept underlying the initial hypothesis for the double-parabolic ultrasonic reflector we employed in **Paper II**. Two PZTs excite mechanical plane waves that enter the metallic structure. The plane waves are then re-directed to the focal point of the big parabola. The small parabola, sharing the same geometrical focus, converts the focus sound waves back into plane waves and directs them onto the microfluidic chip glued on top. Figure adapted from [156], with permission of the Acoustofluidic Society.

I believe that these types of ultrasound resonators/concentrators, capable of delivering high acoustic vibration amplitude in the MHz range, have the potential to better the performance of BAW acoustofluidic devices. Nevertheless, in **Paper II** we also showed that the initial hypothesis that implied the focusing of longitudinal waves was not sufficiently rigorous, as we concluded that transverse waves play a significant role in building the resonating behaviour of the parabolic structure. Hence, more research is needed to identify and optimize designs, materials, and structures suitable to deliver clean and strong vibrations onto the microfluidic chip.

4.3 Need for temperature-controlled devices

As discussed in section 4.1, the actuators we commonly employ in BAW acoustofluidic devices dissipate energy as heat. This can be an issue since temperature increases can damage the biological sample to be processed. Further, the device temperature affects the resonance inside the channel, as it changes the physical properties of the device [157, 158]. Recent publications showcase several approaches to achieve temperature-controlled BAW acoustofluidics by cooling the piezoelectric element via either Peltier elements [159, 160] or forced air convection [161]. Nevertheless, these devices do not account for the possible heat that can be conducted directly to the chip from the piezoelectric element, which is a ceramic material with poor heat conductivity, to the fluidic chamber. Thus temperature regulation of the back surface of the piezoelectric element may be less efficient than regulation via a mechanical interface.

This has been previously accounted for only in a few publications. Grenvall et al placed a block made of aluminium in between the piezoelectric actuator and the chip [162]. The metal acted as a heat sink, thus preventing heat from reaching the fluidic cavity. However, the temperature of the device was not actively regulated. Ohlin et al showed a liquid-cooled device capable of actively regulating the temperature of the chip within ± 0.2 °C from the set temperature [163]. Their well-engineered device was rather complex though, employing an aluminium housing to allow the cooling liquid to flow between the piezoelectric actuator and the microfluidic chip. Such a complex load on the piezoelectric element affects the overall device performance. Hence, to maximize the acoustic energy density in the channel, we hypothesized that the mass and complexity of the layer interposed between the actuator and the resonator should be minimized.

In **Paper IV** we showed such a device, with a thin sheet of copper interposed between the piezoelectric element and the microfluidic chip. With a Peltier element in thermal contact with the copper, we could control the temperature of the chip by placing a thermo-sensitive resistor on top of the chip and using a feedback loop to the Peltier to keep it stable. The device showed very good temperature stability on the chip at set temperatures between 25 °C and 37 °C, with the measured temperature varying less than 0.2 °C.

With this setup, we could assure consistent and robust performance of the device at a wide range of flowrates and applied electrical powers. This design is far from perfect. First, as we measure the temperature at one single location on the chip, we cannot account for uneven heating inside the piezoelectric element. Second, even though the copper sheet we used is rather thin (~ 130 µm), the impedance of the PZT-copper assembly is not matched with its load. This means that there is room for several improvements for such a design to deliver even better performance and increased thermal stability.

Chapter 5

Summary of included papers

In this chapter, I summarise the journal articles included in this thesis. For each, I focus on the most relevant results and what we learned from the project. **Papers I**, **III**, and **V** pertain to thermoacoustics, while **Papers II** and **IV** present two novel mechanical interfaces linking the PZT to the chip. General conclusions for these main topics can be found in the following chapter, Ch.6.

Paper I. Fast Microscale Acoustic Streaming Driven by a Temperature-Gradient-Induced Nondissipative Acoustic Body Force

This work focused on studying the thermoacoustic streaming arising when the fluid in a micro-resonator is heated via the absorption of LED light. We characterised the flow via particle tracking and the temperature field via heat-dependent fluorescence. We validated the thermoacoustic theory by comparing the experimental results with three-dimensional numerical models, which were in excellent agreement.

The resulting thermoacoustic streaming was found to be a markedly three-dimensional phenomenon, Fig. 5.1(a-e). This work confirmed the theoretical description of the effects of fluid inhomogeneities via the acoustic body force for a temperature-induced change in the physical properties. Moreover, according to the simulation results, we showed that a temperature gradient as small as 0.5 K/mm is enough for thermoacoustic streaming to outcompete boundary-driven Rayleigh streaming.

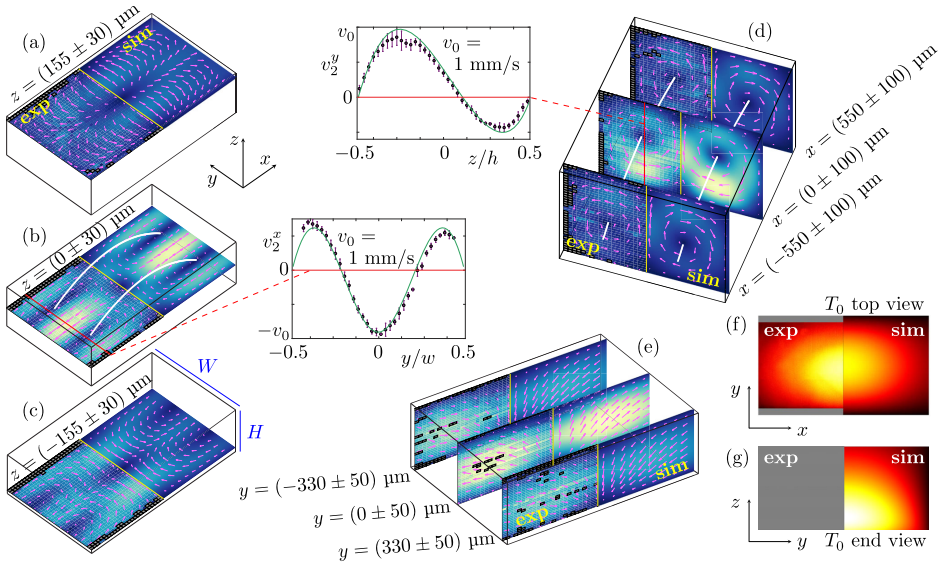

Figure 5.1: (a-e) Measured (exp) and simulated (sim) velocity field for a temperature gradient of 9.76 K/mm. The pairs of white curves represent the centrelines of the counterrotating streaming rolls. The inserts show the velocity profiles (purple dots-exp, green-sim) along the red lines in the plots. (a-c) Flow velocity in the xy plane averaged along the height of thin slabs at the (a) top, (b) middle, and (c) bottom sections of the channel. (d) Flow velocity in the yz plane averaged along the length-direction of the channel in three thin sections. (e) Flow velocity in the xz plane averaged along the width-direction of the channel in three thin sections. (f, g) Temperature map from 25.0 °C (black) to 30.1 °C (white) in the xy plane, but in the yz plane no experimental data was available. Figure from [79], ©(2021) by the American Physical Society.

Paper II. High-energy-density acoustofluidic device using a double parabolic ultrasonic transducer

In this study, we aimed at inducing very strong sound fields inside a microchannel using a different approach compared to classic BAW devices. We employed a metallic double-parabolic reflector to harvest vibrational energy from two large piezoelectric transducers, actuated at constant voltage, Fig. 5.2 . We demonstrated focusing of 5-µm polystyrene particles at a flow rate of 5 ml/min, corresponding to a time-of-flight of ≈ 13.5 ms in the actuated area. We then investigated the acoustic field at the frequency leading to the best focusing, Fig. 5.3. Even though the acoustic energy density was not uniform along the channel, the device indeed reached very high energy values, Fig. 5.3(c).

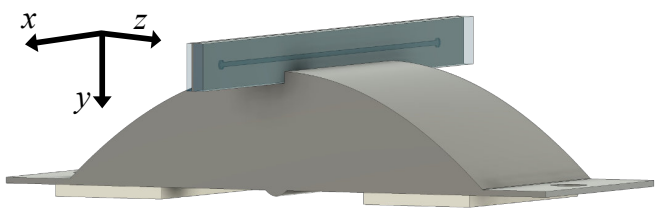

Figure 5.2: Rendering of the aluminium double parabolic reflector, with two large PZT at the bottom. A microfluidic chip is glued on top in side-actuation configuration.

Moreover, we investigated the working mechanism of the double-parabolic reflector via two-dimensional finite element simulations and laser Doppler vibrometry (LDV). The initial hypothesis entailed the focusing of longitudinal waves from the piezoelectric elements onto the microfluidic chip due to the opposite concavity and large size difference of the two parabolas. However, by comparing simulation and LDV data, we showed that also transverse waves do have an important role in the resonance of the structure.

In summary, the double-parabolic reflector we presented here was capable of exciting strong sound fields in the channel, as we reported the highest value for acoustic energy density in literature as of today. This gives encouraging

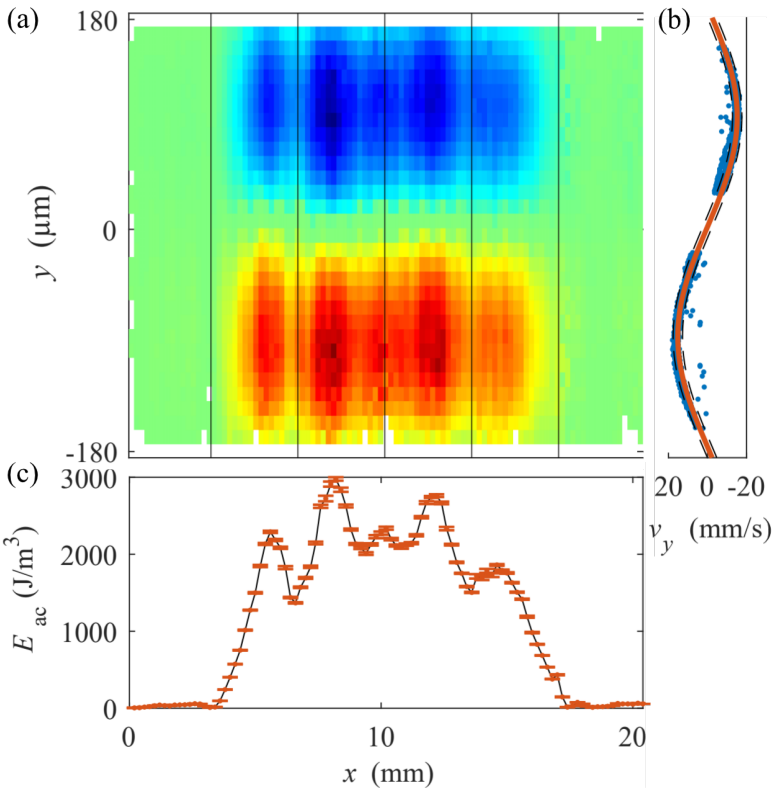

Figure 5.3: (a) 4.9-µm PS particles focusing at the mid-height of the channel, from dark blue (-30 mm/s) to dark red (30 mm/s). (b) Particle velocities (blue dots) along a 0.2-mm section of the channel length. By estimating their sinusoidal fitting (solid orange line), the energy density in each 0.2-mm beam can be calculated. The 95% confidence interval for the fitting is shown by the dashed black lines. (c) Acoustic energy density along the 20-mm-long actuated area of the channel. For each data point, the 95% confidence interval is represented by the orange error bars (overlapping for most of them). Figure from [132].

indications that an optimised mechanical interface would lead to even better performance.

Paper III. Thermoacoustic streaming in a linear temperature gradient

This work showed the interplay of orthogonal sound and temperature fields. With a custom-made setup, shown in Fig. 5.4, we could impose a stable temperature across the internal sidewalls of a microchannel.

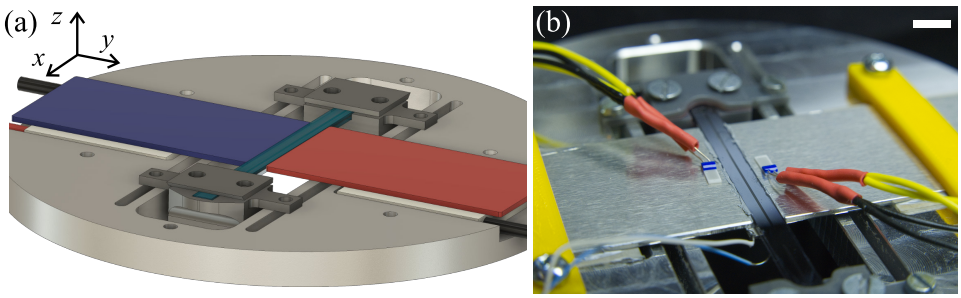

Figure 5.4: Generating a linear temperature gradient across an acoustofluidic microchannel. (a) Rendering of the experimental setup. By controlling the temperature of two aluminium plates placed in thermal contact with the side of the chip, we can generate and maintain a temperature gradient across the microfluidic chip. (b) Photograph of the device mounted on the microscope holder (scale bar is 5 mm).

A standing wave was then excited along the channel height, and we measured the resulting thermoacoustic streaming in three dimensions via particle tracking. The observed thermoacoustic streaming in the channel cross-section was up to 30 times faster than natural convection, Fig. 5.5(b,d).

Even though we did not observe an ideal acoustic field in the channel, our simple finite-element model could capture the pattern of the thermoacoustic streaming that we measured in experiments. However, the numerical simulation could not explain the measured change in temperature inside the channel once the sound was active, Fig. 5.5(a,c).

This work further validated the thermoacoustic theory based on the acoustic body force. Moreover, the decreased temperature difference between the side walls when the sound was on offers good opportunities for designing acoustically-

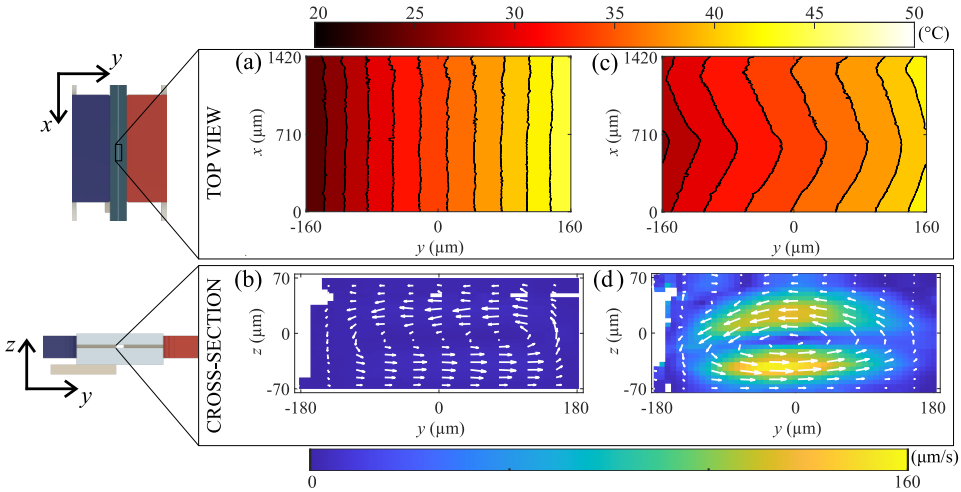

Figure 5.5: Measured (a, c) temperature and (b, d) velocity fields, for (a, b) only temperature gradient condition and (c, d) thermoacoustic streaming. The linear temperature gradient (a) gets deformed when the acoustic field is introduced (c). Black isolines show 2 °C intervals. With only temperature, the fluid flow is rather slow, as it is driven by natural convection (b), while thermoacoustic streaming is ~ 30 times faster (d).

aided heat exchangers. Further studies are needed to investigate the feasibility of this concept and the interplay between acoustic and heat exchange at the micro-scale.

Paper IV. Preliminary investigation report: Simple temperature-controlled device for robust bulk acoustic wave acoustofluidics

This study explores a relatively simple solution to regulate the temperature on an acoustofluidic chip. We controlled the temperature using a Peltier element in thermal contact at one end of a thin copper sheet ($\sim$ 130 µm), while the other end was glued between the chip and the piezoelectric elements, Fig. 5.6. By controlling the Peltier element with a thermo-electric cooler, we could maintain the temperature of the chip at a set level (± 0.2 °C) at various combinations of flowrates and applied electrical powers.

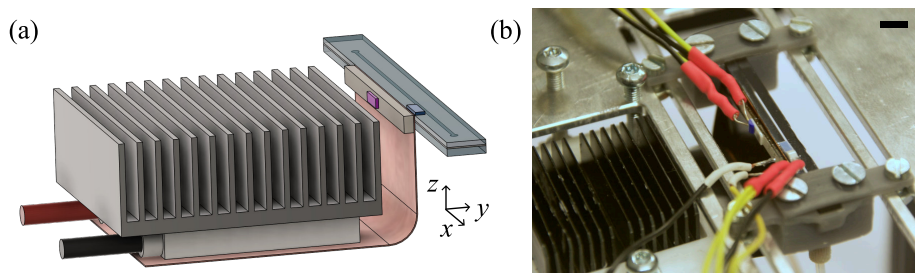

Figure 5.6: Temperature controlled acoustofluidic device. (a) Rendering of the essential parts of the device: a single-inlet, single-outlet microfluidic chip attached to a piezoelectric element, with a thin sheet of copper in between. A Peltier element, placed in thermal contact with the bent copper, allows for regulation of the temperature on the chip. A heat sink (black) helps maintain the Peltier element performance. Thermoresistant probes (blue and magenta) measure the temperature on the chip and the piezoelectric element, respectively. (b) Picture of the device mounted on its microscope holder. The copper sheet is covered with insulating tape to minimize heat exchange with the surrounding ambient air. 3D-printed parts (gray) allow for fluid connection into the chip. The two thermo-sensitive probes are glued on the chip (as close as possible to the copper sheet, without touching it) and on the piezoelectric element. The Peltier element is below a heat sink (black) and it is controlled by a ThermoElectric Cooler that has the probe on the chip as feedback. Scale bar is 5 mm.

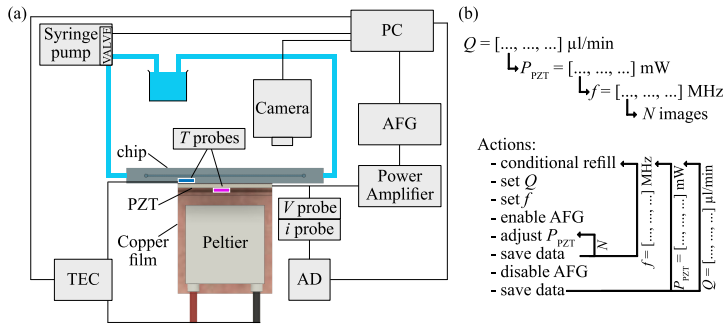

Figure 5.7: (a) Block diagram of the experimental setup, for which a LabView program controls the automated data acquisition. The blue and magenta squares represent the resistance temperature detectors that monitor the temperature on the chip and PZT, respectively. The probe on the chip acts as a target temperature sensor for the temperature controller (TEC). AFG: Arbitrary Function Generator; AD: Analog Discovery, oscilloscope; TEC: ThermoElectric Cooler. (b) Hierarchical diagram of the experiments and actions taken by the LabVIEW program.

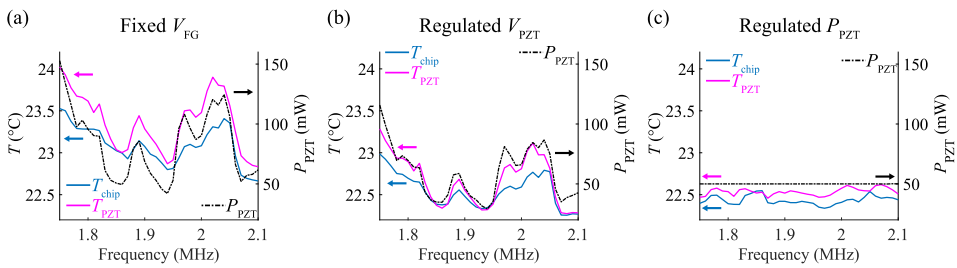

Figure 5.8: Different electrical excitation methods: (a) constant voltage from the function generator; (b) regulated voltage over the PZT; (c) regulated electrical power on the PZT. The temperature variation strongly correlates with the applied electrical power.

With our automated experimental setup, Fig. 5.7, we first showed how constant power is the preferred actuation mode for BAW acoustofluidic devices, especially to achieve constant operating temperature, Fig. 5.8. Moreover, we confirmed that temperature strongly influences the resonance inside the channel.

Paper V. Thermoacoustic streaming around a temporally modulated temperature gradient

With this work, we expanded the characterization of thermoacoustic streaming. We generated a confined temperature gradient by laser heating in a small spot close to the channel side wall and we excited a standing wave along its width. We measured the onset and decay of thermoacoustic streaming by having either the sound or laser turned on (and then off) while maintaining the other field constantly on. We then compared the experimental data with a 3D finite-element simulation.

We showed how the thermoacoustic streaming arises (and decays) faster when the laser heating is constant and the sound is turned on (and off), compared to having constant sound and the laser turned on (and off), Fig. 5.9. This is due to the longer time scale for the thermal gradient to be fully established.

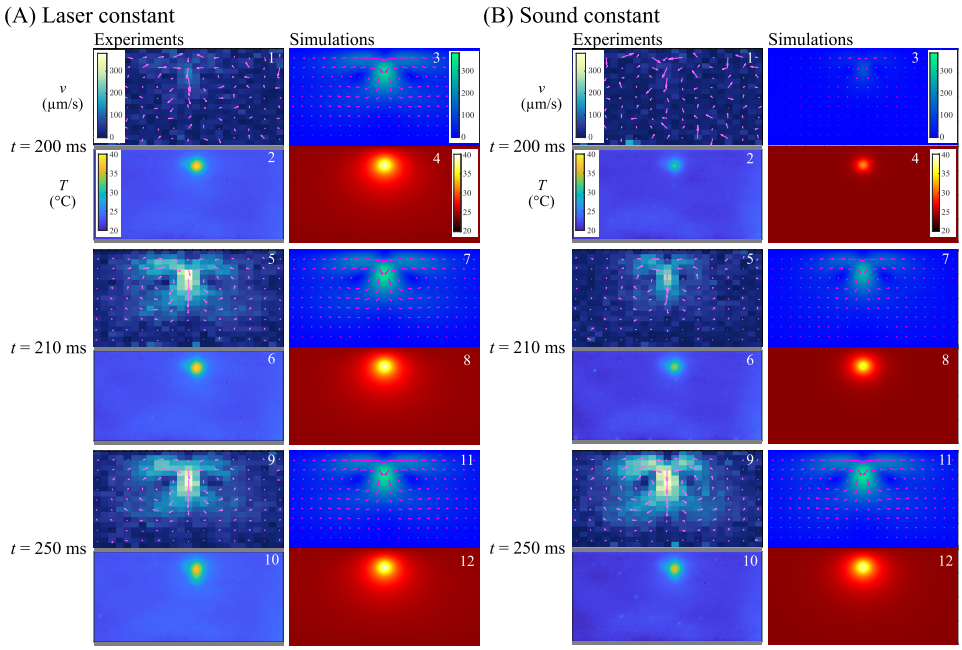

Figure 5.9: (A) Laser constant and sound on at $t = 200$ ms. Left column shows measured data for velocity (panels 1, 5, and 9) and temperature (panels 2,6, and 10). Right column shows simulation results analogously. The results are shown for three frames, $t = 200, 210, 250$ ms and the thermoacoustic field is fully developed at $t = 210$ ms. (B) Sound constant and laser ON at $t = 200$ ms. Left column shows measured data for velocity (panels 1,5, and 9) and temperature (panels 2,6, and 10). Right column shows simulation results analogously. The results are shown for three frames, $t = 200, 210, 250$ ms and the thermoacoustic field is fully developed at $t = 250$ ms.

Chapter 6
Conclusions and outlook

During my PhD studies I have been mainly investigating thermal effects in bulk acoustic wave devices for acoustofluidic applications. Nowadays acoustofluidics has started to be integrated in laboratory equipments, with a few notable examples [164, 165]. Nevertheless, the optimised acoustofluidic device we envisioned at the beginning of my PhD remains a dream still. So, there are a few considerations I would like to make, along with some suggestions for future investigations that build on what we found in these years. In this chapter, I present what I consider the most important conclusions of my PhD journey and some open issues I believe are crucial to the acoustofluidic community for the years to come.

6.1 Thermoacoustics

We have contributed to establishing the theory for thermoacoustic streaming, validating numerical models with experiments and showing how it can arise in different conditions (**Papers I**, **III**, and **V**).

I think thermoacoustic effects play a significant role in the working mechanisms of acoustofluidic devices. This is because heat is inevitably generated in any process of energy dissipation. It happens inside the piezoelectric material acting as an actuator, as discussed in 4.1. It happens also in the fluid itself, especially at the boundaries parallel to the wave propagation direction [130]. This latter phenomenon will become more significant in the near future, when devices capable of higher energy densities become more common. Considering

thermoacoustic effects is of utmost importance to optimize such devices, and more investigations are necessary to conceptualize strategies to avoid it affecting the separation capabilities of acoustofluidic devices. A quick solution for this would be to use the same material for the whole chip, for example, whole-glass devices. However, this would not prevent the liquid from heating the glass close to the fluidic chamber, thus still creating a localized temperature gradient.

Thermoacoustics has indeed potential in the biomedical field, where it could be used to achieve even faster and simpler flow cytometry (as outlined in **Paper V**) or employed for fast mixing in reactions where temperature is tightly regulated, such as even faster polymerase chain reaction. Furthermore, I think it could also be useful in other industrial sectors. For example, it could potentially increase the heat transfer in heat exchangers, hence reducing the need for powerful pumps and complex designs, as we outlined in **Paper III**. This would make the devices more compact and more easily applicable in extreme conditions, such as CubeSat and other space-related applications [166]. Another potential application, fundamental in this era of electrification, is the charging process of lithium-ion batteries. Acoustic streaming has already been shown to aid charging, making it faster and increasing the lifetime of the battery [167, 168]. Considering the inevitable Joule effects in these systems, the design of such acoustically assisted charging could be greatly improved by including thermoacoustic theory.

6.2 Mechanical interfaces

As a PhD student, I have also built a few different mechanical interfaces to be placed between the actuator (piezoelectric elements) and the resonator (microfluidic chip). We showed that these structures can indeed help us reach very high energy density inside the microchannel and that they also prevent unwanted heating from affecting the acoustofluidic performance of the device.

Paper II showed one of our successful attempts in using such interfaces to achieve high acoustic energy density inside the channel. However, as we conclude in the publication, this design is not optimised, as it comprises several unwanted modes of vibration that dissipate energy and thus do not contribute

to the resonance in the channel. Our collaborators at the University of Tokyo, led by prof. Morita, are now investigating new designs that can focus only transverse waves onto the chip [169]. I hope they will eventually succeed in building a more compact and powerful mechanical interface compared to what we have already done.

Moreover, when I was in Tokyo hosted by prof. Nakamura at the Tokyo Institute of Technology, I have also investigated the use of horns to excite acoustic fields. Unsurprisingly, almost every shape I used was leading to some sort of resonance inside the channel, though with different degrees of efficiency and performance. In fact, no horn design that I tried could compare with the simple and elegant solution of gluing the piezoelectric transducer directly on the side of the chip. Nevertheless, I still think that horns or similar designs would be potentially useful for achieving strong and uniform sound fields inside microfluidic channels. However, due to the high frequency, classic approaches in horn theory cannot be directly applied, thus making it necessary to use iterative design aided by computational models to prototype devices. Employing machine learning or genetic algorithms would be extremely beneficial to tackle such problems where no analytical solutions can be derived. Furthermore, horns offer the possibility of backing, stacking, and clamping the piezoelectric materials, potentially enabling better energy extraction from the actuators.

The simplest mechanical interface I have used, shown in **Paper IV**, was also the most surprising to me. By simply placing a thin sheet of copper in between the piezoelectric element and the chip, we could precisely control the temperature of the system and thus make the separation process robust and stable over a wide range of flowrates and applied powers. With this work, we have further confirmed how much temperature can affect the resonance inside the channel and that more electrical power does not always correlate with better performance. The simple design we proposed offers a great solution to perform acoustofluidic applications at controlled temperatures, which is indeed important in biomedical applications, and that can also be significant for various industrial processes. Future work should focus on matching the acoustic impedance of the copper-piezo assembly itself and with the chip, which could greatly improve the device efficiency. Further, by combining this concept

with backing, better thermal regulation of the piezoelectric material itself would be possible. This, together with the more efficient resonance of the whole structure, should lead to radically improved performance of temperature-controlled acoustofluidic devices, whilst maintaining low electrical power consumption.

6.3 Reflections

I would like to conclude by stressing the importance of integrating knowledge across different fields. In a multidisciplinary discipline such as acoustofluidics, it is necessary to juggle various expertise to reach satisfactory device performance. Many publications have already stressed the importance of matching the electrical impedance of the driving circuit with the piezoelectric elements. However, this aspect is often overlooked in published works, including my own. Furthermore, there is an immense expertise regarding transducers from which the whole community could benefit. I am thinking of all the experiences in building ultrasonic motors and actuators, as well as the fascinating field of biomedical ultrasound, especially the devices used for treatment such as ablation and lithotripsy. From these, we could learn not only how to shape the acoustic field according to the intended application, but also how to better match acoustically the transducers with their load.

Last but not least, I feel that acoustofluidics would greatly benefit from creating standards applicable across the various fields where it is employed. By reporting the same values in all experiments, such as temperature and applied electrical power, comparisons will be much easier to make between different devices and the strengths and weaknesses of the experiments at hand could be better assessed by the community. Acoustofluidics has experienced a booming growth in the last two decades and it is time for it to mature into an established scientific field. In my opinion, especially from an experimentalist point of view, it comes down to creating standards for reporting and assessing the various experiments performed. It will not be easy to create a uniform culture in such a diverse field, but I think it will be a necessary step for translating acoustofluidics from a mere research tool into technology fully deployable in the real world.

I am a simple experimentalist, but I am grateful to having played my part in the effort to finding a unifying theory of acoustofluidics. This theory, which is

still in the making, relies only on the shape of the acoustic field and the material properties of the domain, including the fluid and any suspended objects. By only applying body forces based on differences in acoustic properties and boundary conditions, every phenomenon happening in an acoustic resonator could be explained, from acoustic streaming to fluid relocation, up to acoustic radiation force. I believe that the more experiments and specific theories align, the closer we will get to this unifying mathematical description of all acoustofluidic effects.

I have indeed learned a lot, and I have even learned that it is not possible to learn everything, and to make peace with it. A wise man once told me "They have already invented the wheel, just use it". I have here developed a few new spokes, and I hope they can become part of new wheels that people will use in the future.

References

[1] M. Van Dyke. *An Album of Fluid Motion*. An Album of Fluid Motion. Parabolic Press, 1982. ISBN: 9780915760022.

[2] S. C. Terry, J. H. Jerman, and J. B. Angell. "A gas chromatographic air analyzer fabricated on a silicon wafer". In: *IEEE Transactions on Electron Devices* 26.12 (1979), pp. 1880–1886. ISSN: 0018-9383. DOI: 10.1109/t-ed.1979.19791. URL: https://dx.doi.org/10.1109/t-ed.1979.19791.

[3] A. Manz, N. Graber, and H. M. Widmer. "Miniaturized total chemical analysis systems: A novel concept for chemical sensing". In: *Sensors and Actuators B: Chemical* 1.1 (1990), pp. 244–248. ISSN: 0925-4005. DOI: https://doi.org/10.1016/0925-4005(90)80209-I. URL: https://www.sciencedirect.com/science/article/pii/092540059080209I.

[4] A. T. Woolley and R. A. Mathies. "Ultra-high-speed DNA fragment separations using microfabricated capillary array electrophoresis chips". In: *Proceedings of the National Academy of Sciences* 91.24 (1994), pp. 11348–11352. ISSN: 0027-8424. DOI: 10.1073/pnas.91.24.11348. URL: https://dx.doi.org/10.1073/pnas.91.24.11348.

[5] Eric T. Lagally, Charles A. Emrich, and Richard A. Mathies. "Fully integrated PCR-capillary electrophoresis microsystem for DNA analysis". In: *Lab on a Chip* 1.2 (2001), p. 102. ISSN: 1473-0197. DOI: 10.1039/b109031n. URL: https://dx.doi.org/10.1039/b109031n.

[6] Neil Convery and Nikolaj Gadegaard. "30 years of microfluidics". In: *Micro and Nano Engineering* 2 (2019), pp. 76–91. ISSN: 2590-0072. DOI: https://doi.org/10.1016/j.mne.2019.01.003. URL: https://www.sciencedirect.com/science/article/pii/S2590007219300036.

[7] Henrik Bruus. *Theoretical Microfluidics*. Oxford University Press, 2008. ISBN: 978–0–19–923509–4.

[8] COMSOL. *COMSOL Multiphysics 6.2*. Web Page. URL: https://www.comsol.com/.

[9] R. Byron Bird, Warren E. Stewart, and Edwin N. Lightfoot. *Transport Phenomena, Revised 2nd Edition*. John Wiley & Sons, Inc., 2006. ISBN: 978-0-470-11539-8.

[10] Paul Yager, Thayne Edwards, Elain Fu, Kristen Helton, Kjell Nelson, Milton R. Tam, and Bernhard H. Weigl. "Microfluidic diagnostic technologies for global public health". In: *Nature* 442.7101 (2006), pp. 412–418. ISSN: 0028-0836. DOI: 10.1038/nature05064. URL: https://dx.doi.org/10.1038/nature05064.

[11] Tianlong Zhang, Dino Di Carlo, Chwee Teck Lim, Tianyuan Zhou, Guizhong Tian, Tao Tang, Amy Q. Shen, Weihua Li, Ming Li, Yang Yang, Keisuke Goda, Ruopeng Yan, Cheng Lei, Yoichiroh Hosokawa, and Yaxiaer Yalikun. "Passive microfluidic devices for cell separation". In: *Biotechnology Advances* 71 (2024), p. 108317. ISSN: 0734-9750. DOI: https://doi.org/10.1016/j.biotechadv.2024.108317. URL: https://www.sciencedirect.com/science/article/pii/S0734975024000119.

[12] Di Huang, Jiaxiang Man, Di Jiang, Jiyun Zhao, and Nan Xiang. "Inertial microfluidics: Recent advances". In: *ELECTROPHORESIS* 41.24 (2020), pp. 2166–2187. ISSN: 0173-0835. DOI: 10.1002/elps.202000134. URL: https://dx.doi.org/10.1002/elps.202000134.

[13] Dino Di Carlo. "Inertial microfluidics". In: *Lab on a Chip* 9.21 (2009), p. 3038. ISSN: 1473-0197. DOI: 10.1039/b912547g. URL: https://dx.doi.org/10.1039/b912547g.

[14] Majid Ebrahimi Warkiani, Andy Kah Ping Tay, Guofeng Guan, and Jongyoon Han. "Membrane-less microfiltration using inertial microfluidics". In: *Scientific Reports* 5.1 (2015), p. 11018. ISSN: 2045-2322. DOI: 10.1038/srep11018. URL: https://dx.doi.org/10.1038/srep11018.

[15] Joseph M. Martel and Mehmet Toner. "Inertial Focusing in Microfluidics". In: *Annual Review of Biomedical Engineering* 16.1 (2014), pp. 371–396. ISSN: 1523-9829. DOI: 10.1146/annurev-bioeng-121813-120704. URL: https://dx.doi.org/10.1146/annurev-bioeng-121813-120704.

[16] Lotien Richard Huang, Edward C. Cox, Robert H. Austin, and James C. Sturm. "Continuous Particle Separation Through Deterministic Lateral Displacement". In: *Science* 304.5673 (2004). doi: 10.1126/science.1094567, pp. 987–990. DOI: 10.1126/science.1094567. URL: https://doi.org/10.1126/science.1094567.

[17] Axel Hochstetter, Rohan Vernekar, Robert H. Austin, Holger Becker, Jason P. Beech, Dmitry A. Fedosov, Gerhard Gompper, Sung-Cheol Kim, Joshua T. Smith, Gustavo Stolovitzky, Jonas O. Tegenfeldt, Benjamin H. Wunsch, Kerwin K. Zeming, Timm Krüger, and David W. Inglis. "Deterministic Lateral Displacement: Challenges and Perspectives". In: *ACS Nano* 14.9 (2020), pp. 10784–10795. ISSN: 1936-0851. DOI: 10.1021/acsnano.0c05186. URL: https://dx.doi.org/10.1021/acsnano.0c05186.

[18] Alexander Zhbanov, Ye Sung Lee, and Sung Yang. "Current status and further development of deterministic lateral displacement for micro-particle separation". In: *Micro and Nano Systems Letters* 11.1 (2023). ISSN: 2213-9621. DOI: 10.1186/s40486-023-00175-w. URL: https://dx.doi.org/10.1186/s40486-023-00175-w.

[19] Izabella Bouhid De Aguiar and Karin Schroën. "Microfluidics Used as a Tool to Understand and Optimize Membrane Filtration Processes". In: *Membranes* 10.11 (2020), p. 316. ISSN: 2077-0375. DOI: 10.3390/membranes10110316. URL: https://dx.doi.org/10.3390/membranes10110316.

[20] T. Van De Laar, S. Ten Klooster, K. Schroën, and J. Sprakel. "Transition-state theory predicts clogging at the microscale". In: *Scientific Reports* 6.1 (2016), p. 28450. ISSN: 2045-2322. DOI: 10.1038/srep28450. URL: https://dx.doi.org/10.1038/srep28450.

[21] Shosaku Nomura, Narendra N. Tandon, Takashi Nakamura, James Cone, Shirou Fukuhara, and Junichi Kambayashi. "High-shear-stress-induced activation of platelets and microparticles enhances expression of cell adhesion molecules in THP-1 and endothelial cells". In: *Atherosclerosis* 158.2 (2001), pp. 277–287. ISSN: 0021-9150. DOI: https://doi.org/10.1016/S0021-9150(01)00433-6. URL: https://www.sciencedirect.com/science/article/pii/S0021915001004336.

[22] Heng-Dong Xi, Hao Zheng, Wei Guo, Alfonso M. Gañán-Calvo, Ye Ai, Chia-Wen Tsao, Jun Zhou, Weihua Li, Yanyi Huang, Nam-Trung Nguyen, and Say Hwa Tan. "Active droplet sorting in microfluidics: a review". In: *Lab on a Chip* 17.5 (2017), pp. 751–771. ISSN: 1473-0197. DOI: 10.1039/c6lc01435f. URL: https://dx.doi.org/10.1039/c6lc01435f.

[23] Muthusaravanan Sivaramakrishnan, Ram Kothandan, Deenadayalan Karaiyagowder Govindarajan, Yogesan Meganathan, and Kumaravel Kandaswamy. "Active microfluidic systems for cell sorting and separation". In: *Current Opinion in Biomedical Engineering* 13 (2020), pp. 60–68. ISSN: 2468-4511. DOI: https://doi.org/10.1016/j.cobme.2019.09.014. URL: https://www.sciencedirect.com/science/article/pii/S2468451119300492.

[24] Hui Yan and Hongkai Wu. "Magnetophoresis". In: *Encyclopedia of Microfluidics and Nanofluidics*. Ed. by Dongqing Li. Boston, MA: Springer US, 2008, pp. 1043–1048. ISBN: 978-0-387-48998-8. DOI: 10.1007/978-0-387-48998-8_847. URL: https://doi.org/10.1007/978-0-387-48998-8_847.

[25] Fadi Alnaimat, Sawsan Dagher, Bobby Mathew, Ali Hilal Alnqbi, and Saud Khashan. "Microfluidics Based Magnetophoresis: A Review". In: *The Chemical Record* 18.11 (2018), pp. 1596–1612. ISSN: 1527-8999. DOI: 10.1002/tcr.201800018. URL: https://dx.doi.org/10.1002/tcr.201800018.

[26] Ki-Ho Han and A. Bruno Frazier. "Paramagnetic capture mode magnetophoretic microseparator for high efficiency blood cell separations". In: *Lab Chip* 6.2 (2006), pp. 265–273. ISSN: 1473-0197. DOI: 10.1039/b514539b. URL: https://dx.doi.org/10.1039/b514539b.

[27] Brian D. Plouffe, Madhumita Mahalanabis, Laura H. Lewis, Catherine M. Klapperich, and Shashi K. Murthy. "Clinically Relevant Microfluidic Magnetophoretic Isolation of Rare-Cell Populations for Diagnostic and Therapeutic Monitoring Applications". In: *Analytical Chemistry* 84.3 (2012). doi: 10.1021/ac2022844, pp. 1336–1344. ISSN: 0003-2700. DOI: 10.1021/ac2022844. URL: https://doi.org/10.1021/ac2022844.

[28] Khashayar Khoshmanesh, Saeid Nahavandi, Sara Baratchi, Arnan Mitchell, and Kourosh Kalantar-zadeh. "Dielectrophoretic platforms for bio-microfluidic systems". In: *Biosensors and Bioelectronics* 26.5 (2011), pp. 1800–1814. ISSN: 0956-5663. DOI: https://doi.org/10.1016/j.bios.2010.09.022. URL: https://www.sciencedirect.com/science/article/pii/S0956566310006366.

[29] Nurhaslina Abd Rahman, Fatimah Ibrahim, and Bashar Yafouz. "Dielectrophoresis for Biomedical Sciences Applications: A Review". In: *Sensors* 17.3 (2017), p. 449. ISSN: 1424-8220. DOI: 10.3390/s17030449. URL: https://dx.doi.org/10.3390/s17030449.

[30] Jiafeng Yao, Guiping Zhu, Tong Zhao, and Masahiro Takei. "Microfluidic device embedding electrodes for dielectrophoretic manipulation of cells A review". In: *ELECTROPHORESIS* 40.8 (2019), pp. 1166–1177. ISSN: 0173-0835. DOI: 10.1002/elps.201800440. URL: https://dx.doi.org/10.1002/elps.201800440.

[31] Joseph S. Heyman. *Acoustophoresis method and apparatus*. US Patent - 5,147,562|NASA-CASE-LAR-13388-1. 15 Sep 1992. URL: https://ntrs.nasa.gov/citations/19920024367.

[32] Leslie Y. Yeo and James R. Friend. "Surface Acoustic Wave Microfluidics". In: *Annual Review of Fluid Mechanics* 46.Volume 46, 2014 (2014), pp. 379–406. ISSN: 1545-4479. DOI: https://doi.org/10.1146/annurev-fluid-010313-141418. URL: https://www.annualreviews.org/content/journals/10.1146/annurev-fluid-010313-141418.

[33] Xiaoyun Ding, Peng Li, Sz-Chin Steven Lin, Zackary S. Stratton, Nitesh Nama, Feng Guo, Daniel Slotcavage, Xiaole Mao, Jinjie Shi, Francesco Costanzo, and Tony Jun Huang. "Surface acoustic wave microfluidics". In: *Lab on a Chip* 13.18 (2013), p. 3626. ISSN: 1473-0197. DOI: 10.1039/c3lc50361e. URL: https://dx.doi.org/10.1039/c3lc50361e.

[34] Byung Hang Ha, Kang Soo Lee, Ghulam Destgeer, Jinsoo Park, Jin Seung Choung, Jin Ho Jung, Jennifer Hyunjong Shin, and Hyung Jin Sung. "Acoustothermal heating of polydimethylsiloxane microfluidic system". In: *Scientific Reports* 5.1 (2015), p. 11851. ISSN: 2045-2322. DOI: 10.1038/srep11851. URL: https://dx.doi.org/10.1038/srep11851.

[35] Thomas Laurell, Filip Petersson, and Andreas Nilsson. "Chip integrated strategies for acoustic separation and manipulation of cells and particles". In: *Chem. Soc. Rev.* 36.3 (2007), pp. 492–506. ISSN: 0306-0012. DOI: 10.1039/b601326k. URL: https://dx.doi.org/10.1039/b601326k.

[36] Rayisa P. Moiseyenko and Henrik Bruus. "Whole-System Ultrasound Resonances as the Basis for Acoustophoresis in All-Polymer Microfluidic Devices". In: *Physical Review Applied* 11.1 (2019). ISSN: 2331-7019. DOI: 10.1103/physrevapplied.11.014014. URL: https://dx.doi.org/10.1103/physrevapplied.11.014014.

[37] Per Augustsson. "On microchannel acoustophoresis - Experimental considerations and life science applications". PhD Thesis. Lund University, 2011.

[38] Cecilia Magnusson, Per Augustsson, Andreas Lenshof, Yvonne Ceder, Thomas Laurell, and Hans Lilja. "Clinical-Scale Cell-Surface-Marker Independent Acoustic Microfluidic Enrichment of Tumor Cells from Blood". In: *Analytical Chemistry* 89.22 (2017). doi: 10.1021/acs.analchem.7b01458, pp. 11954–11961. ISSN: 0003-2700. DOI: 10.1021/acs.analchem.7b01458. URL: https://doi.org/10.1021/acs.analchem.7b01458.

[39] Per Augustsson and Thomas Laurell. "Acoustofluidics 11: Affinity specific extraction and sample decomplexing using continuous flow acoustophoresis". In: *Lab on a Chip* 12.10 (2012), p. 1742. ISSN: 1473-0197. DOI: 10.1039/c2lc40200a. URL: https://dx.doi.org/10.1039/c2lc40200a.

[40] Per Augustsson, Jonas T. Karlsen, Hao-Wei Su, Henrik Bruus, and Joel Voldman. "Iso-acoustic focusing of cells for size-insensitive acousto-mechanical phenotyping". In: *Nature Communications* 7.1 (2016), p. 11556. ISSN: 2041-1723. DOI: 10.1038/ncomms11556. URL: https://doi.org/10.1038/ncomms11556.

[41] Stephen S. Adler, Emmanuel C. Nyong, Raisa A. Glabman, Peter L. Choyke, and Noriko Sato. "Cell radiolabeling with acoustophoresis cell washing". In: *Scientific Reports* 12.1 (2022), p. 9125. ISSN: 2045-2322. DOI: 10.1038/s41598-022-13144-x. URL: https://doi.org/10.1038/s41598-022-13144-x.

[42] Klara Petersson, Ola Jakobsson, Pelle Ohlsson, Per Augustsson, Stefan Scheding, Johan Malm, and Thomas Laurell. "Acoustofluidic hematocrit determination". In: *Analytica Chimica Acta* 1000 (2018), pp. 199–204. ISSN: 0003-2670. DOI: https://doi.org/10.1016/j.aca.2017.11.037. URL: https://www.sciencedirect.com/science/article/pii/S0003267017313156.

[43] Andreas Lenshof, Asilah Ahmad-Tajudin, Kerstin Järås, Ann-Margret Swärd-Nilsson, Lena Åberg, György Marko-Varga, Johan Malm, Hans Lilja, and Thomas Laurell. "Acoustic Whole Blood Plasmapheresis Chip for Prostate Specific Antigen Microarray Diagnostics". In: *Analytical Chemistry* 81.15 (2009). doi: 10.1021/ac9013572, pp. 6030–6037. ISSN: 0003-2700. DOI: 10.1021/ac9013572. URL: https://doi.org/10.1021/ac9013572.

[44] Cecilia Magnusson, Per Augustsson, Eva Undvall Anand, Andreas Lenshof, Andreas Josefsson, Karin Welén, Anders Bjartell, Yvonne Ceder, Hans Lilja, and Thomas Laurell. "Acoustic Enrichment of Heterogeneous Circulating Tumor Cells and Clusters from Metastatic Prostate Cancer Patients". In: *Analytical Chemistry* 96.18 (2024). doi: 10.1021/acs.analchem.3c05371, pp. 6914–6921. ISSN: 0003-2700. DOI: 10.1021/acs.analchem.3c05371. URL: https://doi.org/10.1021/acs.analchem.3c05371.

[45] David Van Assche, Elisabeth Reithuber, Wei Qiu, Thomas Laurell, Birgitta Henriques-Normark, Peter Mellroth, Pelle Ohlsson, and Per Augustsson. "Gradient acoustic focusing of sub-micron particles for separation of bacteria from blood lysate". In: *Scientific Reports* 10.1 (2020). ISSN: 2045-2322. DOI: 10.1038/s41598-020-60338-2. URL: https://dx.doi.org/10.1038/s41598-020-60338-2.

[46] Joseph Rufo, Feiyan Cai, James Friend, Martin Wiklund, and Tony Jun Huang. "Acoustofluidics for biomedical applications". In: *Nature Reviews Methods Primers* 2.1 (2022), p. 30. ISSN: 2662-8449. DOI: 10.1038/s43586-022-00109-7. URL: https://doi.org/10.1038/s43586-022-00109-7.

[47] Fria Hossein and Panagiota Angeli. "A review of acoustofluidic separation of bioparticles". In: *Biophysical Reviews* 15.6 (2023), pp. 2005–2025. ISSN: 1867-2450. DOI: 10.1007/s12551-023-01112-2. URL: https://dx.doi.org/10.1007/s12551-023-01112-2.

[48] Reza Rasouli, Karina Martinez Villegas, and Maryam Tabrizian. "Acoustofluidics – changing paradigm in tissue engineering, therapeutics development, and biosensing". In: *Lab on a Chip* 23.5 (2023), pp. 1300–1338. ISSN: 1473-0197. DOI: 10.1039/d2lc00439a. URL: https://dx.doi.org/10.1039/d2lc00439a.

[49] Vincent Miralles, Axel Huerre, Florent Malloggi, and Marie-Caroline Jullien. "A Review of Heating and Temperature Control in Microfluidic Systems: Techniques and Applications". In: *Diagnostics* 3.1 (2013), pp. 33–67. ISSN: 2075-4418. DOI: 10.3390/diagnostics3010033. URL: https://dx.doi.org/10.3390/diagnostics3010033.

[50] Z. E. Jeroish, K. S. Bhuvaneshwari, Fahmi Samsuri, and Vigneswaran Narayanamurthy. "Microheater: material, design, fabrication, temperature control, and applications—a role in COVID-19". In: *Biomedical Microdevices* 24.1 (2022). ISSN: 1387-2176. DOI: 10.1007/s10544-021-00595-8. URL: https://dx.doi.org/10.1007/s10544-021-00595-8.

[51] Alejandro A. Dos-Reis-Delgado, Andrea Carmona-Dominguez, Gerardo Sosa-Avalos, Ivan H. Jimenez-Saaib, Karen E. Villegas-Cantu, Roberto C. Gallo-Villanueva, and Víctor H. Perez-Gonzalez. "Recent advances and challenges in temperature monitoring and control in microfluidic devices". In: *ELECTROPHORESIS* 44.1-2 (2023), pp. 268–297. ISSN: 0173-0835. DOI: https://doi.org/10.1002/elps.202200162. URL: https://doi.org/10.1002/elps.202200162.

[52] Hanbin Mao, Tinglu Yang, and Paul S. Cremer. "A Microfluidic Device with a Linear Temperature Gradient for Parallel and Combinatorial Measurements". In: *Journal of the American Chemical Society* 124.16 (2002). doi: 10.1021/ja017625x, pp. 4432–4435. ISSN: 0002-7863. DOI: 10.1021/ja017625x. URL: https://doi.org/10.1021/ja017625x.

[53] Daniele Vigolo, Roberto Rusconi, Roberto Piazza, and Howard A. Stone. "A portable device for temperature control along microchannels". In: *Lab on a Chip* 10.6 (2010), pp. 795–798. ISSN: 1473-0197. DOI: 10.1039/B919146A. URL: http://dx.doi.org/10.1039/B919146A.

[54] Jean Charles Athanase Peltier. *Nouvelles expériences sur la caloricité des courans électriques*. 1834.

[55] George Maltezos, Matthew Johnston, Konstantin Taganov, Chutatip Srichantaratsamee, John Gorman, David Baltimore, Wasun Chantratita, and Axel Scherer. "Exploring the limits of ultrafast polymerase chain reaction using liquid for thermal heat exchange: A proof of principle". In: *Applied Physics Letters* 97.26 (2010), p. 264101. ISSN: 0003-6951. DOI: 10.1063/1.3530452. URL: https://dx.doi.org/10.1063/1.3530452.

[56] Rosanne M. Guijt, Arash Dodge, Gijs W. K. Van Dedem, Nico F. De Rooij, and Elisabeth Verpoorte. "Chemical and physical processes for integrated temperature control in microfluidic devices". In: *Lab on a Chip* 3.1 (2003), p. 1. ISSN: 1473-0197. DOI: 10.1039/b210629a. URL: https://dx.doi.org/10.1039/b210629a.

[57] George Maltezos, Aditya Rajagopal, and Axel Scherer. "Evaporative cooling in microfluidic channels". In: *Applied Physics Letters* 89.7 (2006), p. 074107. ISSN: 0003-6951. DOI: 10.1063/1.2234318. URL: https://dx.doi.org/10.1063/1.2234318.

[58] Mihai P. Dinca, Marin Gheorghe, Margaret Aherne, and Paul Galvin. "Fast and accurate temperature control of a PCR microsystem with a disposable reactor". In: *Journal of Micromechanics and Microengineering* 19.6 (2009), p. 065009. ISSN: 0960-1317. DOI: 10.1088/0960-1317/19/6/065009. URL: https://dx.doi.org/10.1088/0960-1317/19/6/065009.

[59] Tsung-Min Hsieh, Ching-Hsing Luo, Fu-Chun Huang, Jung-Hao Wang, Liang-Ju Chien, and Gwo-Bin Lee. "Enhancement of thermal uniformity for a microthermal cycler and its application for polymerase chain reaction". In: *Sensors and Actuators B: Chemical* 130.2 (2008), pp. 848–856. ISSN: 0925-4005. DOI: https://doi.org/10.1016/j.snb.2007.10.063. URL: https://www.sciencedirect.com/science/article/pii/S0925400507008842.

[60] Ji Peng, Cifeng Fang, Shen Ren, Jiaji Pan, Yudong Jia, Zhiquan Shu, and Dayong Gao. "Development of a microfluidic device with precise on-chip temperature control by integrated cooling and heating components for single cell-based analysis". In: *International Journal of Heat and Mass Transfer* 130 (2019), pp. 660–667. ISSN: 0017-9310. DOI: https://doi.org/10.1016/j.ijheatmasstransfer.2018.10.135. URL: https://www.sciencedirect.com/science/article/pii/S0017931018323548.

[61] David Issadore, Katherine J. Humphry, Keith A. Brown, Lori Sandberg, David A. Weitz, and Robert M. Westervelt. "Microwave dielectric heating of drops in microfluidic devices". In: *Lab on a Chip* 9.12 (2009), p. 1701. ISSN: 1473-0197. DOI: 10.1039/b822357b. URL: https://dx.doi.org/10.1039/b822357b.

[62] Hanyoup Kim, Siarhei Vishniakou, and Gregory W. Faris. "Petri dish PCR: laser-heated reactions in nanoliter droplet arrays". In: *Lab on a Chip* 9.9 (2009), p. 1230. ISSN: 1473-0197. DOI: 10.1039/b817288a. URL: https://dx.doi.org/10.1039/b817288a.

[63] Junguk Ko and Jae-Chern Yoo. "Non-Contact Temperature Control System Applicable to Polymerase Chain Reaction on a Lab-on-a-Disc". In: *Sensors* 19.11 (2019), p. 2621. ISSN: 1424-8220. DOI: 10.3390/s19112621. URL: https://dx.doi.org/10.3390/s19112621.

[64] Aaron T. Ohta, Arash Jamshidi, Justin K. Valley, Hsan-Yin Hsu, and Ming C. Wu. "Optically actuated thermocapillary movement of gas bubbles on an absorbing substrate". In: *Applied Physics Letters* 91.7 (2007), p. 074103. ISSN: 0003-6951. DOI: 10.1063/1.2771091. URL: https://dx.doi.org/10.1063/1.2771091.

[65] Franziska Martens, Wei Qiu, Ola Jakobsson, Christian Cierpka, Andreas Ehn, and Per Augustsson. "Configurable thermoacoustic streaming by laser-induced temperature gradients". In: *Physical Review Applied* 23.2 (2025). ISSN: 2331-7019. DOI: 10.1103/physrevapplied.23.024043. URL: https://dx.doi.org/10.1103/physrevapplied.23.024043.

[66] Hideyuki F. Arata, Yannick Rondelez, Hiroyuki Noji, and Hiroyuki Fujita. "Temperature Alternation by an On-Chip Microheater To Reveal Enzymatic Activity of -Galactosidase at High Temperatures". In: *Analytical Chemistry* 77.15 (2005). doi: 10.1021/ac050385+, pp. 4810–4814. ISSN: 0003-2700. DOI: 10.1021/ac050385+. URL: https://doi.org/10.1021/ac050385+.

[67] Charlie Gosse, Christian Bergaud, and Peter Löw. "Molecular Probes for Thermometry in Microfluidic Devices". In: Springer Berlin Heidelberg, 2009, pp. 301–341. ISBN: 0303-4216. DOI: 10.1007/978-3-642-04258-4_10. URL: https://dx.doi.org/10.1007/978-3-642-04258-4_10.

[68] J. Massing, D. Kaden, C. J. Kähler, and C. Cierpka. "Luminescent two-color tracer particles for simultaneous velocity and temperature measurements in microfluidics". In: *Measurement Science and Technology* 27.11 (2016), p. 115301. ISSN: 0957-0233. DOI: 10.1088/0957-0233/27/11/115301. URL: https://dx.doi.org/10.1088/0957-0233/27/11/115301.

[69] Steven W. Magennis, Emmelyn M. Graham, and Anita C. Jones. "Quantitative Spatial Mapping of Mixing in Microfluidic Systems". In: *Angewandte Chemie International Edition* 44.40 (2005), pp. 6512–6516. ISSN: 1433-7851. DOI: 10.1002/anie.200500558. URL: https://dx.doi.org/10.1002/anie.200500558.

[70] Richard K. P. Benninger, Yasemin Koç, Oliver Hofmann, Jose Requejo-Isidro, Mark A. A. Neil, Paul M. W. French, and Andrew J. deMello. "Quantitative 3D Mapping of Fluidic Temperatures within Microchannel Networks Using Fluorescence Lifetime Imaging". In: *Analytical Chemistry* 78.7 (2006). doi: 10.1021/ac051990f, pp. 2272–2278. ISSN: 0003-2700. DOI: 10.1021/ac051990f. URL: https://doi.org/10.1021/ac051990f.

[71] David-A. Mendels, Emmelyn M. Graham, Steven W. Magennis, Anita C. Jones, and François Mendels. "Quantitative comparison of thermal and solutal transport in a T-mixer by FLIM and CFD". In: *Microfluidics and Nanofluidics* 5.5 (2008), pp. 603–617. ISSN: 1613-4982. DOI: 10.1007/s10404-008-0269-5. URL: https://dx.doi.org/10.1007/s10404-008-0269-5.

[72] Carosena Meola and Giovanni M. Carlomagno. "Recent advances in the use of infrared thermography". In: *Measurement Science and Technology* 15.9 (2004), R27–R58. ISSN: 0957-0233. DOI: 10.1088/0957-0233/15/9/r01. URL: https://dx.doi.org/10.1088/0957-0233/15/9/r01.

[73] G. A. Bennett and S. D. Briles. "Calibration procedure developed for IR surface-temperature measurements". In: *IEEE Transactions on Components, Hybrids, and Manufacturing Technology* 12.4 (1989), pp. 690–695. ISSN: 0148-6411. DOI: 10.1109/33.49034. URL: https://dx.doi.org/10.1109/33.49034.

[74] Christophe Pradere, Mathieu Joanicot, Jean-Christophe Batsale, Jean Toutain, and Christophe Gourdon. "Processing of temperature field in chemical microreactors with infrared thermography". In: *Quantitative InfraRed Thermography Journal* 3.1 (2006), pp. 117–135. ISSN: 1768-6733. DOI: 10.3166/qirt.3.117-135. URL: https://dx.doi.org/10.3166/qirt.3.117-135.

[75] Takatoki Yamamoto, Teruo Fujii, and Takahiko Nojima. "PDMS–glass hybrid microreactor array with embedded temperature control device. Application to cell-free protein synthesis". In: *Lab Chip* 2.4 (2002), pp. 197–202. ISSN: 1473-0197. DOI: 10.1039/b205010b. URL: https://dx.doi.org/10.1039/b205010b.

[76] Kelly Swinney and Darryl J. Bornhop. "Noninvasive picoliter volume thermometry based on backscatter interferometry". In: *ELECTROPHORESIS* 22.10 (2001), pp. 2032–2036. ISSN: 0173-0835. DOI: 10.1002/1522-2683(200106)22:10<2032::aid-elps2032>3.0.co;2-1. URL: https://dx.doi.org/10.1002/1522-2683(200106)22:10<2032::aid-elps2032>3.0.co;2-1.

[77] Michael N. Kammer, Amanda K. Kussrow, and Darryl J. Bornhop. "Longitudinal pixel averaging for improved compensation in backscattering interferometry". In: *Optics Letters* 43.3 (2018), pp. 482–485. DOI: 10.1364/OL.43.000482. URL: https://opg.optica.org/ol/abstract.cfm?URI=ol-43-3-482.

[78] Katherine L. Saenger and Julie Gupta. "Laser interferometric thermometry for substrate temperature measurement". In: *Applied Optics* 30.10 (1991), pp. 1221–1226. DOI: 10.1364/AO.30.001221. URL: https://opg.optica.org/ao/abstract.cfm?URI=ao-30-10-1221.

[79] Wei Qiu, Jonas Helboe Joergensen, Enrico Corato, Henrik Bruus, and Per Augustsson. "Fast Microscale Acoustic Streaming Driven by a Temperature-Gradient-Induced Nondissipative Acoustic Body Force". In: *Physical Review Letters* 127.6 (2021). PRL, p. 064501. DOI: 10.1103/PhysRevLett.127.064501. URL: https://link.aps.org/doi/10.1103/PhysRevLett.127.064501.

[80] L.E. Kinsler, A.R. Frey, A.B. Coppens, and J.V. Sanders. *Fundamentals of Acoustics*. Fourth Edition. John Wiley & Sons, Inc., 2000. ISBN: 9780471847892.

[81] L.D. Landau and E.M. Lifshitz. *Fluid Mechanics: Course of Theoretical Physics, Volume 6*. Second Edition. Pergamon, 1987. ISBN: 978-0-08-033933-7.

[82] Rune Barnkob. "Physics of microparticle acoustophoresis: bridging theory and experiment". PhD Thesis. Technical University of Denmark, 2012.

[83] Peter Muller Tribler. "Acoustic streaming in microchannels: the trinity of analytics, numerics and experiments". PhD Thesis. Technical University of Denmark, 2015.

[84] Jonas Helboe Jørgensen. "Theory and modeling of thermoviscous acoustofluidics". PhD Thesis. Technical University of Denmark, 2022.

[85] Henrik Bruus. "Acoustofluidics 2: Perturbation theory and ultrasound resonance modes". In: *Lab Chip* 12.1 (2012), pp. 20–28. ISSN: 1473-0197. DOI: 10.1039/c1lc20770a. URL: https://dx.doi.org/10.1039/c1lc20770a.

[86] Jurg Dual and Dirk Möller. "Acoustofluidics 4: Piezoelectricity and application in the excitation of acoustic fields for ultrasonic particle manipulation". In: *Lab on a Chip* 12.3 (2012), p. 506. ISSN: 1473-0197. DOI: 10.1039/c1lc20913b. URL: https://dx.doi.org/10.1039/c1lc20913b.

[87] Jürg Dual, Philipp Hahn, Ivo Leibacher, Dirk Möller, and Thomas Schwarz. "Acoustofluidics 6: Experimental characterization of ultrasonic particle manipulation devices". In: *Lab on a Chip* 12.5 (2012), p. 852. ISSN: 1473-0197. DOI: 10.1039/c2lc21067c. URL: https://dx.doi.org/10.1039/c2lc21067c.

[88] Björn Hammarström, Mikael Evander, Jacob Wahlström, and Johan Nilsson. "Frequency tracking in acoustic trapping for improved performance stability and system surveillance". In: *Lab on a Chip* 14.5 (2014), pp. 1005–1013. ISSN: 1473-0197. DOI: 10.1039/C3LC51144H. URL: http://dx.doi.org/10.1039/C3LC51144H.

[89] Valentina Vitali, Giulia Core, Fabio Garofalo, Thomas Laurell, and Andreas Lenshof. "Differential impedance spectra analysis reveals optimal actuation frequency in bulk mode acoustophoresis". In: *Scientific Reports* 9.1 (2019). ISSN: 2045-2322. DOI: 10.1038/s41598-019-55333-1. URL: https://dx.doi.org/10.1038/s41598-019-55333-1.

[90] L. Rayleigh. "I. On the circulation of air observed in Kundt's tubes, and on some allied acoustical problems". In: *Philosophical Transactions of the Royal Society of London* 175.0 (1884), pp. 1–21. ISSN: 0261-0523. DOI: 10.1098/rstl.1884.0002. URL: https://dx.doi.org/10.1098/rstl.1884.0002.

[91] H. Schlichting. "Berechnung ebener periodischer Grenzschichtstromungen". In: *Phys. Z.* 33 (1932), pp. 327–335. URL: https://ci.nii.ac.jp/naid/10010463225/en/.

[92] Sir James Lighthill. "Acoustic streaming". In: *Journal of Sound and Vibration* 61.3 (1978), pp. 391–418. ISSN: 0022-460X. DOI: https://doi.org/10.1016/0022-460X(78)90388-7. URL: https://www.sciencedirect.com/science/article/pii/0022460X78903887.

[93] Peter Barkholt Muller and Henrik Bruus. "Numerical study of thermoviscous effects in ultrasound-induced acoustic streaming in microchannels". In: *Physical Review E* 90.4 (2014). PRE, p. 043016. DOI: 10.1103/PhysRevE.90.043016. URL: https://link.aps.org/doi/10.1103/PhysRevE.90.043016.

[94] Jacob S. Bach and Henrik Bruus. "Theory of pressure acoustics with viscous boundary layers and streaming in curved elastic cavities". In: *The Journal of the Acoustical Society of America* 144.2 (2018), pp. 766–784. DOI: 10.1121/1.5049579. URL: https://asa.scitation.org/doi/abs/10.1121/1.5049579.

[95] L. V. King. “On the acoustic radiation pressure on spheres”. In: *Proceedings of the Royal Society of London. Series A - Mathematical and Physical Sciences* 147.861 (1934), pp. 212–240. ISSN: 0080-4630. DOI: 10.1098/rspa.1934.0215. URL: https://dx.doi.org/10.1098/rspa.1934.0215.

[96] K. Yosioka and Y. Kawasima. “Acoustic radiation pressure on a compressible sphere”. In: *Acta Acustica united with Acustica* 5.3 (1955), pp. 167–173.

[97] Gorkov. “On the forces acting on a small particle in an acoustical field in an ideal fluid”. In: *Soviet Physics - Doklady* 6.9 (1962).

[98] Mikkel Settnes and Henrik Bruus. “Forces acting on a small particle in an acoustical field in a viscous fluid”. In: *Physical Review E* 85.1 (2012). ISSN: 1539-3755. DOI: 10.1103/physreve.85.016327. URL: https://dx.doi.org/10.1103/physreve.85.016327.

[99] Rune Barnkob, Per Augustsson, Thomas Laurell, and Henrik Bruus. “Acoustic radiation- and streaming-induced microparticle velocities determined by microparticle image velocimetry in an ultrasound symmetry plane”. In: *Physical Review E* 86.5 (2012). PRE, p. 056307. DOI: 10.1103/PhysRevE.86.056307. URL: https://link.aps.org/doi/10.1103/PhysRevE.86.056307.

[100] Alexander Edthofer, Jakub Novotny, Andreas Lenshof, Thomas Laurell, and Thierry Baasch. “Acoustofluidic Properties of Polystyrene Microparticles”. In: *Analytical Chemistry* 95.27 (2023), pp. 10346–10352. ISSN: 0003-2700. DOI: 10.1021/acs.analchem.3c01156. URL: https://dx.doi.org/10.1021/acs.analchem.3c01156.

[101] Glauber T. Silva and Henrik Bruus. “Acoustic interaction forces between small particles in an ideal fluid”. In: *Physical Review E* 90.6 (2014). ISSN: 1539-3755. DOI: 10.1103/physreve.90.063007. URL: https://dx.doi.org/10.1103/physreve.90.063007.

[102] Blake E. Simon and Mark F. Hamilton. “Analytical solution for acoustic radiation force and torque on a spheroid near a rigid or free planar boundary”. In: *The Journal of the Acoustical Society of America* 156.2 (2024), pp. 1269–1282. ISSN: 0001-4966. DOI: 10.1121/10.0028165. URL: https://dx.doi.org/10.1121/10.0028165.

[103] Mikkel W. H. Ley and Henrik Bruus. “Continuum modeling of hydrodynamic particle–particle interactions in microfluidic high-concentration suspensions”. In: *Lab on a Chip* 16.7 (2016), pp. 1178–1188. ISSN: 1473-0197. DOI: 10.1039/c6lc00150e. URL: https://dx.doi.org/10.1039/c6lc00150e.

[104] Thierry Baasch and Jürg Dual. “Acoustofluidic particle dynamics: Beyond the Rayleigh limit”. In: *The Journal of the Acoustical Society of America* 143.1 (2018), pp. 509–519. ISSN: 0001-4966. DOI: 10.1121/1.5021339. URL: https://dx.doi.org/10.1121/1.5021339.

[105] Thierry Baasch, Alen Pavlic, and Jürg Dual. "Acoustic radiation force acting on a heavy particle in a standing wave can be dominated by the acoustic microstreaming". In: *Physical Review E* 100.6 (2019). PRE, p. 061102. DOI: 10.1103/PhysRevE.100.061102. URL: https://link.aps.org/doi/10.1103/PhysRevE.100.061102.

[106] Thierry Baasch, Ivo Leibacher, and Jürg Dual. "Multibody dynamics in acoustophoresis". In: *The Journal of the Acoustical Society of America* 141.3 (2017), pp. 1664–1674. ISSN: 0001-4966. DOI: 10.1121/1.4977030. URL: https://dx.doi.org/10.1121/1.4977030.

[107] Melody X. Lim, Bryan Vansaders, and Heinrich M. Jaeger. "Acoustic manipulation of multi-body structures and dynamics". In: *Reports on Progress in Physics* 87.6 (2024), p. 064601. ISSN: 0034-4885. DOI: 10.1088/1361-6633/ad43f9. URL: https://dx.doi.org/10.1088/1361-6633/ad43f9.

[108] Bjørn G. Winckelmann and Henrik Bruus. "Acoustic radiation force on a spherical thermoviscous particle in a thermoviscous fluid including scattering and microstreaming". In: *Phys. Rev. E* 107 (6 2023), p. 065103. DOI: 10.1103/PhysRevE.107.065103. URL: https://link.aps.org/doi/10.1103/PhysRevE.107.065103.

[109] Henrik Bruus. "Acoustofluidics 10: Scaling laws in acoustophoresis". In: *Lab on a Chip* 12.9 (2012), p. 1578. ISSN: 1473-0197. DOI: 10.1039/c2lc21261g. URL: https://dx.doi.org/10.1039/c2lc21261g.

[110] Maria Antfolk and Thomas Laurell. "Continuous flow microfluidic separation and processing of rare cells and bioparticles found in blood – A review". In: *Analytica Chimica Acta* 965 (2017), pp. 9–35. ISSN: 0003-2670. DOI: https://doi.org/10.1016/j.aca.2017.02.017. URL: https://www.sciencedirect.com/science/article/pii/S0003267017302337.

[111] Michael Gerlt, Thierry Baasch, Amal Nath, Wei Qiu, Andreas Lenshof, and Thomas Laurell. "Acoustofluidic Blood Component Sample Preparation and Processing in Medical Applications". In: *Applications of Microfluidic Systems in Biology and Medicine*. Ed. by Manabu Tokeshi. Singapore: Springer Nature Singapore, 2024, pp. 1–55. ISBN: 978-981-97-6540-9. DOI: 10.1007/978-981-97-6540-9_1. URL: https://doi.org/10.1007/978-981-97-6540-9_1.

[112] Jonas T. Karlsen, Per Augustsson, and Henrik Bruus. "Acoustic Force Density Acting on Inhomogeneous Fluids in Acoustic Fields". In: *Physical Review Letters* 117.11 (2016). ISSN: 0031-9007. DOI: 10.1103/physrevlett.117.114504. URL: https://dx.doi.org/10.1103/physrevlett.117.114504.

[113] Sameer Deshmukh, Zbigniew Brzozka, Thomas Laurell, and Per Augustsson. "Acoustic radiation forces at liquid interfaces impact the performance of acoustophoresis". In: *Lab Chip* 14.17 (2014), pp. 3394–3400. ISSN: 1473-0197. DOI: 10.1039/c4lc00572d. URL: https://dx.doi.org/10.1039/c4lc00572d.

[114] Mahdi Rezayati Charan and Per Augustsson. “Acoustophoretic Characterization and Separation of Blood Cells in Acoustic Impedance Gradients”. In: *Physical Review Applied* 20.2 (2023). ISSN: 2331-7019. DOI: 10.1103/physrevapplied.20.024066. URL: https://dx.doi.org/10.1103/physrevapplied.20.024066.

[115] Julia Alsved, Mahdi Rezayati Charan, Pelle Ohlsson, Anke Urbansky, and Per Augustsson. “Label-free separation of peripheral blood mononuclear cells from whole blood by gradient acoustic focusing”. In: *Scientific Reports* 14.1 (2024). ISSN: 2045-2322. DOI: 10.1038/s41598-024-59156-7. URL: https://dx.doi.org/10.1038/s41598-024-59156-7.

[116] Cecilia Magnusson, Mahdi Rezayati Charan, and Per Augustsson. “Two-Step Acoustic Cell Separation Based on Cell Size and Acoustic Impedance□toward Isolation of Viable Circulating Tumor Cells”. In: *Analytical Chemistry* 97.4 (2025). doi: 10.1021/acs.analchem.4c04911, pp. 2120–2126. ISSN: 0003-2700. DOI: 10.1021/acs.analchem.4c04911. URL: https://doi.org/10.1021/acs.analchem.4c04911.

[117] Jonas T. Karlsen, Wei Qiu, Per Augustsson, and Henrik Bruus. “Acoustic Streaming and Its Suppression in Inhomogeneous Fluids”. In: *Physical Review Letters* 120.5 (2018). ISSN: 0031-9007. DOI: 10.1103/physrevlett.120.054501. URL: https://dx.doi.org/10.1103/physrevlett.120.054501.

[118] Wei Qiu, Jonas T. Karlsen, Henrik Bruus, and Per Augustsson. “Experimental Characterization of Acoustic Streaming in Gradients of Density and Compressibility”. In: *Physical Review Applied* 11.2 (2019). ISSN: 2331-7019. DOI: 10.1103/physrevapplied.11.024018. URL: https://dx.doi.org/10.1103/physrevapplied.11.024018.

[119] Wei Qiu, Henrik Bruus, and Per Augustsson. “Particle-size-dependent acoustophoretic motion and depletion of micro- and nano-particles at long timescales”. In: *Physical Review E* 102.1 (2020). ISSN: 2470-0045. DOI: 10.1103/physreve.102.013108. URL: https://dx.doi.org/10.1103/physreve.102.013108.

[120] P. Vainshtein, M. Fichman, and C. Gutfinger. “Acoustic enhancement of heat transfer between two parallel plates”. In: *International Journal of Heat and Mass Transfer* 38.10 (1995), pp. 1893–1899. ISSN: 0017-9310. DOI: https://doi.org/10.1016/0017-9310(94)00299-B. URL: https://www.sciencedirect.com/science/article/pii/001793109400299B.

[121] Michael W. Thompson, Anthony A. Atchley, and Michael J. Maccarone. “Influences of a temperature gradient and fluid inertia on acoustic streaming in a standing wave”. In: *The Journal of the Acoustical Society of America* 117.4 (2005), pp. 1839–1849. ISSN: 0001-4966. DOI: 10.1121/1.1859992. URL: https://dx.doi.org/10.1121/1.1859992.

[122] Islam A. Ramadan, Hélène Bailliet, and Jean-Christophe Valière. "Experimental investigation of the influence of natural convection and end-effects on Rayleigh streaming in a thermoacoustic engine". In: *The Journal of the Acoustical Society of America* 143.1 (2018), pp. 361–372. DOI: 10.1121/1.5021331. URL: https://asa.scitation.org/doi/abs/10.1121/1.5021331.

[123] K. T. Feldman. "Review of the literature on Rijke thermoacoustic phenomena". In: *Journal of Sound and Vibration* 7.1 (1968), pp. 83–89. ISSN: 0022-460X. DOI: https://doi.org/10.1016/0022-460X(68)90159-4. URL: https://www.sciencedirect.com/science/article/pii/0022460X68901594.

[124] Guillaume Michel and Christophe Gissinger. "Cooling by Baroclinic Acoustic Streaming". In: *Physical Review Applied* 16.5 (2021). PRAPPLIED, p. L051003. DOI: 10.1103/PhysRevApplied.16.L051003. URL: https://link.aps.org/doi/10.1103/PhysRevApplied.16.L051003.

[125] Guillaume Michel and Gregory P. Chini. "Strong wave–mean-flow coupling in baroclinic acoustic streaming". In: *Journal of Fluid Mechanics* 858 (2019), pp. 536–564. ISSN: 0022-1120. DOI: 10.1017/jfm.2018.785. URL: https://dx.doi.org/10.1017/jfm.2018.785.

[126] Jacques Abdul Massih, Remil Mushthaq, Guillaume Michel, and Gregory P. Chini. "Aspect-ratio-dependent heat transport by baroclinic acoustic streaming". In: *Journal of Fluid Mechanics* 997 (2024), A7. ISSN: 0022-1120. DOI: 10.1017/jfm.2024.744. URL: https://www.cambridge.org/core/product/1E29DF7F98412D0BE6EFF49BD84CB383.

[127] Rana A. Fine and Frank J. Millero. "Compressibility of water as a function of temperature and pressure". In: *The Journal of Chemical Physics* 59.10 (1973), pp. 5529–5536. DOI: 10.1063/1.1679903. URL: https://aip.scitation.org/doi/abs/10.1063/1.1679903.

[128] W. Wagner and A. Pruß. "The IAPWS Formulation 1995 for the Thermodynamic Properties of Ordinary Water Substance for General and Scientific Use". In: *Journal of Physical and Chemical Reference Data* 31.2 (2002), pp. 387–535. ISSN: 0047-2689. DOI: 10.1063/1.1461829. URL: https://dx.doi.org/10.1063/1.1461829.

[129] Jonas Helboe Joergensen and Henrik Bruus. "Theory of pressure acoustics with thermoviscous boundary layers and streaming in elastic cavities". In: *The Journal of the Acoustical Society of America* 149.5 (2021), pp. 3599–3610. DOI: 10.1121/10.0005005. URL: https://asa.scitation.org/doi/abs/10.1121/10.0005005.

[130] Jonas Helboe Joergensen, Wei Qiu, and Henrik Bruus. "Transition from Boundary-Driven to Bulk-Driven Acoustic Streaming Due to Nonlinear Thermoviscous Effects at High Acoustic Energy Densities". In: *Phys. Rev. Lett.* 130 (4 2023), p. 044001. DOI: 10.1103/PhysRevLett.130.044001. URL: https://link.aps.org/doi/10.1103/PhysRevLett.130.044001.

[131] Wei Qiu. "High-Performance and Environmentally-Friendly Bulk-Wave-Acoustofluidic Devices Driven by Lead-Free Piezoelectric Materials". In: *Small* 21.10 (2025), p. 2407453. DOI: https://doi.org/10.1002/smll.202407453. URL: https://onlinelibrary.wiley.com/doi/abs/10.1002/smll.202407453.

[132] Enrico Corato, Ola Jakobsson, Wei Qiu, Takeshi Morita, and Per Augustsson. "High-energy-density acoustofluidic device using a double-parabolic ultrasonic transducer". In: *Phys. Rev. Appl.* 23 (2 2025), p. 024031. DOI: 10.1103/PhysRevApplied.23.024031. URL: https://link.aps.org/doi/10.1103/PhysRevApplied.23.024031.

[133] Lizebona August Ambattu and Leslie Y. Yeo. "Sonomechanobiology: Vibrational stimulation of cells and its therapeutic implications". In: *Biophysics Reviews* 4.2 (2023). ISSN: 2688-4089. DOI: 10.1063/5.0127122. URL: https://dx.doi.org/10.1063/5.0127122.

[134] Martin Wiklund. "Acoustofluidics 12: Biocompatibility and cell viability in microfluidic acoustic resonators". In: *Lab on a Chip* 12.11 (2012), p. 2018. ISSN: 1473-0197. DOI: 10.1039/c2lc40201g. URL: https://dx.doi.org/10.1039/c2lc40201g.

[135] Jacques Curie and Pierre Curie. "Développement par compression de l'électricité polaire dans les cristaux hémièdres à faces inclinées". In: *Bulletin de Minéralogie* (1880). doi:10.3406/bulmi.1880.1564, pp. 90–93. ISSN: 0150-9640. URL: https://www.persee.fr/doc/bulmi_0150-9640_1880_num_3_4_1564.

[136] J. A. Gallego-Juarez. "Piezoelectric ceramics and ultrasonic transducers". In: *Journal of Physics E: Scientific Instruments* 22.10 (1989), pp. 804–816. ISSN: 0022-3735. DOI: 10.1088/0022-3735/22/10/001. URL: https://dx.doi.org/10.1088/0022-3735/22/10/001.

[137] *Ferroperm Piezoceramics*. Web Page. URL: www.meggittferroperm.com.

[138] K. Uchino and S. Hirose. "Loss mechanisms in piezoelectrics: how to measure different losses separately". In: *IEEE Transactions on Ultrasonics, Ferroelectrics, and Frequency Control* 48.1 (2001), pp. 307–321. ISSN: 1525-8955. DOI: 10.1109/58.896144.

[139] Seyit O. Ural, Safakcan Tuncdemir, Yuan Zhuang, and Kenji Uchino. "Development of a High Power Piezoelectric Characterization System and Its Application for Resonance/Antiresonance Mode Characterization". In: *Japanese Journal of Applied Physics* 48.5R (2009), p. 056509. ISSN: 1347-4065 0021-4922. DOI: 10.1143/JJAP.48.056509. URL: https://dx.doi.org/10.1143/JJAP.48.056509.

[140] Shinjiro Tashiro, Masahiko Ikehiro, and Hideji Igarashi. “Influence of Temperature Rise and Vibration Level on Electromechanical Properties of High-Power Piezoelectric Ceramics”. In: *Japanese Journal of Applied Physics* 36.Part 1, No. 5B (1997), pp. 3004–3009. ISSN: 0021-4922. DOI: 10.1143/jjap.36.3004. URL: https://dx.doi.org/10.1143/jjap.36.3004.

[141] Mikio Umeda, Kentaro Nakamura, and Sadayuki Ueha. “Effects of Vibration Stress and Temperature on the Characteristics of Piezoelectric Ceramics under High Vibration Amplitude Levels Measured by Electrical Transient Responses”. In: *Japanese Journal of Applied Physics* 38.9S (1999), p. 5581. ISSN: 0021-4922. DOI: 10.1143/jjap.38.5581. URL: https://dx.doi.org/10.1143/jjap.38.5581.

[142] K. Uchino, J. H. Zheng, Y. H. Chen, X. H. Du, J. Ryu, Y. Gao, S. Ural, S. Priya, and S. Hirose. “Loss mechanisms and high power piezoelectrics”. In: Springer US, 2006, pp. 217–228. DOI: 10.1007/978-0-387-38039-1_20. URL: https://dx.doi.org/10.1007/978-0-387-38039-1_20.

[143] Kenji Uchino, Jiehui Zheng, Amod Joshi, Yun-Han Chen, Shoko Yoshikawa, Seiji Hirose, Sadayuki Takahashi, and J. W. C. De Vries. “High Power Characterization of Piezoelectric Materials”. In: *Journal of Electroceramics* 2.1 (1998), pp. 33–40. ISSN: 1385-3449. DOI: 10.1023/a:1009962925948. URL: https://dx.doi.org/10.1023/a:1009962925948.

[144] A. V. Mezheritsky. “Elastic, dielectric, and piezoelectric losses in piezoceramics: how it works all together”. In: *IEEE Transactions on Ultrasonics, Ferroelectrics and Frequency Control* 51.6 (2004), pp. 695–707. ISSN: 0885-3010. DOI: 10.1109/tuffc.2004.1304268. URL: https://dx.doi.org/10.1109/tuffc.2004.1304268.

[145] Mikio Umeda, Kentaro Nakamura, and Sadayuki Ueha. “The Measurement of High-Power Characteristics for a Piezoelectric Transducer Based on the Electrical Transient Response”. In: *Japanese Journal of Applied Physics* 37.Part 1, No. 9B (1998), pp. 5322–5325. ISSN: 0021-4922. DOI: 10.1143/jjap.37.5322. URL: https://dx.doi.org/10.1143/jjap.37.5322.

[146] Richard S. C. Cobbold. *Foundations of Biomedical Ultrasound*. Electronic Book. 2006. DOI: 10.1093/oso/9780195168310.001.0001. URL: https://doi.org/10.1093/oso/9780195168310.001.0001.

[147] Björn Hammarström, Karl Olofsson, Valentina Carannante, Sarah Alberio, Patrick A. Sandoz, Björn Önfelt, and Martin Wiklund. “Adaptive ultrasonic actuation for dynamic formation and characterization of 3D cell cultures”. In: *Sensors and Actuators B: Chemical* 427 (2025), p. 137173. ISSN: 0925-4005. DOI: https://doi.org/10.1016/j.snb.2024.137173. URL: https://www.sciencedirect.com/science/article/pii/S0925400524019038.

[148] Amir Tahmasebipour, Leanne Friedrich, Matthew Begley, Henrik Bruus, and Carl Meinhart. "Toward optimal acoustophoretic microparticle manipulation by exploiting asymmetry". In: *The Journal of the Acoustical Society of America* 148.1 (2020), pp. 359–373. ISSN: 0001-4966. DOI: 10.1121/10.0001634. URL: https://dx.doi.org/10.1121/10.0001634.

[149] Wei Qiu, Thierry Baasch, and Thomas Laurell. "Enhancement of Acoustic Energy Density in Bulk-Wave-Acoustophoresis Devices Using Side Actuation". In: *Physical Review Applied* 17.4 (2022). ISSN: 2331-7019. DOI: 10.1103/physrevapplied.17.044043. URL: https://dx.doi.org/10.1103/physrevapplied.17.044043.

[150] O. Manneberg, J. Svennebring, H. M. Hertz, and M. Wiklund. "Wedge transducer design for two-dimensional ultrasonic manipulation in a microfluidic chip". In: *Journal of Micromechanics and Microengineering* 18.9 (2008), p. 095025. ISSN: 0960-1317. DOI: 10.1088/0960-1317/18/9/095025. URL: https://dx.doi.org/10.1088/0960-1317/18/9/095025.

[151] I. Iranmanesh, R. Barnkob, H. Bruus, and M. Wiklund. "Tunable-angle wedge transducer for improved acoustophoretic control in a microfluidic chip". In: *Journal of Micromechanics and Microengineering* 23.10 (2013), p. 105002. ISSN: 0960-1317 1361-6439. DOI: 10.1088/0960-1317/23/10/105002. URL: http://dx.doi.org/10.1088/0960-1317/23/10/105002.

[152] Kang Chen, Takasuke Irie, Takashi Iijima, and Takeshi Morita. "Double-parabolic-reflectors acoustic waveguides for high-power medical ultrasound". In: *Scientific Reports* 9.1 (2019). ISSN: 2045-2322. DOI: 10.1038/s41598-019-54916-2. URL: https://dx.doi.org/10.1038/s41598-019-54916-2.

[153] Kang Chen, Takasuke Irie, Takashi Iijima, and Takeshi Morita. "Double-Parabolic-Reflectors Ultrasonic Transducer With Flexible Waveguide for Minimally Invasive Treatment". In: *IEEE Transactions on Biomedical Engineering* 68.10 (2021), pp. 2965–2973. ISSN: 0018-9294. DOI: 10.1109/tbme.2021.3057087. URL: https://dx.doi.org/10.1109/tbme.2021.3057087.

[154] Xiaogang Wu, Kang Chen, Yasushi Hoshijima, Taro Hariu, Hiroki Yamazaki, Susumu Miyake, and Takeshi Morita. "High-Power Ultrasonic Transducer for Effective Hemolysis". In: *IEEE Transactions on Ultrasonics, Ferroelectrics, and Frequency Control* 69.1 (2022), pp. 181–186. ISSN: 0885-3010. DOI: 10.1109/tuffc.2021.3116977. URL: https://dx.doi.org/10.1109/tuffc.2021.3116977.

[155] Qingyang Liu, Kang Chen, Junhui Hu, and Takeshi Morita. "An Ultrasonic Tweezer With Multiple Manipulation Functions Based on the Double-Parabolic-Reflector Wave-Guided High-Power Ultrasonic Transducer". In: *IEEE Transactions on Ultrasonics, Ferroelectrics, and Frequency Control* 67.11 (2020), pp. 2471–2474. ISSN: 0885-3010. DOI: 10.1109/tuffc.2020.3014352. URL: https://dx.doi.org/10.1109/tuffc.2020.3014352.

[156] Enrico Corato, Ola Jakobsson, Wei Qiu, Takeshi Morita, and Per Augustsson. *High-power bulk wave acoustofluidics*. Peer-reviewed abstract, Acoustofluidics 2023, St. Louis, USA. 2023.

[157] Per Augustsson, Rune Barnkob, Steven T. Wereley, Henrik Bruus, and Thomas Laurell. "Automated and temperature-controlled micro-PIV measurements enabling long-term-stable microchannel acoustophoresis characterization". In: *Lab on a Chip* 11.24 (2011), pp. 4152–4164. ISSN: 1473-0197. DOI: 10.1039/C1LC20637K. URL: http://dx.doi.org/10.1039/C1LC20637K.

[158] Jonathan D. Adams, Christian L. Ebbesen, Rune Barnkob, Allen H. J. Yang, H. Tom Soh, and Henrik Bruus. "High-throughput, temperature-controlled microchannel acoustophoresis device made with rapid prototyping". In: *Journal of Micromechanics and Microengineering* 22.7 (2012), p. 075017. ISSN: 0960-1317. DOI: 10.1088/0960-1317/22/7/075017. URL: https://dx.doi.org/10.1088/0960-1317/22/7/075017.

[159] Bettina Sailer, Rune Barnkob, and Oliver Hayden. "Acoustophoretic particle motion in a spherical microchamber". In: *Physical Review Applied* 22.4 (2024). PRAPPLIED, p. 044034. DOI: 10.1103/PhysRevApplied.22.044034. URL: https://link.aps.org/doi/10.1103/PhysRevApplied.22.044034.

[160] Mehrnaz Hashemiesfahan, Pierre Gelin, Antonio Maisto, Han Gardeniers, and Wim De Malsche. "Enhanced Performance of an Acoustofluidic Device by Integrating Temperature Control". In: *Micromachines* 15.2 (2024), p. 191. ISSN: 2072-666X. DOI: 10.3390/mi15020191. URL: https://dx.doi.org/10.3390/mi15020191.

[161] Anke Urbansky, Franziska Olm, Stefan Scheding, Thomas Laurell, and Andreas Lenshof. "Label-free separation of leukocyte subpopulations using high throughput multiplex acoustophoresis". In: *Lab on a Chip* 19.8 (2019), pp. 1406–1416. ISSN: 1473-0197. DOI: 10.1039/c9lc00181f. URL: https://dx.doi.org/10.1039/c9lc00181f.

[162] Carl Grenvall, Per Augustsson, Jacob Riis Folkenberg, and Thomas Laurell. "Harmonic Microchip Acoustophoresis: A Route to Online Raw Milk Sample Precondition in Protein and Lipid Content Quality Control". In: *Analytical Chemistry* 81.15 (2009). doi: 10.1021/ac900723q, pp. 6195–6200. ISSN: 0003-2700. DOI: 10.1021/ac900723q. URL: https://doi.org/10.1021/ac900723q.

[163] Mathias Ohlin, Ida Iranmanesh, Athanasia E. Christakou, and Martin Wiklund. "Temperature-controlled MPa-pressure ultrasonic cell manipulation in a microfluidic chip". In: *Lab on a Chip* 15.16 (2015), pp. 3341–3349. ISSN: 1473-0197. DOI: 10.1039/c5lc00490j. URL: https://dx.doi.org/10.1039/c5lc00490j.

[164] *Attune Flow Cytometers*. Web Page. URL: https://www.thermofisher.com/se/en/home/life-science/cell-analysis/flow-cytometry/flow-cytometers/attune-nxt-flow-cytometer.html.

[165] *AcouSort and Werfen POC system*. Web Page. URL: http://acousort.com/mfn_news/the-leading-diagnostics-company-werfen-launches-groundbreaking-poc-system-with-integrated-acoustofluidic-technology/.

[166] NASA. *State-of-the-Art of Small Spacecraft Technology*. Web Page. URL: https://www.nasa.gov/smallsat-institute/sst-soa/thermal-control/.

[167] An Huang, Haodong Liu, Ping Liu, and James Friend. "Overcoming the Intrinsic Limitations of Fast Charging Lithium-Ion Batteries Using Integrated Acoustic Streaming". In: *Advanced Energy and Sustainability Research* 4.2 (2023), p. 2200112. ISSN: 2699-9412. DOI: 10.1002/aesr.202200112. URL: https://dx.doi.org/10.1002/aesr.202200112.

[168] James Friend and An Huang. *Acoustic wave based dendrite prevention for rechargeable batteries*. US Patent 12,142,736, 2024. 12 Nov 2024. URL: https://patents.google.com/patent/US12142736B2/en.

[169] Shoki Ieiri, Kyohei Yamada, Tatsuki Sasamura, Shinsuke Itoh, Takashi Kasashima, and Takeshi Morita. "An ultrasonic transducer focusing ultrasound into a thin waveguide by two elliptical reflectors". In: *Applied Physics Express* 17.6 (2024), p. 064001. ISSN: 1882-0778. DOI: 10.35848/1882-0786/ad4d3c. URL: https://dx.doi.org/10.35848/1882-0786/ad4d3c.